



Energy Saving through Urban Design

A Microclimatic Approach

Mohamed M. El Nahas

B. Sc., M. Sc. (Ain Shams (Cairo))

A thesis submitted in fulfilment of
the requirements for the degree of
Doctor of Philosophy in Architecture
at The University of Adelaide

1996

Table of Contents

List of Figures	v
List of Tables	vii
Abstract	viii
Declaration	ix
Acknowledgments	x

1 Introduction 1

2 Radiation Fluxes Availability 13

2.1 Urban Radiation Balance 14
2.1.1 Short-wave Radiation 14
2.1.2 Long-wave Radiation 20
2.1.3 Net Radiation 23
2.2 Solar Access/Shading 24
2.2.1 Levels of Solar Access 25
2.2.2 Solar Access Techniques 27
2.3 Solar Obstruction Model 31

3 Controlling Wind Field 33

3.1 Wind Field Characteristics 34
3.1.1 Urban Wind Speed 34
3.1.2 Wind Turbulence 37
3.2 Urban Wind Conditions 37
3.2.1 Wind Shelter 37
3.2.2 Urban Ventilation 40
3.3 Ventilation and Infiltration 44
3.3.1 Air flow caused by Wind 45
3.3.2 Air flow caused by Buoyancy 49
3.3.3 Airflow caused by Both Forces 49
3.4 Airflow Model 51

4 Temperature Modification 53

4.1 Urban Air Temperature 54
4.1.1 Heat Island Effect 54
4.2 Factors contributing to the Development of the Heat Island Effect 59
4.2.1 Absorption of Short-wave Radiation 59
4.2.2 Long-wave Radiation Loss 61
4.2.3 Turbulent Heat Transport 63
4.2.4 Sensible Heat Storage 64
4.2.5 Evapotranspiration 65
4.2.6 Anthropogenic Heat 68
4.5 Temperature Prediction Model 70
4.3.1 The Developed CTTC Model 71
4.3.2 Verifying the Model 72

List of Figures

1.1	Internal environment control chart.	5
2.1	Heat exchange at noon for a summer day.	15
2.2	The difference between surface and air temperatures versus solar reflectivity of paint and roofing materials facing the sun	18
2.3	Schematic diagram of two symmetrical parallel surfaces and two perpendicular surfaces	22
2.4	Ground solar access for differently oriented streets in Adelaide.	25
2.5	Monthly average wall solar access indices by aspect ratio.	26
2.6	Effects of surface orientation and local screening on annual global radiation in Sweden	29
3.1	Diagrammatic mean horizontal wind velocity profiles above urban, rural and sea surfaces.	35
3.2	Wind speed distributions between two bldgs by wind tunnel tests.	42
3.3	Thresholds for flow regimes in urban canyons as functions of canyons H/W and L/H ratios.	43
3.4	Mean pressure difference between windward and leeward facade	48
4.1	Typical isotherms in Sydney as measured at street level at about 1 am on 24 April 1971.	54
4.2	Generalised cross-section of a typical urban heat island.	55
4.3	Normalised solar radiation and air temperature above bare soil at Scottsbluff, Nebraska on Sept. 4, 1963.	60
4.4	Simulated effects on cooling of varying the area of a city covered by evapotranspiring surfaces.	66
4.5	The man-made heating and observed screen temperatures in Sydney at 8 am in July.	68
4.6	An assumed diurnal artificial heat profile for major Australian cities.	69
4.7	The experimental urban canyons at the University of Adelaide	73
4.8	Skyline diagram (Kent Town Weather Station)	75
4.9 a	Measured meteorological and urban air temperatures for N-S axis canyon in December 1993.	76
4.9 b	Predicted versus measured urban temperatures for N-S axis canyon in December 1993.	76
4.10 a	Measured meteorological and urban air temperatures for E-W axis canyon in December 1993.	77
4.10 b	Predicted versus measured urban temperatures for E-W axis canyon in December 1993.	77
5.1	Schematic illustration of simulation models.	84
5.2	A practicable zone of urban forms defined by two urban design variables.	88
5.3	Cross-section through urban configurations.	89
5.4	Diagrammatic plans of the design options.	90
5.5	House plan	97
6.1 a	Simulated air temperature profiles for two different building density's sites compared with that at the weather station in Adelaide (15 Jul., 1986)	115
6.1 b	Simulated air temperature profiles for two different building density's sites compared with that at the weather station in	

5 Simulation and Modelling 79

5.1 Simulation Procedure 80

5.1.1 Assumptions & Restrictions 80

5.1.2 Simulation Approach 81

5.2 Simulation Models 82

5.2.1 The Building Energy Simulation Program 82

5.2.2 Climate Modifier Models 84

5.3 Data Input 85

5.3.1 Climatic Data 85

5.3.2 Urban Configurations 87

5.4 Building Analysis 91

5.4.1 Heating/Cooling Model 92

5.4.2 Building Constuction 100

6 Results and Discussion 105

6.1 Design Objectives 106

6.1.1 Solar Access 106

6.1.2 Wind Shelter 108

6.1.3 Urban Warmth 110

6.1.4 Isolated Analysis 111

6.3 Design Variables 113

6.2.1 Building Density 114

6.2.2 Building Spacing 115

6.2.3 Building Orientation 117

6.4 Energy Analysis 118

7 Summary and Recommendations 123

Bibliography 133

Appendices 145

Appendix1: CONSECTTC Program 146

Appendix2: The TEMPAL Package (Summary Documentation) 159

Appendix3: TDINPUT (TEMPAL Data Input File) 165

	Adelaide (10 Jan., 1984)	115
6.2 a	Simulated Air temperature profiles for two sites with different aspect ratios compared with that at the weather station in Adelaide (15 Jul., 1986)	116
6.2 b	Simulated air temperature profiles for two sites with different aspect ratios compared with that at the weather station in Adelaide (10 Jan., 1984)	116
6.3 a	Simulated air temperature profiles for differently-oriented urban street canyons in Adelaide (15 July, 1986)	118
6.3 b	Simulated air temperature profiles for differently-oriented urban street canyons in Adelaide (10 January, 1986)	118

List of Tables

2.1	The albedo of some typical urban materials.	17
	The yearly average albedo and absorption increment for different street aspect ratios.	19
4.1	Input data requirements for the CTTC Model.	74
4.2	Urban characteristics of the weather station and University sites.	74
4.3	Effect of excluding the new features on mean temperature values	78
5.1	Selected representative periods as typical meteorol. seasons.	85
5.2	Average annual climatic data for Perth, Adelaide and Melbourne.	86
5.3	Urban characteristics of urban weather stations.	86
5.4	Thermal properties of construction elements used in the simulations	91
5.5	Range of comfort with normal clothes suggested by some researchers	93
5.6	The effect of thermostat setting on predicted energy use.	98
5.7 a	The impact of hypothetical times and spaces on predicted heating energy use.	99
5.7 b	The impact of hypothetical times and spaces on predicted cooling energy use.	99
5.8	Heating/cooling energy use with various bldg. elements	102
	Total solar heat gains (GJ/m ² of glass area) by street aspect ratio in Adelaide	107
6.2	Total solar heat gains (GJ/m ² of glass area) by orientation in Adelaide.	108
6.3	Solar heat gain and ventilation heat loss (GJ) by street aspect ratio for the narrow-frontage dwelling in Adelaide.	109
6.4 a	Percentage frequency of air temperature within range for both cases in the heating season.	111
6.4 b	Percentage frequency of air temperature within range for both cases in the cooling season.	111
	Predicted heating/cooling energy use (GJ) in various urban configurations for three simulation sets	112
6.6	Heating and cooling energy use for various urban configurations in Perth	121
6.7	Heating and cooling energy use for various urban configurations in Adelaide	121
6.8	Heating and cooling energy use for various urban configurations in Melbourne	121

Energy Saving through Urban Design

A Microclimatic Approach

Mohamed M. El Nahas

Abstract

This thesis investigates the impact on residential energy use for climate control of urban design variables such as building density, spacing and orientation. Energy use for heating/cooling is predicted in a range of urban configurations that are compatible with the following climate-adapted design objectives: wind shelter and solar access in winter and urban ventilation and shading in summer. It is hypothesised that this range of urban configurations would have roughly the same total heating/cooling energy use.

As the urban configuration influences the microclimate at a particular urban site, some climatic elements such as solar radiation, air temperature and wind speed need to be modified to be site-specific. Climate modifier models are adopted and/or developed to make these climatic elements more closely approximate the urban microclimate. A heating/cooling model is proposed as a simplified description of use-patterns of heaters and coolers in buildings. Energy use of dwellings in hypothetical urban sites is predicted in three Australian cities located in the temperate region.

The results support the hypothesis and show that higher urban densities and deeper canyons than those based on solar access criteria will not result in a noticeable increase in the residential heating/cooling energy use in moderate and cool-temperate climates. A unique aspect of the results is based on quantifying the heat island effect as a counterbalance to reduced solar access in medium-density developments. In addition, the advantageous shading effects of high-density developments result in notable energy savings in warm-temperate climates.

Declaration

This work contains no material which has been accepted for the award of any other degree or diploma in any university or other tertiary institution and, to the best of my knowledge and belief, contains no material previously published or written by another person, except where due reference has been made in the text.

I give consent to the copy of my thesis, when deposited in the University Library, being available for loan and photocopying.

© 1996, Mohamed M. El Nahas

16/4/1996

To my dearest parents,
my adored wife,
and my beloved kids.

Acknowledgments

The author wishes to thank all the following persons/organisations for their help throughout the course of the degree:

- **Ass. Prof. Susan Coldicutt:** (joint supervisor) Department of Architecture, the University of Adelaide, whose substantial help and advice in connection with the thesis preparation were invaluable.
- **Mr. Terry Williamson:** (joint supervisor) Dean, Faculty of Architecture and Urban Design, the University of Adelaide, whose computing assistance in improving the CTTC model was valuable.
- **Dr. Milo Hoffman:** National Building Research Institute, Haifa, who provided the original CTTC model.
- **Dr. Milton Behrendroff:** Department of Mechanical Engineering, the University of Adelaide, who set up the climatic measurements.
- **Prof. Edward Arens:** Centre for Environmental Design Research, University of California, who supplied the UCB wind flow model.
- **Prof. Tadahisa Katayama:** Thermal Energy System, Kyushu University 39, Kasuga-shi, who provided a number of papers on wind flow in urban canyons.
- **Prof. Richard Aynsley:** Director, AITA, James Cook University of North Queensland, who sent some recent literature about wind and pedestrian comfort.
- **Bureau of Meteorology:** General Office, Melbourne, which supplied the meteorological sites characteristics.

Introduction

"Settlements are continually expanding to accommodate the influx of migrants from rural areas and the natural increase of population, and by the year 2000 it is estimated that 60% of the world's people will live in towns with 5000 or more inhabitants. This makes study of urban climates doubly important; first to ensure a pleasant and healthy environment for urban dwellers, and second to see that the effects of urbanisation do not have harmful repercussions on large scale (even planetary) climates." [Oke 1992: 273].

In the 1990's, society's growing concerns about the environment and the quality of urban life will be a challenge to which urban designers, architects and engineers should respond. The demands for a comfortable living and a safe environment will be the forefront. Comfort in the urban environment will refer to many aspects of the physical environment. Improving urban thermal comfort involves research into the development of more hospitable outdoor spaces for pedestrians and more comfortable indoor climates at reduced energy levels.

Urban outdoor areas could be designed for human relaxation. One important condition for relaxation is a pleasant climate. To maintain the importance of sheltered sunlit outdoor areas, architects and planners need well-founded arguments and defined goals. However, they also need instructive planning tools for quantification of climatic differences and prediction of how the climate in a certain location is altered by building development. The climatic aspects must be considered throughout all levels of the planning process.

The energy demands in buildings can be reduced by appropriate urban and building design. An appropriate urban design would leave proportionally less to be achieved by passive building design, that is by appropriate selection of building form, orientation and the thermal properties, proportions and porosity of the facade. The fine tuning of the internal environment conditions, if required, can then be achieved by active controls, that is heating/cooling systems.



BACKGROUND

Since the far past, health and hygiene have been important considerations in the planning of ancient cities. Sun and wind have played a considerable role in influencing the overall form and orientation of such cities. Modern excavations indicate that climate-adapted architecture flourished in civilised nations in the ancient world (for example Egyptian, Greek and Roman). The awareness of solar and wind orientation was developed in the ancient cities to ensure an equitable access to the sun in winter and exposure to a cool breeze in summer [Abdou 1987].

Climate adaptation is not a new criterion of design. The context of building has always been defined by climatic and material limitations. Even when these limitations are oppressive, they have not prevented designers from developing solutions of great adeptness and distinction. Watson [1979: 3] points out that "Indigenous and vernacular building at its best is a direct expression of adaption to climate and resource constraints". A principal purpose of building is to change the micro-climate. Early men built houses to control climatic elements, such as rain, wind, sun and snow. For example, ancient city plans reveal that sunlight was an important enough element to exert some influence on house and street orientation.

An analysis of *Pueblo Bonito* in the American South-west shows how the ancients naturally controlled seasonal climatic impacts [Knowles 1974]. Solar irradiation in winter proved to be constant from 8:00 am to 4:00 pm and greater than in summer, during which it decreases during the afternoon when the sol-air temperature is greatest. In ancient Egypt, a more sophisticated and complex approach was implemented in the workers' city of *Tel El-Amarna*. Narrow streets served as an access to back-to-back residential units. This solution was formulated to reduce the area exposed to the sun and hot dust-bearing winds and to create shaded cool paths.

Wind direction and its effects figured prominently in the planning and orientation of ancient cities. Opposing views were held by theorists of that time, as to the benefits of wind at an angle or parallel to the streets. Although no significant relationship has been established between the orientation of ancient cities' streets and prevailing winds, such orientation

is just as likely to be function of wind direction as sun position. Hitherto archaeology has not provided the evidence to situate the link between the theories of wind influence on urban planning and the application of those theories in the practice of town planning [Kenworthy 1985].

These successful solutions of manipulating climatic problems did not result from deliberate scientific reasoning. They grew out of countless experiments and accidents and the experience of generations of builders who continued to use what worked and rejected what did not. They were conveyed in the form of traditional, rigid, and apparently arbitrary rules for selecting sites, orienting the building, and choosing the material, building method, and design [Fathy 1986].

Recently, the human-environment relationship has encountered several challenges. One of these is inadvertent climate modification. In other words, it is the climatic side-effects of human activities. They are the result of interference in the operation of natural systems. These climate modifications—for example the urban heat islands—are recorded as well as their effect on the energy demand for climate control [Taha 1990]. Therefore, designers need to understand these issues and need to be able to make conscious modifications of the microclimate. Ideally, this would entail full awareness of the various environmental effects of these modifications.

CLIMATE-ADAPTED DESIGN

Scales of climate vary from thousands of kilometres down to fractions of a centimetre, that is, from global to molecular or from macro- to micro-climatological [Chandler 1976]. Macroclimate exercises a first-order control on internal climates and affects those aspects of design intended to improve the internal climate and maintain it at acceptable comfort levels. Microclimate is the climate variations, over distances up to a few tens of meters, because of changes in surface terrain and cover. In urban areas, climate is affected by the presence of obstructive structures and materials. The microclimate, rather than the climate, is dominant when selecting a site or designing a building.

Individual buildings react with their envelope of air, and small groups of buildings exercise a considerable effect on the external climate. On the

other hand, the thermal performance of a building is dependent on the micro-meteorological conditions outside the building, the thermal behaviour of the building fabric, and the internal thermal loads. Figure 1.1 represents the different energy sources involved in the process of controlling the internal environment conditions. For a given total energy input, an appropriate urban design would reduce the reliance on generated energy by optimising the benefit from ambient energy.

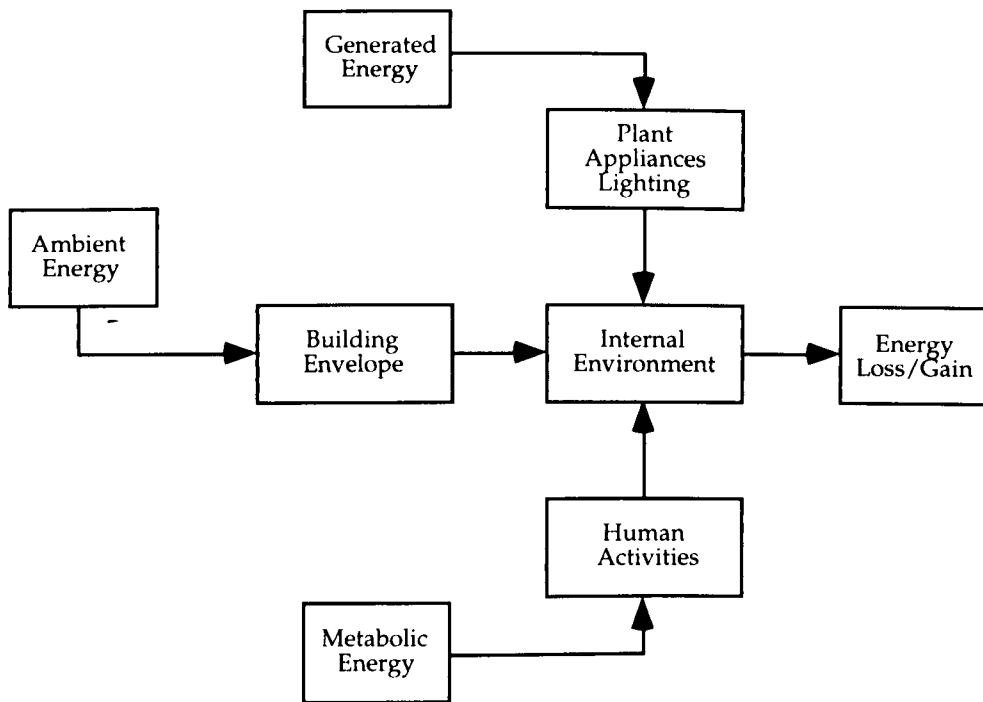


Figure 1.1 Internal environment control chart

Improving the microclimate of built-up areas can be a functional step towards enhancing the energy efficiency of buildings, with added benefits for the habitability and value of outdoor spaces. Complex interaction and feedback exist between the buildings and their outdoor environment. The internal climate in any given building depends on the local climate conditions around this building. Nevertheless, the building itself will change this microclimate by its presence.

Various neighbourhoods within the overall urban area usually differ in the details of their structure, density, street orientation, and so on. In many cases even a given neighbourhood is not homogeneous in its details. Numerous design details can modify the urban temperature, wind conditions and solar exposure of the building and the street [Givoni 1989]. These modifications are not always in favour of improving the

internal climate. However, the building energy demand would be affected by the end result of all these modifications.

PROBLEM STATEMENT

Much has been written about the nature of cities from a general urban design and architectural theory aspect. On the other hand, a great amount of work has been produced on the urban environment and microclimate. However, between the two extremes of urban academic theory and urban geography, lies a body of urban research work that needs to be addressed [Steemers 1991]. The environmental impact of buildings on the urban microclimate has been investigated by climatologists and meteorologists, but little has been done to study the effects of the urban context on buildings.

Energy efficient design of individual buildings on open sites, that is free standing buildings, has received much attention in research and practice. Nevertheless, the complexities of the urban environmental interactions have not been explored. Urban design variables, such as building density, spacing and orientation, help to control the climate around the buildings. Designers' intervention can modify the environment close to buildings, creating more favourable microclimatic conditions. In this sense, the task of designing buildings suitable for a particular climate could be made easier.

Making choices between alternatives in planning and in design could be difficult. Although the case in this research is mainly concerned with physical outcomes rather than social or cultural values, it is not clear what choices should be made. The relative importance of the urban effects on air temperature (heat island effect) versus that on solar access to the building in winter cannot be simply decided, nor the urban effects on shading versus that on ventilation in summer. Moreover, in temperate climates where the weather conditions are not so extreme, summer and winter considerations may be of equal importance in design. This fact complicates rather than simplifies climate-adapted design.

Climate-adapted design objectives are directed to optimising ambient energy from the sun and wind to reduce the energy consumption for improving human thermal comfort. They include access to the sun and

exposure to the wind. Solar access is solar radiation availability at a particular surface as a ratio to total unobstructed solar radiation. It is of major significance to the heat budgets of the buildings, and hence to the energy costs of heating and/or cooling them. Wind shelter contributes to energy conservation by reducing turbulent heat losses in the cold season. In the hot season, inducing higher ventilation rates could have a great effect in reducing heat gains.

In temperate climates, these objectives are likely to be providing solar access and wind shelter in the cold season, and urban shading and ventilation in the hot season. It seems difficult to achieve a balance between those objectives due to their conflicting nature in different seasons. For example, an open geometry could have the advantages of welcoming natural ventilation and mitigating the heat island effect in summer and allowing solar access to buildings and streets in winter. On the other hand, the disadvantages would be reducing urban shading by opposite buildings flanking the streets in summer and exposing streets and open areas to chilling wind in winter.

PURPOSE/HYPOTHESIS

The main purpose of the research is to investigate the role of urban design in achieving thermally improved environments. This climate-oriented design approach is helpful for developing more favourable outdoor spaces and hence more comfortable indoor climates at reduced energy use for climate control. The objectives of the research are to:

- investigate the impact of urban configurations on indoor climate and energy consumption for heating/cooling;
- incorporate local microclimatic effects into building performance simulations;
- determine urban forms that are consistent with the climate-adapted design objectives; and
- propose some guidelines for energy-conscious urban design in temperate climates.

For testing the foregoing research objectives, a hypothesis is required for this research. It is hypothesised that effects of applying mutually exclusive design objectives might offset each other. Therefore, there might be a range of urban configurations that have roughly the same total

energy use for climate control. If the hypothesis is shown to be supported, this could give urban designers a simple and easily applicable design guideline. If on the other hand great variations in the total energy use were obtained, this would imply that applying one or more of these objectives might have a considerable effect on energy use.

RESEARCH METHODOLOGY

Field studies might be a trustworthy method for similar research. Sioufi points out that

"The ideal approach to investigating the effects of the urban context on the thermal performance of buildings and spaces they constitute would be to take actual measurements of air and surface temperature, solar radiation, and wind speed in an existing built environment." [Sioufi 1987: 39].

Nevertheless, this would entail the use of extensive resources—in terms of instrumentation and data management—and the existence of a built environment that has a particular urban density with various building spacings but similar heights in one location. As these conditions are not readily available, simulation models of built environment-climate interactions are an alternative approach.

The methodology for conducting this research includes:

- Reviewing the literature on controlling urban climate and its modification by buildings.
- Selecting microclimate models for modifying conventional climatic data to represent the local climatic conditions around the building, to be linked thereafter to a building energy simulation program.
- Testing hypothetical layout positions considering the variations of microclimate in different sites.
- Illustrating the deviations in predicted building energy use between these cases. From this, the impact of urban geometry on building energy use for space heating and cooling could possibly be revealed.

The research focuses on thermal environments in parallel block layouts as formed by row buildings (urban canyons). The urban street canyon is adopted as the basic structural unit in medium- and high-density built-up urban areas. At its simplest, the urban canyon may be conceived as a

rectangular groove composed from a street of width (W) and buildings flanking this street of average height (H), with specific surface materials and oriented at some angle (θ), measured in this thesis clock-wise from north. The absolute dimensions of the canyon are not relevant in many applications, as its geometry may be characterised by its aspect ratio H/W .

The selected urban forms and dwellings are not representative of the major sector of Australian housing; however, they have been chosen for the following reasons:

- Such dwellings combine some of the advantages, from the energy viewpoint, of both multi-storey apartment buildings (smaller external wall area) and of single-family houses (natural ventilation and solar heating options).
- Except for the end units, all dwellings have essentially two external orientations. Because of this, orientation with respect to the sun is a much more sensitive issue than in the case of detached houses.
- Matching with the policy of urban consolidation recently adopted in most of Australia, town-houses enable higher urban density as compared with detached single-family houses.

The thermal environment being considered is limited to mid-latitude cities (temperate climates). Temperate climates encompass perhaps, to lesser extremes, the characteristics of other climates, but what distinguishes temperate climates further from other climates is the wide variety of weather conditions one can expect within the same season [Serra 1988]. Furthermore, in these climates housing has both a heating season and a (potential) cooling season. Three different categories of temperate climates are to be dealt with—warm, moderate and cool temperate climates. Three Australian capital cities are to be selected in the temperate region for the purpose of this study.

THESIS OUTLINE

The thesis is organised in five main parts as follows. The first and second parts present a literature review on solar radiation and wind flow field. The **first** part deals with the radiation fluxes availability in urban areas. Possibilities of controlling urban solar radiation to produce improved microclimates are studied. Levels of solar access (floor, wall and roof) are

studied and applied in some case studies. Then, different techniques of protecting solar access are evaluated to select an appropriate method for determining shading effects on solar radiation received on building surfaces.

The **second** part describes the urban wind field and the different scales of air movement modelling. The importance of wind shelter is highlighted and shelter requirements have been assessed by various criteria based on different combinations of climate elements. Then, predictive models of air flow rates caused by wind and buoyancy are researched towards proposing a ventilation/infiltration model suitable for the purposes of this research. The model is used as a replacement to the empirical model adopted in TEMPAL the building energy simulation program used in this research.

The **third** part outlines the temperature modification by built-up areas, in order to improve a model for predicting urban temperatures. The climate changes are related to the effects of intrusive structures and materials. These changes include the effects of building geometry, materials and heat losses. Urban climate modifications involve increased absorption of short-wave radiation, decreased long-wave radiation loss, and decreased total turbulent heat transport. Urban built-up areas result in increasing the anthropogenic heat and sensible heat storage, and reducing evapotranspiration. A model for predicting urban air temperatures is developed and tested.

The **fourth** part describes the simulation procedure and its restrictions. The assumptions that are adopted in the simulations are discussed. Simulation models are selected—microclimate modifier models plus the building energy simulation program TEMPAL. Input data is classified to urban form characteristics and the dwelling description. A model heating/cooling routine is proposed to approximate real occupancy and use patterns. A building analysis is performed to investigate the impact of the building description and energy use patterns on heating/cooling energy use.

The **fifth** part analyses the urban effects on residential energy demands for heating and cooling in case study examples. A preliminary building energy analysis is performed to separately consider the effects of an urban

design variable on each climatic element affected by this variable. In order to complete the building energy analysis, however, all of these effects are analysed in an integrated form. In this analysis, effects of selected urban design variables on climatic elements affected by these variables are all considered.

Radiation Fluxes Availability

2.1 URBAN RADIATION BALANCE	14
2.1.1 Short-wave Radiation	14
2.1.2 Long-wave Radiation	20
2.1.3 Net Radiation	23
2.2 SOLAR ACCESS/SHADING	24
2.2.1 Levels of Solar Access	25
2.2.2 Solar Access Techniques	27
2.3 SOLAR OBSTRUCTION MODEL	31

"There are four main factors responsible for weather and climate. First comes the atmosphere itself, set into motion by the second factor, radiation from the sun. Thirdly, water in the air creates humidity and precipitation. Lastly, the Earth's rotation and topography control the pattern of the winds." [Linacre & Hobbs 1977:13].

This chapter is about radiation from the sun that is the source of power for all atmospheric processes. It deals with radiation fluxes availability in urban areas. Then, levels of solar access are studied and solar access techniques are evaluated to select an appropriate solar obstruction model.

2.1 URBAN RADIATION BALANCE

The solar radiation input to built-up areas impinges on the urban facets, such as walls, roofs and the ground (streets and open areas). The radiation falling on the vertical walls is partly reflected, mostly towards other walls of nearby buildings. The percentage of solar radiation reflected from the walls can vary greatly, from about 20% to 80%, depending upon the exterior colour of these walls [Givoni 1989]. Similarly, the percentage of solar radiation reflected off the roofs towards the sky is relative to the colour of the roofs, and thus varies from 80% in the case of white painted roofs to 20% in the case of black tarred roofs.

The walls and the ground surfaces lose heat by long-wave radiation to the sky. The intensity of this radiant heat loss depends upon the fraction of the sky which the wall or the street *sees*. The outgoing long-wave radiation from a vertical wall is only one-half of that emitted from a roof of similar area. As most of the sky dome *seen* by the walls is blocked by other buildings, the long-wave radiation exchange between walls does not result in significant radiant heat loss. When the buildings are of different heights, the higher buildings block the sky and reduce the amount of solar reflection and long-wave radiation from the roofs of the lower buildings, thus reducing the overall amount of radiant heat loss from the urban canopy.

2.1.1 Short-wave Radiation

Any exposed surface on Earth gains heat from solar radiation (short-wave) and loses heat by outgoing long-wave radiation. The solar

radiation actually received by a surface (insolation) is reduced by the obliqueness of the sun's rays and by absorption by cloud, dust and the gases of the atmosphere. The incoming solar radiation is ultimately subdivided into two fractions: the radiation that is absorbed at some point and converted into heat (sensible and/or latent); and the fraction that is reflected away towards the sky, without any effect on the temperature and humidity conditions of the environment [Givoni 1989].

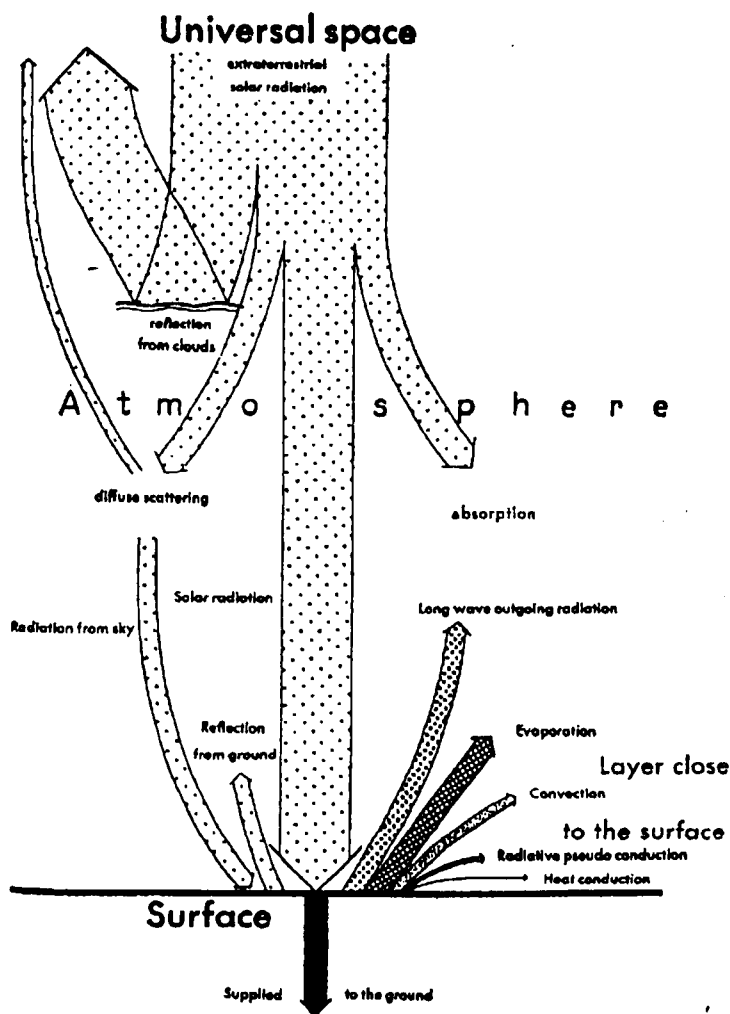


Figure 2.1 Heat exchange at noon for a summer day (Geiger 1959 : 4)

Clouds reduce the portion of solar radiation reaching the ground as they increase the radiation reflection and reduce its transmission. With an overcast sky, the fraction of radiation reaching the ground is only about one third that with a clear sky. In the latter case, the incoming solar radiation represents about 75% of the total radiation on a horizontal surface above the atmosphere (extra-terrestrial). This reduction is caused by the absorption of radiation within the atmosphere and the scattering of

radiation back into space. Gases and aerosols in the air result in this absorption and scattering. Figure 2.1 shows the relationship among those various radiation fluxes.

Part of the extra-terrestrial radiation is scattered back to space and about 20% is scattered downwards to the Earth as diffuse radiation. This diffuse radiation is a component of the global radiation, the solar radiation reaching a horizontal surface on the ground. The other component comes straight from the sun, that is direct radiation. The ratio of direct radiation to diffuse radiation tends to be less when the sun is low, at high latitudes and in winter [Rosenberg 1974]. In the mid latitudes, diffuse sky radiation may contribute 30% - 40% of the total solar radiation. Before sunrise and after sunset, all the total solar energy received is diffuse sky radiation.

The short-wave input to urban areas is considerably altered in its passage through a polluted atmosphere. A depletion is caused by the absorption of radiation within the atmosphere and the scattering of radiation back into the space. This absorption and scattering is called *turbidity* and results from the gases and aerosols in the air [Linacre & Hobbs 1977]. The attenuation of the incoming radiation varies with height as the concentration of the pollutants varies. In a heavy industry city short-wave input may be reduced by 10% - 20% in comparison with its surrounding rural areas. In less industrialised cities where transportation is the prime source of pollution concentration the range is 2% - 10% [Oke 1992].

The presence of geometric obstructions has a major influence on the solar radiation received at street-level. Geometric obstructions include local planting of vegetation and the shape, size and position of buildings (urban geometry). Therefore, both turbidity and urban geometry are contributory causes of the depletion of short-wave input to urban areas. Since studying the effects of turbidity is beyond the scope of this research, the thesis will consider the impact of urban geometry only. The reflection of short-wave radiation from urban areas is affected both by the albedo of the reflecting surfaces, and by their geometrical arrangement.

Albedo effect

Albedo is a wavelength-weighted and spatially-averaged reflectivity. The surface albedo (α) is a fundamental property that directly determines the absorptivity of an opaque surface and could be altered by a surface

treatment. Low-albedo surfaces absorb a larger portion of the incident insolation and become hotter than high-albedo surfaces. Table 2.1 shows the albedo of some typical urban materials. The albedo increases with increasing solar zenith angle; therefore, its value is lower during winter. The albedo daily values generally increase from the city centre to the residential suburbs, but net short-wave and net radiation on ground decrease from the city centre to the residential areas at the city periphery [Arnfield 1982].

On the basis of available measurements, urban areas have albedo range (0.10 - 0.27) and average of about 0.15 [Oke 1992]. These values apply to mid-latitude cities in the absence of snow. Mid-latitude urban albedos tend to be lower than their rural counterparts. Due to the surface irregularity of urban structures, it is expected that short-wave input will be less in urban areas compared with the surrounding rural areas. Nevertheless, this deficit is partially offset by a lower urban albedo. Therefore, urban/rural net short-wave radiation differences are not large.

Table 2.1

The albedo of some typical urban materials [Data from Oke 1992 : 281]

Surface	Albedo
1. Roads	
Asphalt	0.05 - 0.20
2. Walls	
Concrete	0.10 - 0.35
Brick	0.20 - 0.40
Stone	0.20 - 0.35
3. Roof	
Tar and gravel	0.08 - 0.18
Tile	0.10 - 0.35
Slate	0.10
Thatch	0.15 - 0.20
Corrugated iron	0.10 - 0.16
4. Windows	
Clear glass	
zenith angle less than 40°	0.08
zenith angle 40° to 80°	0.09 - 0.52

The albedos of land surfaces are greater when the sun is within 30° of the horizon, when the surface colour is lighter and for soil when it is dry - for example $\alpha = 0.10$ for wet soil and 0.35 for dry sand [Linacre & Hobbs

1977]. As lower albedos increase the solar radiation absorbed by active surfaces (street and building facades in this case), they contribute to keep their surface temperature higher. Consequently, the ambient air temperature is kept higher by increasing the amount of convective heat flux. Taha *et al.* [1988] categorised the effects of albedo on building energy use as direct and indirect. Modifications in the absorptive and reflective characteristics of the building envelope directly affect building energy use and indirectly cause micro-climate changes mainly in dry bulb temperature.

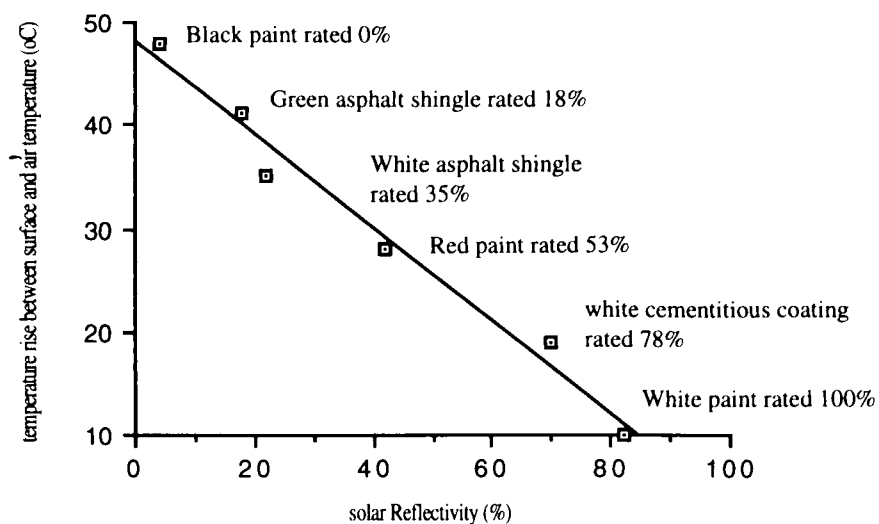


Figure 2.2 The difference between surface and air temperatures versus solar reflectivity of paint and roofing materials facing the sun [Data from Rosenfeld *et al.* 1995: 256]

Direct effects of albedo are affected by surface colour and texture (for example $\alpha = 0.9$ for white-washed exterior finish and 0.1 for dark brown paint). Most high-albedo surfaces are light-coloured, but some surfaces which reflect a large portion of the infra-red solar radiation and absorb some visible light may be coloured, though have relatively high albedos [Rosenfeld *et al.* 1995]. Figure 2.2 shows the midday temperatures of some horizontal surfaces exposed to sunlight. It can be noted that the difference between the surface and ambient air temperature for low-albedo surfaces may be up to 50°C, while that difference for high-albedo surfaces is down to 10°C. Field observations have shown that pavement materials such as granite slab, terracotta bricks and coloured concrete interlocking blocks result in lower heat output to the environment than the conventional asphaltic concrete pavements [Tan & Fwa 1992].

It is reported that 4 - 8°C higher air temperature throughout the course of a hot day is predicted for the internal air temperature in a normal sized building of heavy structure with a black coloured surface rather than a white one [Bansal *et al.* 1992]. In the case of building surfaces and components, these effects vary with orientation. In mid-latitudes, west- and south-facing (in northern hemisphere) and horizontal surfaces are most sensitive to albedo modification [Taha *et al.* 1988]. Nevertheless, the effect of exterior colour is further complicated, and its effectiveness as a conservation strategy becomes less obvious. Temperate climates have both cooling and heating extremes, and therefore it is highly possible that benefits in one season, from albedo modification, offset drawbacks in another season.

Geometry effect

The urban geometry has a great variety of shapes and orientations. The walls, roofs and streets of urban canyons perform like a maze of reflectors, absorbing some of the energy they receive and directing much of the rest to other absorbing surfaces [Lowry 1967]. Yet, the effect of the urban geometry is to decrease the albedo in comparison with the value for a horizontal surface. The decrease is due to radiation trapped within the canyons. Better use of available short-wave radiation can often be accomplished by manipulating surface geometry to take advantage of the direct-beam short-wave radiation.

Table 2.2

The yearly average albedo and absorption increment for different street aspect ratios (H/W) [Data from Aida 1982: 412]

H/W	Average Albedo	Absorption increment (%)
0.00	0.40	—
0.25	0.32	13
1.00	0.27	21
2.00	0.23	27

Using different scale model arrays, Aida [1982] reported that the surface irregularity decreases the surface albedo in the urban areas and tends to increase surface temperatures due to additional absorption of solar radiation. Table 2.2 shows the average yearly albedo and absorption increment for block-canyon models in Yokohama (c. 35°N). The surface irregularity increases the surface absorption of solar radiation by more

than 10% throughout the year compared with a flat surface of the same material. When the solar elevation is low in winter the absorption increment exceeds ~~by~~ 20%. The results show that as the buildings become taller, the urban areas absorb more solar radiation per canyon top area, due to multiple reflections from the canyon walls. In addition, the N-S axis canyon shows almost the same property as the E-W axis canyon in the absorption of solar radiation.

Using a numerical simulation, Aida and Gotoh [1982] suggest that in cases where solar absorption needs to be maximised, such as mid-latitude cities in the cold season, canyon width ~~is~~^{needs} to be about twice the block width. Nevertheless, if the urban geometry is designed to have minimum albedo in the cold season, this geometry also absorbs the maximum solar radiation in the warm season. Therefore, it may be desirable to introduce seasonal modifications in the reflectivity of urban surfaces, particularly for ~~building~~^{building} tops and canyon bottoms. These may be introduced with the help of certain types of planting that change with seasons (deciduous).

2.1.2 Long-wave Radiation

Long-wave radiation is the radiation emitted by the Earth in the infra-red spectral range from about 3.5 μm to 50 μm , with a peak near 10 μm [Linacre & Hobbs 1977]. Long-wave radiation is not visible. The reflectivity of long-wave radiation for most materials is negligible—about 0.1 [Arnfield 1982]. The amount of long-wave radiation from a material depends on the temperature difference between its surface temperature and mean radiant temperature of the surroundings. In this sense, the warmer the surface is, the greater the radiation emittance. Long-wave radiation is emitted from gases and aerosols as well as from the ground and oceans. Therefore, clouds and the clear atmosphere also radiate long-wave radiation. The influence of clouds on long-wave radiation exchange depends upon the cloud height. The lower the clouds, the warmer the cloud temperature and thus the more contribution to the sky radiation.

The long-wave radiation loss is the major cooling factor of an area as a whole. The amount of the long-wave radiation loss from the ground level differs in an open country from that in a densely built-up area. This is one of the major factors that generates the differences between the urban and the country's climatic conditions [Givoni 1989]. The intensity of the

outgoing long-wave radiation depends on the Earth's surface temperature (average $\cong 15^{\circ}\text{C}$) and its emissivity ($\cong 1.0$). Although long-wave emission is the major radiative flux at night, it also occurs during the day. In fact, long-wave radiation flux will be more intense during the daytime because of the higher terrestrial temperatures then.

Although the urban geometry results in decreased long-wave radiation loss, the urban area emits more long-wave radiation to the atmosphere as it is usually warmer than its environs at night. The long-wave radiation emitted down in the lower atmosphere is also greater in urban areas because of overlying pollution layer. Therefore, the changes in the long-wave radiation fluxes tend to oppose each other. Again, similar to the net short-wave radiation, urban/rural differences of the net long-wave radiation are small [Oke 1992].

Direct measurements of the long-wave intensity have been difficult to make and many equations have been developed to describe it. There are two different approaches for estimating atmospheric radiation. The first assumes that the atmosphere is a black-body, then the atmospheric radiation is estimated in terms of the effective sky temperature and according to Stefan-Boltzmann law:

$$Q_{Ld} = \sigma T_{sky}^4 \quad (2.1)$$

where Q_{Ld} = long-wave radiation received from the atmosphere (W/m^2), σ = Stefan-Boltzmann constant ($= 5.67 \times 10^{-8} \text{ W}/\text{m}^2\text{K}^4$) and T_{sky} = effective sky temperature (K). The second approach for estimating the atmospheric radiation is based on ambient air temperature and atmospheric emissivity according to the following equation:

$$Q_{Ld} = \epsilon \sigma T^4 \quad (2.2)$$

where T = air temperature (K), ϵ = atmospheric emissivity. As it is much simpler to calculate atmospheric emissivity than effective sky temperature, Equation 2.2 is used in this research (see Section 4.2.2).

The contribution of the net outgoing long-wave radiation flux to air cooling is affected by the neighbourhood geometry. Obstruction of urban canopy layer (UCL) surfaces from the sky temperature sink for long-wave

radiation exchange is usually represented by the sky view factor (SVF). A view factor is defined as a geometric ratio that expresses the fraction of the radiation output from one surface that is intercepted by another. It is a dimensionless number between zero and unity. The view factors (F) for infinitely long canyons are given by two generic equations [Sioufi 1987 : 157] one for the view factor between two symmetrical parallel surfaces and the second the view factor between two perpendicular surfaces (figure 2.3).

$$F_{1-2} = F_{2-1} = \sqrt{1 + H^2} - H \tag{2.3}$$

where $H = h/w$, h = spacing between the two plates, and w = width of each of the two plates.

$$F_{1-2} = 0.5 (1 + H - \sqrt{1 + H^2}) \tag{2.4}$$

where $H = h/w$, h = width of plate A_2 , and w = width of plate A_1 . These two view factors constitute the canyon view factor, and hence, the remainder is the sky view factor ($SVF = 1 - F_{\text{canyon}}$). However, the real world is usually not symmetrical and certainly is not infinite.

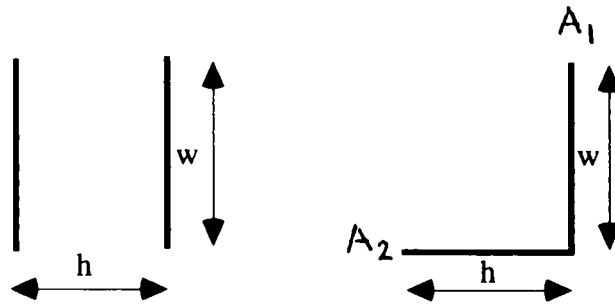


Figure 2.3 Schematic diagram of two symmetrical parallel surfaces and two perpendicular surfaces

The sky view factor is the ratio of the radiation received by a planar surface from the sky to that received from the entire hemispheric radiating environment. Sky view factors in urban environments may be determined by a number of methods as reported by Watson and Johnson

"Analytically—where it is calculated directly once angles from the planar surface to the tops and sides of surrounding buildings are known...Photographically—where a fish-eye lens photograph is used to project the hemispherical radiating environment onto a circular image plane...Video imagery—where a video image either of a fish-

eye lens photograph or directly from a video camera equipped with a fish eye lens is digitised and analysed to distinguish between sky and buildings, thereby determining the sky view factor." [Watson & Johnson 1987: 193].

2.1.3 Net Radiation

The net radiation is the difference between total upward and downward radiation fluxes and is a measure of the energy available at the ground surface. It depends on all factors which influence the radiation fluxes—such as the sun's elevation, the cloudiness, albedo, the temperature and humidity of the atmosphere and the altitude. Daily mean net radiation is positive during summer, reaching its peak value at about the time of the summer solstice. In winter, the daily mean net radiation is negative since daytime solar energy receipts are low and the nights are long [Rosenberg 1974]. The net of all the fluxes of radiant energy is positive by day and negative at night, and can be written as:

$$Q_n = (Q_{dir} + Q_{dif}) (1 - \alpha) + Q_{Ld} - Q_{Lu} \quad (2.5)$$

where Q_{dir} = direct short wave radiation, Q_{dif} = diffuse short wave radiation, α = urban surface albedo (solar reflectivity), Q_{Ld} = long wave radiation received from the atmosphere, and Q_{Lu} = long wave radiation emitted upwards by the urban surfaces.

The radiation fluxes at the ground are much reduced at the poles than at the equator. The net radiation flux tends to be positive towards the equator and negative towards the poles. These differences between the net radiation fluxes make the overall net radiation flux less until it eventually reached zero. The overall *balance* between incoming and outgoing radiation covers variations with latitude. The annual short-wave input of radiant energy exceeds the long-wave loss at latitudes less than about 40° latitude, with a corresponding deficit of heating at higher latitudes [Linacre & Hobbs 1977]. Simple regression models relating net and solar radiation have been developed—for example Linacre's empirical equation [Rosenberg 1974 : 38]:

$$Q_n = (1 - \alpha) Q_s - 16 \times 10^{-4} (0.2 + 0.8 n/N) (100 - T) \quad (2.6)$$

where Q_s = total global radiation (W/m^2), n/N = percent possible sunshine, and T = temperature.

2.2 SOLAR ACCESS/SHADING

Solar radiation received by unit area of surfaces (irradiation) within urban canyons is of major significance to the efficiency of solar collector systems in urban environments, to the heat budgets of the buildings flanking the canyons and, hence, to the energy costs of heating and/or cooling them. In addition, solar access could be important to the day-lighting of building interiors, to illumination levels on the street and to the radiation budgets of humans and vegetation at street level [Arnfield 1990]. For the purpose of this thesis, solar access is studied in terms of its impact on the energy needs for internal climate control.

The approach to improving thermal environments varies with season. In the hot season, shading is one of the goals for reducing thermal loads and producing more hospitable urban environments than the macroclimate in which they are built. Shading improves outdoor thermal conditions by reducing the amount of solar radiation input to the environments. Therefore, the outdoor ambient temperature and the thermal loads on buildings are reduced. Shading strategies include the use of architectural and urban shading. Despite the variability of urban shading strategies (such as opposite buildings, awnings, corbels, arcades and vegetation), this thesis focuses only on shading by opposite buildings.

Providing solar access to each site is one of the goals in the cold season. Solar radiation reaching a site improves the microclimate by raising surface temperatures, thus counter-acting the cold ambient air temperatures. In these days, for reasons like the availability of land and the cost of services and energy, cities in temperate and cool climates may find it difficult to apply solar access regulations particularly in the city centre. Furthermore, there are urban consolidation strategies directed, in Australia, at reducing the size of new allotments, zoning newly developed areas to allow more blocks of dwellings and town-houses to be built, and re-zoning established residential areas to encourage houses to be replaced by medium- and high-density developments [Ballinger 1992]. The likely impact of these strategies needs further investigation, as whether and to

what extent it would affect the residential energy use for climate control in these developments.

2.2.1 Levels of Solar Access

In the case of an urban canyon, that is adopted in this research, solar access can be categorised, according to the level at which access is provided, into three categories: ground, wall and roof.

Ground access level is where an urban street or park is protected from shading by other buildings and vegetation in certain times. The most logical period for ground solar access to mixed-use streets is lunchtime (2 hours from 12 noon to 2 pm Standard Time) [Hayman 1988]. Figure 2.4 shows an application of that level in Adelaide (c. 35°S) for different street orientations. To provide two hours solar access to one of the sidewalks, a street aspect ratio between 0.5 - 1.0 is needed. This level of solar access is a major component in the energy budget of the canyon floor and, as such, will play an important role in the thermal and moisture status of low vegetation at street level, in the thermal stress placed on paving materials and in the general illumination level for pedestrians and traffic within the canyon.

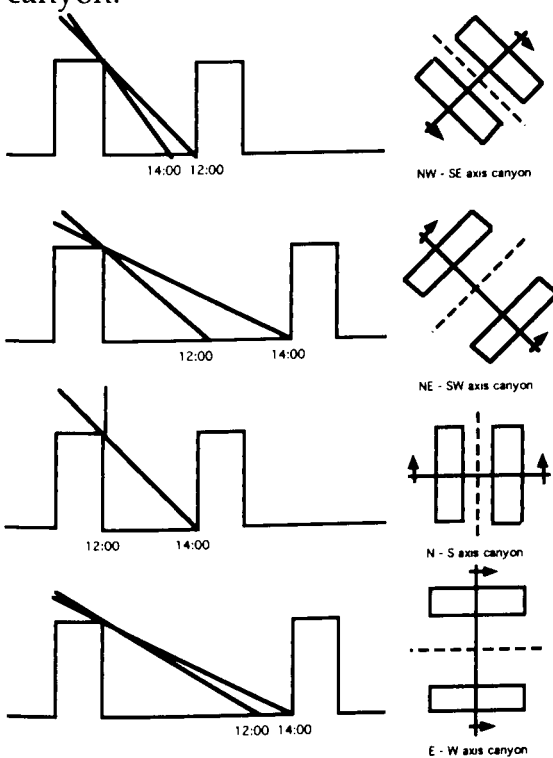


Figure 2.4 Ground solar access for differently oriented streets in Adelaide (winter solstice)

Wall solar access is the second level of access and is a concern of this research. This level refers to the protection from shadows, if possible, in mid-winter - in other words, allowing the sun to penetrate buildings in certain times throughout the year. It is suggested to be between 9 am and 3 pm in mid-winter [Kay *et al.* 1982]. Wall solar access is a significant component in the energy budgets of buildings and affects the costs of heating and cooling them to maintain a comfortable environment for human activities within. Moreover, it may affect the day-lighting of interior building spaces through fenestration.

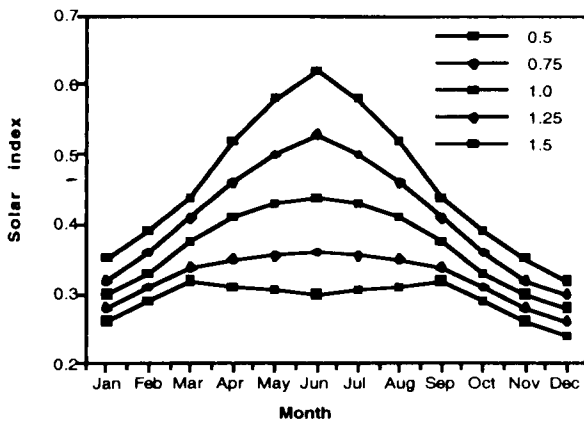


Figure 2.5 Monthly average wall solar access indices by street aspect ratio (Lat. 35° S) [Data from Arnfield 1990: 123]

In a numerical simulation, Arnfield [1990] explored the dependence of irradiance on the urban street facets on aspect ratio and season. The results are presented in street wall, floor and top solar access indices that are the relevant irradiances divided by the unobstructed global solar irradiance on a horizontal surface (I_G). Wall access indices are smaller in the high sun season, so that wall irradiance will not increase as much from winter to summer as will (I_G), a desirable attribute in the temperate climates where buildings may require heating in winter and cooling in summer. Figure 2.5 shows the average monthly wall access indices by aspect ratio at latitude 35° South.

There is a third level of solar access, roof access which aims to protect roof solar collector systems from shading at certain times. Although this level of solar access allows maximum density to be achieved, it hinders some options for future development. The definition of roof access is

particularly dependent upon the definition of the solar collector (whether passive or active). In this sense, it is relevant to domestic solar water heating and passive building design applications, besides active space heating and day-lighting applications.

Solar access legislation could be related to the development density as the Australia Energy in Building Consultative Committee points out

"In selecting a suitable system of solar access protection, it will be necessary for the level of protection provided in a given neighbourhood to be related to the density of development likely to occur in that neighbourhood. Thus, in areas where only low-rise development is expected, it would be reasonable to provide protection for roof-top collectors and north-facing vertical wall (passive) systems. In areas where high-rise development is common, only roof-top protection could reasonably be provided." [EBCC 1984: 7].

As this thesis is concerned with medium-density developments, wall solar access will be considered the level of access assigned to these developments.

2.2.2 Solar Access Techniques

There are two different technical methods for protection of solar access: shadowing and total radiation. The former is by far the most commonly used technique for protecting a solar collector from overshadowing by a proposed development at critical times of the year. This traditional method inherently considers only the direct radiation from the sun, ignoring the contribution of the diffuse and reflected radiation. The importance of the diffuse radiation should be highlighted; as it represents a considerable ratio of the total (direct and diffuse) radiation—for example it is between 20% - 40% in Adelaide. Any method for solar access protection which is based on shadowing considerations clearly accounts only for the direct component of radiation and, as such, overestimates the real effect of any obstruction [EBCC 1984].

Shadowing technique

A system of solar access protection should be constructed for ensuring a reasonable balance between the rights of a site-owner to effectively use a solar system and the rights of neighbouring land-owners to adequately

develop their properties. In this respect, concepts like solar envelope and fence, which were originally developed in the United States, are applicable. A solar envelope defines the limiting volume for development of a site to provide nominated levels of solar access to adjacent sites [Knowles 1981]. The solar envelope is a feasible protection mechanism to guide urban development if suitable criteria for solar access and implementation are selected. The limits imposed by the envelope can be incorporated into planning codes using conventional indicators such as plot ratios and building heights and lines.

Different factors have a direct influence on the volume enclosed by the envelope, such as periods of solar access and urban grid orientations. The minimum duration of access ranges from 2 to 6 hours based on building density and type. Solar access is preferably required within the six hours of useful insolation each day of the year (from 9 am to 3 pm). Various grid orientations produce solar envelopes with different bulks. Solar envelopes over plots with frontages on streets running E-W have considerably less bulk than those on streets running N-S. Street grids with intermediate orientations (NE/SW-NW/SE) produce envelopes with the least bulk [Knowles 1981].

A related concept is that of the hypothetical solar fence which was pioneered in Boulder, Colorado. For each allotment to be protected, a solar fence which completely encircles the allotment is hypothesised. This fence is vertical, uniformly opaque and of negligible thickness. A development would be prohibited in other allotments if they shade the allotment concerned to a greater degree between 10 am and 2 pm (solar time) on a clear winter solstice day than would a solar fence [Danielson 1982]. The height prescribed for the solar fence varies according to the building density where it is about 3.5 m within outer residential areas and 7 m within inner city zones. The technique will produce similar results as that of the solar envelope. However, it is claimed to be much easier to understand.

Limits of accuracy of shadowing methods

Graphical shadowing methods are limited in their accuracy due to systematic and random errors [Hayman 1989]. These errors are associated with calculation and presentation of the solar angles. Systematic errors could appear due to lack of information for a specific location, the

difference between solar time and local standard time, and solar time variation within a year and between years. The total systematic errors could be significant in some methods, particularly if they are to be applied to a tall structure. On the other hand, computer methods using an analytical approach offer greater accuracy but they do not consider the full effect of leap year variation. In addition, computer-based studies are dependent upon the accuracy of the algorithm used.

Total radiation technique

Providing reasonable estimates are available for direct and diffuse solar radiation, an estimate of the actual level of radiation reduction on a solar collector system due to a proposed development of arbitrary geometry is, in principle, a simple technique. Such a technique could be programmed for a micro-computer for rapid and accurate calculations. The main feature of this technique is that it involves the total radiation incident on a solar collector system rather than simply the direct component. In addition, it does not put arbitrary restrictions on the placement or form of proposed development as do the shadowing techniques.

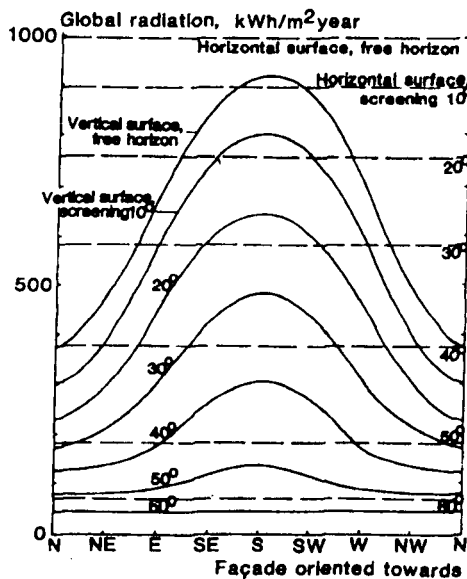


Figure 2.6 Effects of surface orientation and local screening on annual global radiation in Sweden [Taesler 1988: 80]

A technique of this type has been developed at the Swedish Meteorological and Hydrological Institute [Taesler 1988]. The technique uses the screening level in conjunction with recorded weather data to assess solar radiation conditions in local environments. It calculates

screening caused by surrounding topography, buildings and trees. The screening is evaluated as elevation angles in 8 compass directions around the tested point. The mean global radiation on differently inclined surfaces is affected by both the screening and orientation. In the case of a uniform screening, the global radiation for vertical surfaces is far less than that for horizontal surfaces as a result of the partly obstructed sky. Figure 2.6 shows the dependence of annual global radiation on screening and orientation. The effect of orientation on the global radiation is weakened with increasing the screening until it diminishes with screening of more than 60° .

Computer-aided design of solar access controls enables rapid and accurate calculations. A computer program of this type has been written at the University of Adelaide [Williamson 1986]. The following are considered as main elements of this program: it applies to existing solar collector systems; any new development on an adjacent land is required not to reduce the incident solar radiation by more than 5%; and all proposed objects below the height of a hypothetical solar fence will automatically comply with the requirements without any further calculations. This program has been further developed, few years later, to calculate solar heat gains through windows (SHADING program). In this thesis, this program is used to assess the impact of urban geometry on solar heat gains (see Section 6.1.1) [Williamson et al. 1993a].

These techniques are intended to optimise mid-winter solar access, however, the design problem of the research is based on optimising access and shading in different seasons. Therefore, solar access techniques might be considered a one-sided approach to the problem. It can be argued that solar access should be the objective, as shading can be achieved by other strategies rather than urban (namely architectural). These strategies are good for reducing or eliminating solar radiation received on a particular building surface. However, they have no influence on ambient air temperature that could be reduced by urban shading (as shown in Section 4.2.1). This gives urban shading strategy a double-sided advantage as it contributes to reduce solar radiation input and ambient air temperature.

In this case, a solar access technique could be used to determine the right distance between opposite buildings flanking the street, which ensures protection from shadows in particular times. This is done by a shadowing

method and forms a base case for investigating the impact of the distance between buildings on solar access to a particular building in different seasons. A total radiation technique is used to estimate the extent to which radiation received on a building is obstructed by opposite buildings when the distance between them gets smaller. This technique is annexed to a building energy simulation program as a solar obstruction model.

2.3 SOLAR OBSTRUCTION MODEL

Meteorological sunshine data can be converted to radiation received at a particular spot by accounting for obstructions which are immediately adjacent to it. These obstructions will cast shadows in bright sunshine or reduce diffuse radiation on cloudy days. The solar obstruction routine PCSHAD (annexed to TEMPAL the building energy simulation program) used in this thesis exemplifies this type of technique. Program PCSHAD was developed by T. J. Williamson at the University of Adelaide. This program uses the computational techniques of ray tracing to estimate radiation on surfaces and is used primarily to determine the effects of shading on radiation received on building surfaces.

Input data into PCSHAD includes surfaces and obstructions geometry in 3-dimensions, which cover surface area, orientation and inclination. Using the altitude and azimuth of the sun, it determines the hourly shaded area of the building surfaces (opaque and diathermic) by the obstructions. In addition, it calculates different view factors between the surface and the sky, ground and obstructions.

The output of this model is, then, used in TEMPAL to determine the adjusted direct and diffuse radiation on the building surfaces. The amount of adjustment is also dependent upon the type of obstruction, ranging from solid objects to trees of varying transmissivities. Diffuse radiation is calculated on the basis of the sky and reflected radiation from surrounding objects (reflected sky diffuse and direct radiation). The computation is for unit area of unobstructed external surface and for radiation transmitted through unit area of the nominated glass type in four components—direct and diffuse transmitted and direct and diffuse absorbed and re-radiated and convected into the space [Coldicutt 1985].

Controlling Wind Field

3.1 WIND FIELD CHARACTERISTICS	34
3.1.1 Urban Wind Speed	34
3.1.2 Wind Turbulence	37
3.2 URBAN WIND CONDITIONS	37
3.2.1 Wind Shelter	37
3.2.2 Urban Ventilation	40
3.3 VENTILATION AND INFILTRATION	44
3.3.1 Airflow caused by Wind	45
3.3.2 Airflow caused by Buoyancy	49
3.3.3 Airflow caused by Both Forces	49
3.4 AIR FLOW MODEL	51

The airflow patterns around and above buildings are fundamental to nearly all the meteorological processes occurring in urban areas. They affect the temperature and the humidity as well as the air quality in a city. Urban development has a complex effect on wind. Overall, it slows wind down, making cities more susceptible to stagnant air. However, increasing the surface roughness makes the wind gustier and more filled with dust and contaminants. In either case, the people on the street may end up with eye discomfort. This chapter describes urban wind field and researches predictive airflow models to propose a ventilation/infiltration model suitable for the purposes of this research.

3.1 WIND FIELD CHARACTERISTICS

When wind flowing over a rural area approaches the boundaries of an urban area, it encounters a higher surface roughness created by the buildings. The increased flow resistance resulting from the higher roughness decelerates the flow at the urban canopy level [Givoni 1989]. The air flow above and around the buildings is characterised by a lower average speed but higher speed variations (turbulence) as compared to the wind flow over open rural areas. Above the roof-level, there is a sharp increase in the wind speed until the wind reaches the speed it has in the open country at the same height.

When the wind is calm or light in the surrounding rural areas, the heat island of the city generates an air flow driven by urban-rural temperature gradients. The warm air over the city centre rises up and moves outwards. This warm air is replaced by a cooler air flow from the surrounding country which converges near the ground and moves towards the centre. However, these heat island winds are relatively weak (under 4 m/s) and are quickly slowed down over the city roughness [Chandler 1976].

3.1.1 Urban Wind Speed

The wind field is characterised by two parameters: the vertical profile of the mean wind speed and the turbulence spectrum. The pattern of wind speed with elevation above a surface is known as the wind speed profile. With knowledge of wind speed at a fixed or reference level, it is possible

to estimate wind speed at other levels. The mean horizontal wind speed profile is related to the gradient wind speed. This gradient wind is the regional (undisturbed) wind which is generated by differences in the atmospheric pressure. The speed of the gradient wind decreases with reducing height as a result from the friction with the Earth's surface.

Models have been developed for describing the vertical profile of the wind speed. The urban effect on the wind speed is expressed by modifications of the parameters of these models. A parameter used by some models, which is greatly affected by the urban structure, is the aerodynamic roughness. The surface roughness length is an indicator of the drag effect of this surface on the wind flow. At locations upwind of a change in surface roughness, the wind speed profile (Figure 3.1) is assumed to be fully developed and well represented by Landsberg's logarithmic law:

$$U_z = (u^* / k) \ln (z / z_0) \quad (3.1)$$

where U_z = mean wind speed at height z (m/s), u^* = characteristic friction velocity (m/s), k = Von Karman's constant (0.4), and z_0 = surface roughness length (m). For example, a low-density urban area can have roughness lengths around 0.5 m, a medium-density urban area's roughness length can be about 0.7 m and a high-density urban area can have roughness lengths up to 10 m [Landsberg 1981].

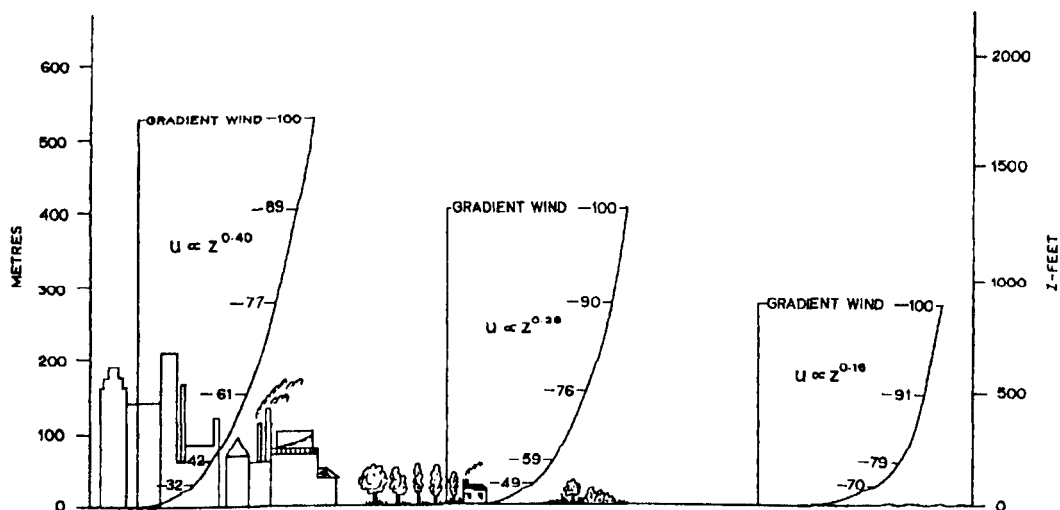


Figure 3.1 Diagrammatic mean horizontal wind velocity profiles above urban, rural and sea surfaces (Chandler 1976: 18)

Landsberg's model has a theoretical limitation, which results in a zero wind speed at the height of the roughness parameter that is not experienced in reality. A simple model developed by Davenport [1960] does not have this limitation and is given by the expression:

$$U_z / U_{zG} = (z / z_G)^\varphi \quad (3.2)$$

where U_z = wind speed at height z (m/s), U_{zG} = gradient wind speed (m/s), z = height at which speed is calculated (m), z_G = gradient height (m), and φ = mean speed exponent. Gradient height and mean speed exponent are functions of the ground roughness. Nevertheless, the wind profile described by this power law does not represent the realistic wind conditions near the ground level (up to about 5-10m) because of the high turbulence of the urban wind at that layer.

Local wind conditions can be modified by the presence of vegetation, buildings and built screens. The shielding effects of these obstacles produce large-scale turbulence that not only reduces effective wind speed but also alters wind direction. Therefore, meteorological wind speed data must be modified carefully when applied to low buildings. De Gids *et al.* [1977] noted that, in the cool-temperate climate of The Hague, there is no clear linear relationship between the meteorological wind velocity and the measured ventilation rate. When the wind velocity is corrected for the local roughness of the building in site, it is possible to find such relation. This is due to taking into account the influence of surroundings on the wind velocity at the location.

Australian Standard AS 1170.2 [1989] gives design wind speeds that vary with terrain and height. For example, at a height of 10 m (reference height) the predicted wind speed in an urban area is 0.7 times the speed in a suburban area (where urban meteorological stations are normally located). The former is defined as open terrain with well scattered obstacles having heights generally 1.5 to 10m, while the latter is a terrain with numerous closely spaced obstacles having the size of domestic houses. Therefore, wind speed can be corrected for the local roughness if it is multiplied by a suitable wind factor. These wind multipliers are used in this research to adjust meteorological wind speed to be site-specific.

3.1.2 Wind Turbulence

The turbulence or gustiness is defined as the standard deviation or root-mean-square value of deviations of the instantaneous speed from the mean [Aynsley *et al.* 1977]. The relative gustiness or the intensity of turbulence is the turbulence normalised to the mean wind speed. It should be pointed out that both quantities, the mean speed and the gustiness, are required for an adequate representation of the wind effects. Therefore, the term equivalent wind speed (U_e) is introduced, which denotes the mean hourly wind speed adjusted to account for the expected turbulence intensity at the site. The equivalent wind speed is calculated by multiplying the mean velocity at the point (U) by a weighting factor according to the following formula:

$$U_e = U(2 \sigma_u + 0.7) \quad (3.3)$$

where σ_u is the turbulence intensity, and for turbulence intensities less than 0.15, U_e is taken to be equal to U [Bosselmann & Arens 1991]. As turbulence intensity is not available in weather data used in this research, wind speed will not be adjusted to account for turbulence.

3.2 URBAN WIND CONDITIONS

The wind conditions within the urban area are a major factor affecting the comfort of the pedestrians and dwellers either in cold or warm climates. The urban wind conditions determine the potential for natural ventilation of buildings and the wind exposure of the pedestrians outside the buildings. In cold or temperate climates, heat losses resulting from uncontrolled ventilation (infiltration) of buildings constitute a large part of the total heat load. In addition, pedestrians in the street need a wind shelter against the chilling effect of wind in cold seasons. On the other hand, wind-driven natural ventilation can be used to improve human thermal comfort in warm seasons and reduce the need for mechanical cooling and hence reduce cooling energy use in buildings.

3.2.1 Wind Shelter

The impact of wind on convective heat losses from buildings ranges from slight to large depending on the building insulation and exposure. Where

this impact on well-insulated parts of a building is generally insignificant, it makes a difference with poorly insulated surfaces such as glass areas on greenhouses and solar collectors. In addition, the difference in energy consumption between a normally insulated building in a sheltered and very exposed position could be remarkable. Keeble *et al.* [1990] reported on a study undertaken in Ireland showing space-heating energy saving of around 5% for wind shelter effects only. However, the height of windbreak used was only two metres, protecting single-storey buildings.

The wind statistics from a nearby weather station should never be used unmodified, since every place has its unique surroundings. Several methods have been developed for calculating, in any positions, the impact of the surroundings on wind conditions [Arens *et al.* 1985, Glaumann & Westerberg 1991]. These methods, to estimate windiness, take base velocities in eight wind directions as median velocities for an unobstructed locality (regional winds). Then, the base velocities are corrected for surface roughness in different directions, and must also, where relevant, be corrected with reference to the topography of the immediate surroundings. Finally, windiness is estimated as a result of the height of the building's projection above its surroundings in different directions, since height is the most influential individual factor.

Planning with reference to the wind in the outdoor environment needs to take account of subjective experience of the wind. Roughly speaking, wind speeds above 5 m/s begin to be a nuisance, with hair and clothing fluttering about, dust and paper whirling up from the ground and sand escaping from the children's sandpits [Bosselmann & Arens 1991]. This value for wind speed is considered the limit above which building windows are assumed to be closed in the ventilation control strategy adopted in this research (see Section 3.4).

Assessment of shelter requirements

Wind comfort criteria and guidelines for the pedestrian level have recently attracted the attention of researchers and city governments particularly in North America, Scandinavia and New Zealand. Some cities adopted a wind ordinance containing specific legal and technical requirements for compliance. Since the wind speed fluctuation is fast, it is probably more important how often rather than for how long the wind speed exceeds an annoying level. Wind engineering has indicated that

gust wind velocities typically have the greatest wind force impact on pedestrians. At the National Swedish Institute for Building Research, the following expression for estimating wind perception is proposed:

$$U_s = 0.85 U (1 + \sigma_u) \quad (3.4)$$

where U_s is standard mean wind speed, which is the mean wind speed in an open field (standard conditions $\sigma_u \cong 0.2$) corresponding to mean wind speed in any environment with respect to wind perception. This expression is preferably used for classifying outdoor areas with respect to wind comfort [Glaumann & Westerberg 1991].

The concept of a wind-chill index has found considerable application in terms of human comfort outdoors. Wind-chill is based on wind velocity and temperature, it combines wind velocity and air temperature to determine the chilling effect of the two combined elements on exposed skin. Evaluation of the wind-chill component is currently based on comfortable conditions occurring at least 80% of the time [Prior & Keeble 1991]. It is possible to represent wind-chill in terms of an index of the rate of heat loss (H) in kcal/m²h of an object using the following formula:

$$H = (h_c + h_v) (t_s - t_a) \quad (3.5)$$

where h_c and h_v are heat transfer coefficients of conduction and convection in kcal/m²h°C respectively, t_s is the surface temperature of the object and t_a is the ambient air temperature in °C.

A comprehensive outdoor comfort criterion, proposed at Delft University of Technology, includes temperature, solar radiation, wind velocity and wind turbulence [Tacken 1989]. These criteria suggest that with temperatures between 18 - 23°C and wind velocity of less than 2.5 m/s, depending upon the amount of solar radiation, the climate is usually suitable for outdoor relaxation. An estimate of the perception of climate is attainable using the following formula:

$$\text{perception of climate} = - 0.329 + 0.215 t - 0.6 U + 0.0024 Q \quad (3.6)$$

where t = air temperature ($^{\circ}\text{C}$), U = wind speed (m/s) and Q = solar irradiation of land area (W/m^2). A score of 4.0 is considered the lower limit for a comfortable climate.

The aforementioned expressions have no direct relationship to the urban configuration. There is not a full relationship between wind speed reduction and measures of canyon geometry. However, Oke [1988] suggests the simple linear form:

$$U_{\text{canyon}} = p U_{\text{roof}} \quad (3.7)$$

where U is the mean horizontal wind speed and p is diminution factor which depends on H/W and the measurement levels. It is shown that $p \cong 2/3$ for wind speeds up to 5 m/s, with $H/W \cong 1$, and canyon centre and above-roof measurement at heights of about 0.06 H and 1.2 H respectively. Presumably at smaller H/W , p approaches unity and shelter is lost. It is suggested that $H/W \cong 0.65$ should ensure considerable protection and, therefore, a minimum acceptable value may be at about 0.4. This value is used as a base line for investigating the wind shelter effects on building ventilation heat losses (see Section 6.1.2).

3.2.2 Urban Ventilation

Urban characteristics have a great impact on the urban wind conditions. These characteristics include orientation of the streets with regard to the wind direction, building density and height, and distribution of high-rise buildings among lower ones. Urban density may affect the ventilation conditions in the street and thus also the potential for natural ventilation of buildings. It is usually assumed that an increase in building density reduces the air flow in an urban area, as a result of increased friction near the ground. However, this influence depends mainly on various physical details of urban space, including differences in heights of neighbouring buildings and their orientation with respect to the wind direction.

The dimensions, shape, and spacing of buildings also influence wind conditions. A combination of buildings can deflect the wind or can channel it. Where buildings converge in the direction of the flow, the wind speed is locally increased; where the gap between buildings gets wider in the direction of the flow, the wind speed is decreased. A city of

pyramidal shape, with building elevations gradually increasing from the edge to the centre, (for example Adelaide City) will cause less drag on the wind than one with a line of high rises at the edge of the city. Studying a single wind direction (prevailing wind direction) does not give a complete determination of the wind environment found in the built-up area. This is because the wind pattern at a particular site depends upon several factors such as wind direction, surrounding topography, and the form of buildings immediately surrounding the site.

Givoni [1989] reported on wind-tunnel research carried out on the effects of building density, determined by average height of buildings and the distance between them, on the wind speed in the open spaces between the buildings. With buildings of the same height placed normal to the wind (windward side at a right-angle to the direction of the flow), it has been found that urban density has a relatively small effect, because even under low urban density conditions the free wind flow is blocked by the buildings. In addition, the quantitative effect of high rise buildings, interspersed among lower buildings, on the air speed in the streets around them has been investigated. It has been found that they increased significantly the air speed in the streets, however, it depends mainly on street aspect ratio.

In the same study, the wind speeds have been measured in the open spaces between nine rows of buildings where the height to spacing ratio was changed from 1:3 to 3:1. A significantly higher speed has been measured in the first space (between the first and second row of buildings) and to a lesser degree in the second space. After the second row the relative speed has been gradually stabilised, with little difference between the different spaces. This pattern has been observed in all the combinations of height of buildings and width of space between them. When wind blowing over an open space encounters a steep resistance in the form of a series of long buildings placed normal to its direction, the highest suction is formed above and immediately behind the first line of buildings. This suction generates the turbulent air flow between the buildings, apparently in proportion to the pressure differences.

Katayama *et al.* [1988] studied the wind speed distribution in urban canyons using a wind tunnel. The distribution of the ratio of mean airflow speed to mean reference speed (U/U_r) in the urban canyon is

shown in Figure 3.2. The airflow speed at height of 5 mm from the wind tunnel floor (U) is equivalent to 2m from the ground surface in full scale. The airflow speed in the urban canyon is smaller than that above the street; the difference between them increases as building density (BV) or number of building storeys (F) increases. The airflow speed right behind the building is especially small. The wind speed in the urban canyon increases and is nearly equal to that above the street when the angle between the wind and the building axis (θ) = 45° . It is almost twice as fast as that in the case when $\theta = 90^\circ$ (the wind flow is normal to the building).

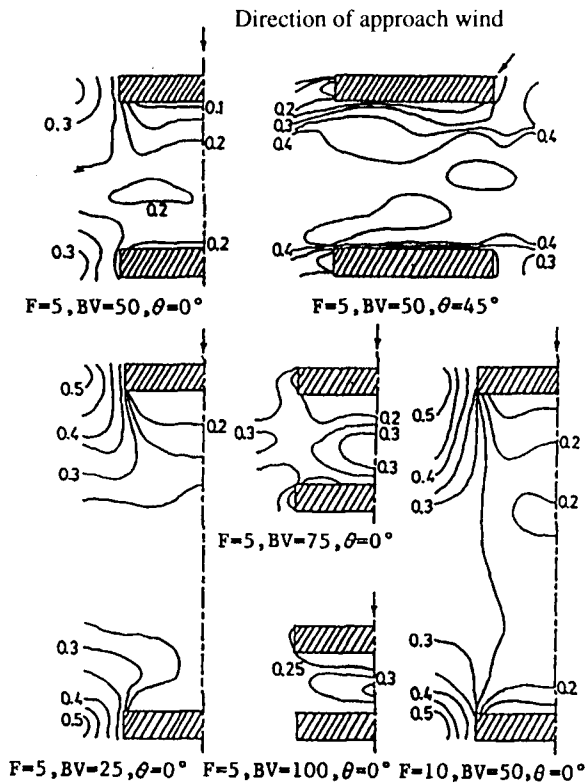


Figure 3.2 Wind speed distributions between two buildings by wind tunnel tests (U/U_T) (Katayama *et al.* 1988: 656)

Bauman *et al.* [1988] describe the results of a wind tunnel investigation of wind pressure distributions over an attached two-storey housing unit contained in long building rows. Surface pressure measurements were made on a scale model as a function of wind direction, spacing between opposite building rows, and building geometry. In urban areas, where buildings are grouped closely together, these surface pressures are strongly influenced by the surrounding buildings. The sheltering effect of the opposite buildings can make it more difficult to obtain large enough

pressure differences across a building necessary to produce adequate ventilation airflow rates. It is indicated that, at upwind spacing between opposite buildings equal to or greater than building height, the ventilation potential is negligible.

Air movement modelling

Field studies are usually carried out on a small scale because of the difficulties inherent to the establishment of a comprehensive network for the collection of urban climatological data in terms of the expense and inconvenience to inhabitants. Approaches to observation of air flow within canyons vary considerably; they include visual tracers and measurements of vertical wind speeds, tracked tracer balloons, and two-dimensional ultrasonic anemometers [Johnson *et al.* 1991]. Air movements within the urban canopy layer (UCL) are extremely complex regarding both mean flow and turbulence characteristics. Wind tunnels as well as numerical modelling have been used to simulate the micro-scale flow patterns [Taesler 1984].

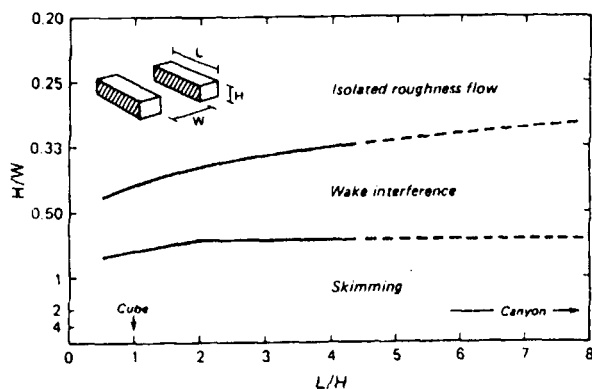


Figure 3.3 Thresholds for flow patterns in urban canyons as functions of canyon H/W and L/H ratios (Oke 1988: 105)

Despite the advantages of wind tunnel programs over field observations, there are some problems with wind tunnel modelling. One of these problems is the need to achieve similarity to gain adequate representation of the flow pattern. In addition, friction on the wind tunnel boundaries affects the observed flow. Special consideration must be given to the length of the wind tunnel, as large wind tunnel facilities are required for modelling complex urban flows. Wind tunnel tests can be used to study the dispersion of pollutants as well as the air flow around and within

scale-models. Based on wind tunnel tests, Hussain and Lee [1980] confirmed the existence of three flow patterns—isolated roughness, wake interference and skimming—and established the critical H/W ratios for transition between these patterns (Figure 3.3). Oke explains these flow patterns as functions of building spacing

"When the buildings are relatively widely spaced (...H/W < 0.3 for row buildings) their flow pattern appears almost the same as if they were isolated. At closer spacing (...H/W up to about 0.65) the wake of any building interferes with that of the next downstream leading to a complicated pattern. At spacings closer than these the main flow starts to skim over the building tops and drives a *lee vortex* in the cavity (often a street)...The preceding flow types are found when the wind is normal to the long axis of the street. If the wind is oriented at some other angle the vortex takes on a *cork-screw* motion with an elongation along the street. If the approach flow is parallel to the street the shelter is destroyed and channelling may cause a jetting effect so that speeds are *greater* than the open."
[Oke 1992: 266-7].

Numerical models might offer the sort of flexibility that enables flow patterns in urban areas to be investigated in a way that has hitherto been beyond the scope of field measurements programs. Numerical simulations can be associated by techniques of visual animation which represent useful tools for analysing unsteady flow and diffusion fields around buildings [Murakami 1991]. Numerical models can be used to simulate the major canyon air flow patterns and to illustrate the relationship between canyon geometry and transition from one pattern to another [Hunter *et al.* 1991]. In this research, the results of wind tunnel tests done by others together with simplified numerical models are used to predict ventilation rates in buildings.

3.3 VENTILATION AND INFILTRATION

The word ventilation is derived from the Latin *ventus* (wind), and is an air current, either through open spaces or through the interior of buildings. Natural ventilation, therefore, is a process that exchanges indoor air for outdoor air without mechanical power [Al-Megren 1987]. Natural ventilation is generally caused by two forces—wind and buoyancy. Wind-driven ventilation tends to dominate in summer where there is no significant difference between internal and external air temperatures nor difference in height between inlet and outlet openings in the building

envelope. On the other hand, heating of building interiors in winter creates a significant indoor-outdoor temperature difference that can be used to provide ventilation rates by the stack effect [Aynsley *et al.* 1977].

ASHRAE points out the importance of outdoor air as follows

"Outdoor air that flows through a building either intentionally as ventilation air or unintentionally as infiltration (and exfiltration) is important for two reasons. Outdoor air is often used to dilute indoor air contaminants, and the energy associated with heating or cooling this outdoor air is a significant space-conditioning load. The magnitude of these airflow rates should be known at maximum load to properly size equipment and at average conditions, to properly estimate average or seasonal energy consumption. Minimum air exchange rates need to be known to assure proper control of indoor contaminant levels." [ASHRAE 1989: 23.1].

3.3.1 Airflow caused by Wind

Two techniques can be used to estimate airflow through buildings due to wind; they are wind tunnel tests and wind predictive models. Wind tunnel tests of scale-models determine the ratios of wind speeds at points of interest inside the building to an external reference wind speed at a height for which wind records are available. Predictive models make use of wind pressure differences across a building, size and airflow discharge characteristics of building openings, to estimate volumetric flow rate. The accuracy of air change rate predictions depends upon interrelationships among airflow coefficients, flow exponents, and pressure differences. Nantka [1990] reported that the average percentage difference between the predictions and the results of the measurements are about $\pm 20\%$.

Relative wind speed

The only source for relative wind speed is wind tunnel measurements of points of interest on a scaled model of the buildings. Average wind speed between buildings is reduced relative to free-air upwind speed at the same height. The difference between free-air upwind speed and the wind speed between buildings increases as building density and height increases, or as building spacing decreases. Givoni [1989] reported Paciuk's wind-tunnel research on the effects of building geometry on relative wind speed between buildings, when the buildings of uniform

height are perpendicular to the wind direction. The effects as obtained from the measurements have been expressed by a regression analysis.

$$U_r = 10 + [66 (1 - e^{-0.08 h})] e^{-0.18 D/W} \quad (3.8)$$

where D = distance travelled by the wind (m) = $n(b+W) - 0.5 W$, U_r = relative wind speed (%), b = depth of the buildings (m), n = serial number of the space (downwind), h = height of the buildings (m), and W = width of the space between buildings (m). In many cases, however, the growing sources of wind pressure distribution data make it more convenient and easier to use predictive methods without resorting to wind tunnel tests. Therefore, pressure coefficient is used in this research to predict airflow rates in buildings rather than using relative wind speed.

Discharge coefficient

Airflow rate through openings is mainly dependent on free area of openings, wind speed and discharge coefficient. The ratio between actual airflow rate and theoretical (ideal) flow rate is called discharge coefficient. Dissipation due to viscous friction and blockage of flow area are the main causes of reductions in the velocity below the theoretical flow. The discharge coefficient is a function of Reynolds flow number, shape of the opening and its size with reference to the wall area. Discharge characteristics of large openings like windows are sometimes called the effectiveness or efficiency of openings [Al-Megren 1987]. Discharge coefficients for a variety of openings are available from Aynsley *et al.* [1977: 203].

The *ASHRAE Handbook of Fundamentals* [1989] gives an equation, to estimate airflow rate through inlet openings, of the form:

$$Q = C A U \quad (3.9)$$

where Q = airflow rate (m^3/s), A = area of inlet (m^2), U = wind velocity (m/s), and C = effectiveness of opening. C is assumed to be 0.5 to 0.6 for perpendicular winds and 0.25 to 0.35 for diagonal winds. The equation applies for the case where the area of inlet is the same as the area of outlets. Where they are different, then a correction factor has to be applied. An increase in the airflow caused by excess of one opening over another is up to 35% when the ratio of the outlet to the inlet (or vice-versa)

is about 3. However, the increase in the airflow is not proportional to the added area. Therefore, greatest flow per unit area of openings is obtained when inlets and outlets are equal.

The ASHRAE equation has its simplicity in application, and hence, has its drawbacks in terms of accuracy of prediction. The equation does not account for the influence on the airflow pattern of nearby obstructions, architectural projections or size and proportion of openings. Unlike the ASHRAE equation, Aynsley's method takes into account the effect of each opening in terms of size and discharge coefficient. Aynsley *et al.* [1977] give an equation of the form:

$$Q = C_d A U_z (C_{pw} - C_{pl})^{0.5} \quad (3.10)$$

where U_z = reference wind velocity at a height z (m/s), C_d = discharge coefficient of opening, C_{pl} = leeward pressure coefficient, and C_{pw} = windward pressure coefficient. The permeability coefficient ($C_d A$) for the building is calculated, for any number of openings (n) in series through which the air flows, as:

$$C_d A = ((C_{d1} A_1)^{-2} + (C_{d2} A_2)^{-2} + (C_{d3} A_3)^{-2} + \dots + (C_{dn} A_n)^{-2})^{-0.5} \quad (3.11)$$

Average wind pressure differences at mid wall height give satisfactory estimates of airflow for openings up to 20% of wall area. Disadvantages of this method - as reported by its authors - are:

- when openings are in excess of 20% of the wall area, it becomes difficult to determine the wind pressure difference;
- when the flow is divided into two or more branches, there is difficulty in getting pressure coefficients inside the building; and
- for shapes of buildings other than simple forms, it is incorrect to use the available pressure coefficients.

Pressure coefficient

The ventilation rate due to wind forces is mainly affected by average wind speed, prevailing direction, seasonal and daily variation in speed and direction, and local obstructions such as nearby buildings, hills, trees, and shrubbery. Pressure difference usually results from the wind flow being obstructed and deflected by objects and buildings. Pressure acting on the surface of any building is usually presented in the form of coefficient.

Values of the pressure coefficient (C_p) depend on building shape, wind direction, and the influence of nearby buildings, vegetation, and terrain features. Accurate determination of C_p can be obtained only from wind tunnel model tests of the specific site and building.

The source of pressure distribution data for the building form adopted in this research, namely terrace housing, is that of Bauman *et al.* [1988]. The data was based on wind tunnel tests done at University of California, Berkeley (UCB). It is applicable to an attached low-rise housing unit contained in long building rows, and to semi-infinite urban canyons as it does not consider edge effects. Simplified correlations developed from these tests are used to predict wall pressure coefficients. Using the wind direction and the ratio of building spacing to height, pressure coefficients can be determined by:

$$C_{pw} = 0.095 - 0.519 \cos^2\theta + 0.571 \ln(S) \cos \theta \quad (3.12)$$

$$C_{pl} = -0.602 \cos^2\theta \quad (3.13)$$

where θ = wind approach angle, and S = height-normalised spacing of upwind rows. S is assumed to be between 1- 5, but if $0.25 < S < 1$, then use $S = 1$. Figure 3.4 shows the mean pressure difference between windward and leeward facade for values of S between 1 and 3.

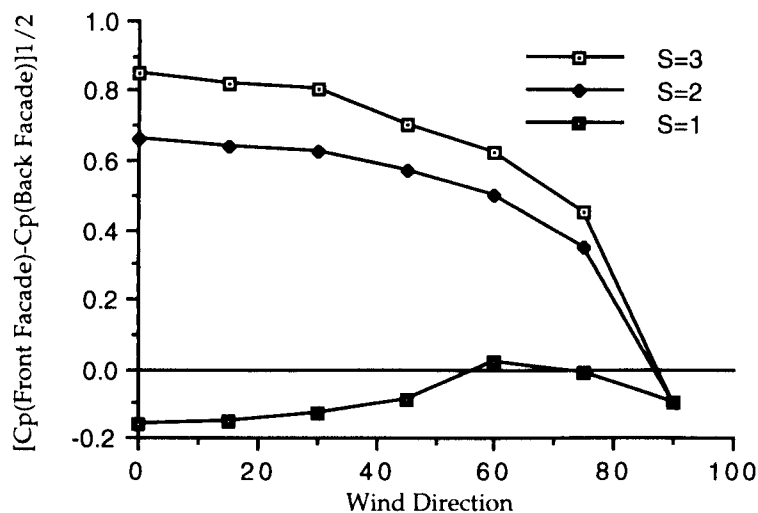


Figure 3.4 Mean pressure difference between windward and leeward facade

3.3.2 Airflow caused by Buoyancy

The key factors that influence stack effect (buoyancy) are height and temperature difference. The stack effect increases linearly with the increase in height between the inlet and outlet. It also increases linearly with the increase in temperature difference between inside and outside air. The buoyancy flow relates to height and temperature in linear fashion, while wind flow relates to the square of wind velocity. In the heating season, buoyancy flow can dominate especially in buildings of more than one storey.

ASHRAE Fundamentals [1989] gives the pressure difference due to the stack effect as follows:

$$\Delta P_T = g (h - h_{NPL}) (\rho_o - \rho_i) \quad (3.14)$$

where g = gravitational acceleration (9.81 m/s^2), h = observation height (m), NPL = neutral pressure difference, and ρ = air density (about 1.2 kg/m^3). Subscripts i = inside and o = outside.

If the openings are uniformly distributed vertically and there is no internal airflow resistance, the NPL is at the midheight of the building. If $\rho_o = \rho T/T_o$, $\rho_i = \rho T/T_i$, $T = 273 \text{ K}$ and $h - h_{NPL} = z$, then the equation is re-written as:

$$\Delta P_T = 273 \rho g z (T_i - T_o) / T_o T_i \quad (3.15)$$

where T = absolute temperature (K). Subscripts i = indoor and o = outdoor. When applying SI units to this equation providing that the indoor and outdoor temperatures are given in degrees Centigrade (namely t_i and t_o) and are not greatly different from 10°C , then the above equation is approximately:

$$\Delta P_T = 0.043 z (t_i - t_o) \quad (3.16)$$

3.3.3 Airflow caused by Both Forces

In a simple case with buoyancy dominant, air flows in to a building at the lower level and out at the upper level. With wind dominant there is a

flow across the building from windward to leeward. In an intermediate situation the flow pattern derives from a combination of these characteristics. Based on a series of measurements in a two-storey house under exposed winter conditions, in which the wind was fairly constant in direction, Wise [1978] calculated the wind speed below which buoyancy dominated as 1.5 m/s. He shows that the relationship between flow rate and wind speed above 1.5 m/s is closely proportional. Below 1.5 m/s wind plays only a secondary role and has a little effect on ventilation rate.

The natural ventilation flow rate is proportional to the square root of the pressure difference of either the wind or stack pressure. Therefore, the combined effect can be considered as the algebraic sum of both effects. This method produces large errors when the stack and wind effects are equal (up to 50%). As mentioned by Givoni [1981], the airflow as a result of the combined effect is slightly higher than it will be with only the greater effect of wind or stack pressure. Instead, pressure addition is physically realistic, simple and has maximum errors of about $\pm 15\%$ which is less than an hourly natural variability measured infiltration [Walker & Wilson 1993]. This method appears to be a good choice for combining independent wind and stack effect flows to estimate their combined effect.

When the building openings are open (cross-ventilation), and hence, the difference between outdoor and indoor temperatures is negligible, then the pressure difference due to stack effect diminishes. When the openings are closed (infiltration), the airflow rate through leakage openings in the building envelope is:

$$Q = L (2 \Delta P / \rho)^{0.5} \quad (3.17)$$

where L is effective leakage area which is estimated to be 3×10^{-4} building envelope area [Wiren 1983], providing that the leakage openings are uniformly distributed over the building surfaces. The combined pressure difference (ΔP) is the sum of the individual pressure difference due to wind and stack effect. Pressure difference due to stack effect (ΔP_T) can be estimated by equation (3.15) and pressure difference due to wind (ΔP_w) can be expressed as [Wiren 1983]:

$$\Delta p_w = \rho U^2 (C_{pw} - C_{pl}) \quad (3.18)$$

All symbols retain their previous meanings.

3.4 AIR FLOW MODEL

A simple algorithm for predicting the infiltration/ventilation rates is adopted in TEMPAL. It is a commonly used simplified procedure derived from measurements in buildings with diverse geometries and window placement:

$$ACH = a + b U \quad (3.19)$$

where ACH = air change rate (hr^{-1}), U = wind speed at a reference height (m/s) -and a and b are empirically determined coefficients. This correlation equation is applicable to a specific building type, namely detached houses, which is different from the modelled building in this research. It is replaced, for the purposes of this research, by the following calculation procedure to make allowance for simulation of some of the most important building characteristics, such as the internal volume and total open areas, in addition to wind direction and local shelter effects.

The combined effect on air flow of the wind and stack effect is, in practice, very complex. However, this research is concerned, in the airflow modelling, with local shelter effects caused by various urban configurations. Therefore, airflow caused by wind is considered to be variable to correct for these surrounding effects. Stack effect while not being ignored is assumed to be constant during the simulations. Air flow caused by stack effect is determined by equation 3.16 and 3.17 providing that the difference between indoor and outdoor temperature is 10°C . All the simulated housing units are assumed to have the same height; therefore, stack effect is not modified by the urban configurations considered in this research.

Since the meteorological data on the weather tape is not obtained at the same site as the buildings being investigated, the data need to be modified to be site-specific. Thus, local shelter effects on the airflow rate by opposite buildings should be considered. For the hypothetical terrace

housing with openings only on two walls, which is the subject of this research, the airflow caused by wind can be determined by equations 3.10 through 3.13. The wind speed is modified to account for terrain roughness based on wind multipliers adopted from AS 1170.2 [1989]. Variations in infiltration/ventilation rates occur due to wind through cracks and vents, due to opening of doors and windows and due to mechanical systems; they are hourly altered in TEMPAL, the building energy simulation program, according to wind speed and user behaviour.

A ventilation control strategy is employed to approximate the user's behaviour. For this study, windows are assumed to be closed if the ambient or indoor temperatures are less than 15 and 20°C respectively (*chilly*), or the wind speed is greater than 5 m/sec (*windy*). In summer, windows are assumed to be open when the indoor temperature is higher than outdoor's, or if relative humidity is greater than 80% associated with temperature less than 30°C (*stuffy*). But in winter, windows are open if relative humidity is greater than 80% associated with temperature greater than 20°C, or the indoor temperature is greater than 26°C and higher than the ambient temperature by 2°C (*overheating*). The simulations assume that when windows have just been opened (open window area is typically 40% of the rough opening in the wall for sliding or hung windows) or closed they will be left unchanged at least 3 hours.

Limitations

The following assumptions affect the sensitivity of the proposed airflow prediction model:

- The model is based on the assumption of quasi-steady flow, which is a necessary and justifiable assumption for an engineering approach to the problem [Etheridge 1988]. Therefore, infiltration associated with pressure fluctuations arising from wind turbulence is neglected.
- Wind pressure is uniform on any given surface, so that only one average coefficient is considered. The error resulting from using only averaged pressure coefficient for each wall in calculating the wind-induced heat loss is < 10% for all wind angles except 90° [Taha 1990].
- Distribution of openings on one wall (or the leakage) is uniform and between walls (the wall distribution) is fixed. These assumptions are valid when wind pressures dominate and for the simple terrace housing considered here. No pressure drop inside building, negligible effects due to partitions.

Temperature Modification

4.1 URBAN AIR TEMPERATURE 54

4.1.1 Heat Island Effect 54

4.2 FACTORS CONTRIBUTING TO THE DEVELOPMENT OF THE URBAN HEAT ISLAND 59

4.2.1 Absorbtion of Short-wave Radiation 59

4.2.2 Long-wave Radiation Loss 61

4.2.3 Turbulent Heat Transport 63

4.2.4 Sensible Heat Storage 64

4.2.5 Evapotranspiration 65

4.2.6 Anthropogenic Heat 68

4.3 TEMPERATURE PREDICTION MODEL 70

4.3.1 The Developed CTTC Model 71

4.3.2 Verifying the Model 72

The outdoor air temperature describes the thermal ambience of a place. It depends on two factors; incoming air flows driven by large-scale weather systems, and local climatic energy inputs. The latter modifies the temperature of the incoming air to a greater or lesser extent, according to the wind speed. When the wind speed is slow, site factors such as the heating of the ground by sunshine and night-time cooling from outgoing long-wave radiation exert a major influence on the air temperature close to the ground. With high wind speeds, the temperature of the incoming air mass is less affected by local factors. This chapter deals with the temperature modification by built-up areas, in order to develop a model for predicting urban air temperatures.

4.1 URBAN AIR TEMPERATURE

In winter, most urban climates are more moderate than those found in suburban or rural areas. The temperature modifications by an urban area are expressed mainly in the heat island phenomenon, especially during calm and clear nights, when the urban air temperature is usually higher than the temperature of the surrounding open country. In big cities, it is actually common to observe nocturnal air temperature 3 - 5 °C higher than in the surrounding areas, and in extreme cases, up to 8 °C higher. During the daytime hours this difference in air temperature between the city and its surrounding area is smaller, about 1 - 2 °C [Givoni 1989].

4.1.1 Heat Island Effect

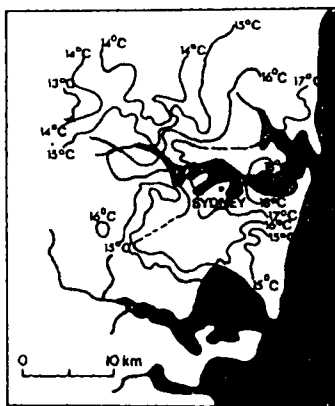


Figure 4.1 Typical isotherms in Sydney as measured at street level at about 1 am on 24 April 1971 (Linacre & Hobbs 1977: 34)

The profile of temperature through a city shows its highest values roughly coincident with the Central Business District (CBD), so that temperatures increase with building density. Measurements in central Sydney have shown temperatures 3 °C hotter than on the outskirts (Figure 4.1) and similar heat islands could exist in most capital Australian cities. The intensity of the heat island is related more to density of buildings rather than to city size [Chandler 1976]. In most cases the density of buildings and energy consuming activities in the centre of cities increase with the size of the city. Therefore, there is also a relationship between the size of the city and the intensity of the heat island of the city centre.

Air temperature variations with distance

Figure 4.2 shows the characteristic variations of air temperature with distance whilst traversing from the countryside to the centre of an urban area under fair weather conditions (calm wind and cloudless sky). Oke explains urban temperature gradients as follows

"The rural/urban boundary exhibits a steep temperature gradient, or *cliff* to the urban heat island. In this area the horizontal gradient may be as great as 4 °C/km. Much of the rest of the urban area appears as a *plateau* of warm air with a steady but weaker horizontal gradient of increasing temperature towards the city centre...the urban core shows a final *peak* to the heat island where the urban maximum temperature is found." [Oke 1992: 289].

Sometimes there would be a number of such peaks each associated with areas of especially dense development; these could be called *heat archipelago*.

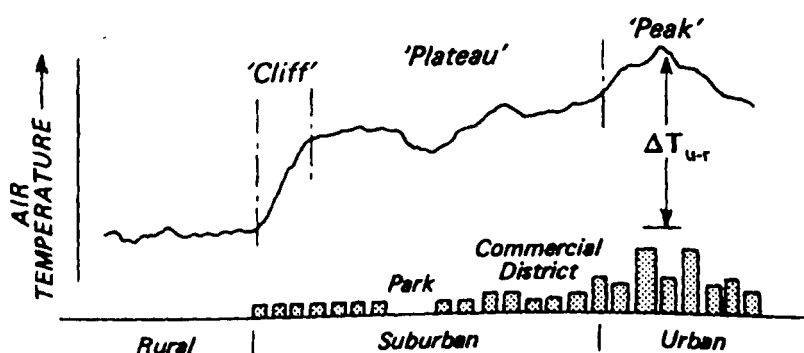


Figure 4.2 Generalised cross-section of a typical urban heat island (Oke 1992: 288)

The temperature profile through the city reflects in its minor fluctuations changes of relief, vegetation and building density. The uniformity of the plateau is interrupted by the influence of distinct intra-urban land-uses such as parks, lakes and open areas (cool), and commercial, industrial or dense building areas (warm). McBoyle [1970] observed and measured the temperature distribution across Hamilton city in New Zealand (Population 65,800). A noticeable rise occurs as a dairy factory is passed within a residential area. This shows that the heat island can be developed even on a relatively small scale urban area.

Heat island statistical models

Heat island development has been studied using full-scale measurements with which scale models have been compared [Oke 1981]. Statistical models have been developed based on field observations. It is difficult to express the planning details of the city in a statistical form to describe the effects of these details on the city's air temperature. Most of the statistical models that deal with the heat island phenomenon express the intensity of the heat island as a function of various meteorological factors such as cloud cover, wind speed, specific humidity, and so on. At night when the heat island is best developed, the intensity of the heat island is inversely related to wind speed (U) and cloud cover. It appears that for a given city with no clouds, the intensity of heat island near sunset is approximately related to $U^{-0.5}$ [Oke 1992].

Ludwig [1970] proposed a model based on a statistical analysis of measurements of the intensity of heat island in different American cities and the corresponding low-level rural lapse rate (the rate of change of temperature with pressure). Although the heat island intensity cannot be explained as being the result of lapse rate, the relationship has a considerable practical significance to those who would use an airport's climatic data in the planning of heating/cooling systems. The proposed relationship which covers data from the cities in question is:

$$\Delta T = 1.85 - 7.4 \gamma \quad (4.1)$$

where ΔT is the intensity of heat island in $^{\circ}\text{C}$ and γ is the lapse rate in $^{\circ}\text{C}/\text{mb}$.

Reduction of sky view factor causes decreased long-wave radiation loss to the sky from the ground level of densely built urban centres. In urban areas, most of the radiation is emitted from the roofs and the walls of the upper storeys of the buildings. Oke [1981] shows that maximum heat island values are related to urban canyon geometry through a sky view factor. This relation demonstrates that urban geometry is a fundamental control on the urban heat island. The geometry of the urban canyon is expressed by the relationship between the building height (H) and the street width (W), namely the street aspect ratio (H/W).

$$\Delta T_{u-r(max)} = 7.54 + \ln(H/W) \quad (4.2)$$

$$= 15.27 - 13.88 SVF \quad (4.3)$$

The relationship between H/W and SVF for the case of a symmetric canyon is:

$$SVF = \cos(\tan^{-1}(H/0.5W)) \quad (4.4)$$

Oke [1992] shows that the heat island intensity is also related to the size of the city. Using population (P) as a surrogate of the city size, the intensity of heat island is found to be proportional to $\log P$. In the case of fair weather, the maximum heat island is very well related to $\log P$ for many North American and European settlements. The relationship between the heat island intensity and city size involves rural wind speed (U) at a height of 10 m.

$$\Delta T_{u-r} = P^{0.25} / 4 U^{0.5} \quad (4.5)$$

Very strong winds might eliminate the heat island effect. However, the above relationship does not easily allow the identification of the critical wind speed at which this happens in a given city. Based on field observations, Oke reported that these values appear to be about 9, 5 and 2 m/s in the case of a city with one million, hundred thousands and ten thousands inhabitants respectively.

Bornstein reports the nature, limitations and applications of statistical models

"Statistical models generally do not require large computing facilities, but do require good data bases to develop accurate predictor equations. While they can be used to forecast urban climatological parameters, they do not generally provide significant insight into the basic physical processes producing urban climate." [Bornstein 1984: 239].

In addition, these models usually deal with the maximum intensity of heat island. Therefore, they cannot be applied to estimating the effect of the heat island on energy needs for heating and cooling, which are related to the average rather than to the extreme conditions. Such models will be of limited relevance to urban design unless urban effects are expressed as functions of urban design factors.

Unlike with the solar access and wind shelter regulations, temperature (heat island) is not normally a matter for regulatory control. However, Oke [1988] has proposed a canyon geometry that retains a desirable proportion of the heat island. It is suggested that a considerable control over the heat island can be achieved with small changes in canyon geometry at low values of street aspect ratio (H/W). Under ideal heat island conditions, Oke has shown that one third of the maximum intensity is gained with H/W of 0.4. In this case, this street aspect ratio might be considered the minimum acceptable for maintaining about one third of the heat island potential for a given mid-latitude city.

Impact of the heat island on energy use

The impact of the urban heat island on thermal comfort and in turn on the energy needs for heating and cooling the buildings is dependant upon the geographic location and synoptic weather conditions. Heat islands in low-latitude cities are totally undesirable as they contribute to thermal discomfort and higher cooling loads particularly at night. At the other end of the scale, heat islands in high-latitude cities are desirable as they reduce the required heating energy. Mid-latitude heat islands are only welcome in the heating season as they are unwanted in the cooling season. Therefore, the overall effect of the heat island needs some evaluation.

The heat island effects on energy use could be estimated through their impact on heating and cooling degree-days in a certain location. The number of degree-days is a climatic indicator roughly proportional to the energy requirements for heating and cooling. The number of degree-days

is defined as the cumulative temperature deficit or excess below or over a base temperature. This number can then be summed for any given period, for example a month or a year. Taha [1991] reported the beneficial and detrimental effects of heat islands on reducing heating and increasing cooling energy requirements respectively. At selected locations in the United States, the reduction in heating degree-days is 6% - 32% and the increase in cooling degree-days is 11% - 92% due to the heat island effect.

4.2 FACTORS CONTRIBUTING TO THE DEVELOPMENT OF THE URBAN HEAT ISLAND

Recently, the heat island effect has been well documented in mid-latitude cities [Chandler 1976, Givoni 1989, Oke 1992]. Different and independent factors may be involved in the production of an urban heat island. Firstly, there are differences in the overall net radiation balance between the urban area and the surrounding open country. Secondly, there is the effect of storage of solar energy in the mass of the buildings in the city during the day and its release during the night. Thirdly, there is artificial heat generation by the activities taking place in the urban area. Fourthly, there is lower evaporation from soil and vegetation in the urban area as compared to a rural area. In the following sections, these factors are discussed in detail and a developed model for predicting urban air temperature is proposed.

4.2.1 Absorbtion of Short-wave Radiation

The ground is heated by incoming solar radiation and is cooled by convection, long-wave radiation and evaporation of water. The Sun heats the ground surface, which then heats the adjacent air as well as the ground beneath. Heat is transferred from the ground surface to the air principally by conduction and vertical convection. There are two types of convection usually distinguished; these are free and forced convection. Free convection is caused by density differences (buoyancy), but forced convection is induced by mechanical forces (wind). Then, heat is removed aside by advection, which is horizontal transport by the wind.

There is a daily temperature swing with maximum temperatures usually occurring in the afternoon sometime after peak solar radiation and the minimum temperatures occurring just after dawn before sunrise. In

overcast weather the daily temperature swing is usually small. The pattern of air temperature waves is not necessarily regular when tested on the basis of individual days, especially in climates that experience irregular cloudiness or strong advection. Nevertheless, the longer the period over which hourly air temperatures are averaged, the more evident the regularity of the waves becomes [Rosenberg 1974]. Figure 4.3 shows the variation of diurnal temperature near the ground as a result of solar radiation changes.

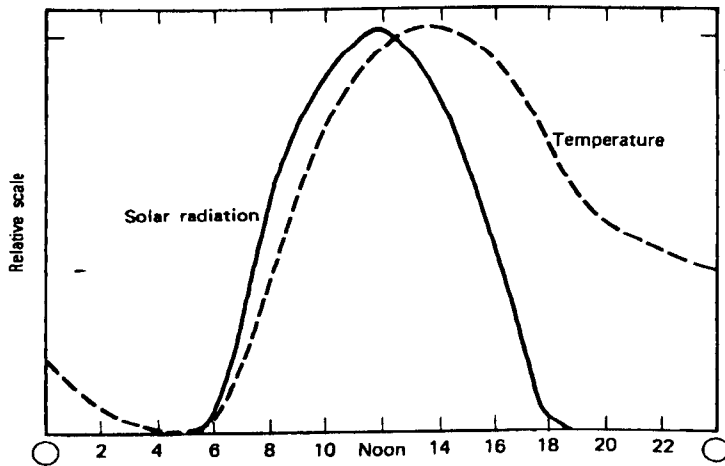


Figure 4.3 Normalised solar radiation and air temperature above bare soil at Scottsbluff, Nebraska on Sept. 4, 1963 (Rosenberg 1974 : 91)

Katayama *et al.* [1988] reported that the dominant factor of the thermal environment in an urban canyon is the direct solar radiation. Solar radiation input to the urban canopy layer (UCL) is affected by the duration of exposure to direct solar radiation [Geiger, 1965]. The extent to which that particular canyon is shaded by its walls (building facades) is represented in the model by the partial shaded area (PSA). Assuming that the solar radiation absorbed at UCL surfaces is released to the air and follows an exponential decay, then the resulting air temperature change ($\Delta T_{sol}(t)$) is as given by Sharlin & Hoffman [1984]:

$$\Delta T_{sol}(t) = \sum_{\lambda=0}^{\lambda=t} (m/h) \Delta I(l) (1 - \exp((\lambda - t)/CTTC)) \quad (4.6)$$

where CTTC = cluster thermal time constant (hr), h = overall heat transfer coefficient (W/m^2K), m = surface solar absorptivity, t = time (h), ΔI = step change in direct solar intensity (W/m^2), and λ = time (hr). In the original formulation, only direct solar radiation incident on a surface is

considered. However, the total solar radiation (direct, diffuse and reflected) incident on a surface (A) should be included such as:

$$I(t) = I_{dir}(t)(1 - PSA(t)) + I_{dif}(t)SVF + \sum_i I_{dir+dif}(t)_i(1 - m_i)(VF_{i-A}) \quad (4.7)$$

where $I(t)$ = hourly mean total solar radiation incident on a surface (W/m^2), $I_{dir}(t)$ = hourly mean unobstructed direct solar radiation incident on a surface (W/m^2), $I_{dif}(t)$ = hourly mean unobstructed diffuse solar radiation on a horizontal plane, $I_{dir+dif}(t)$ = hourly mean direct and diffuse solar radiation incident on a surface, PSA = partial shaded area, SVF = sky view factor for a surface, and VF = view factor for two surfaces. Subscript i is the i th surface type. The direct radiation is corrected for specific solar zenith angle, the incoming diffuse radiation is assumed to be isotropic, and the first reflection is only included as it is very difficult to model multiple reflection. Direct and diffuse radiations are derived from observed values at the meteorological site and are assumed to be representative of the urban site. Partial shaded area is calculated as follows:

$$PSA = (H/W + PSA_h) / (2H/W + 1) \quad \text{if } PSA_h < 1 \quad (4.8)$$

$$= (1 + PSA_v + W/H) / (2 + W/H) \quad \text{if } PSA_h > 1 \quad (4.9)$$

where

$$PSA_h = H/W \cos(AZI - ORI) / \tan ALT \quad (4.10)$$

$$PSA_v = 1 - (W/H \tan ALT / \cos(AZI - ORI)) \quad (4.11)$$

Symbols: H/W = street aspect ratio; AZI = solar azimuth ($0 - 360^\circ$); ORI = orientation (azimuth of the surface normal, $0 - 360^\circ$) and ALT = solar altitude (from horizontal, zenith = 90°). Subscripts: h = horizontal and v = vertical.

4.2.2 Long-wave Radiation Loss

Empirical formulae have been developed for estimating long-wave radiation. Assuming that the emissivity of all surfaces of the urban canopy layer (UCL) is uniform and equals unity, and on average the difference between surface temperatures and air temperatures is negligible, then the surface net long-wave radiation with cloudless skies ($L^*_{(0)}$) is as expressed by Oke [1992]:

$$L^*_{(0)} = \sigma (T_a + 273)^4 (1 - \epsilon) \quad (4.12)$$

where σ is the Stefan-Boltzmann constant ($= 5.67 \times 10^{-8} \text{ W/m}^2\text{K}^4$), T_a is air temperature ($^{\circ}\text{C}$) and ϵ is atmospheric emissivity. The net long-wave radiation contribution to air temperature variations is governed by the urban geometry. The effect of urban geometry on surface temperature patterns is evident from infra-red thermography studies. The results of Swedish studies show that infra-red thermography with good accuracy could be used for determination of intra-urban surface temperature variations [Eliasson 1990]. Swaid and Hoffman [1990a] propose the following expression for estimating the contribution to urban air temperatures of the net long-wave radiation:

$$\begin{aligned} \Delta T_{lw}(t) = & \sigma (T_a + 273)^4 (1 - Br) (SVF/h) (1 - (FA/S)) \\ & + \sigma (T_a + 273)^4 (1 - Br) (SVF_{roof}/h_{roof}) (FA/S) \end{aligned} \quad (4.13)$$

where

$$Br = 0.605 + 0.048 \sqrt{e_a} \quad (4.14)$$

Symbols: Br = Brunt number, FA = plan area of building roofs (m^2), h = overall heat transfer coefficient at street level ($\text{W/m}^2 \text{K}$), h_{roof} = overall heat transfer coefficient at roof level ($\text{W/m}^2 \text{K}$), e_a = vapour pressure (mb), S = site area (m^2), SVF = sky view factor at street level, and SVF_{roof} = sky view factor at roof level. Obstruction of UCL surfaces from the sky temperature sink for long-wave radiation exchange is represented by the sky view factor. The atmospheric emissivity (Br) is estimated by the Brunt equation [Brunt 1932].

The original formulation does not account for the effects of clouds on net long-wave radiation. Clouds have a strong influence on long-wave exchange because they are full radiators. The effects of clouds on net long-wave radiation can be accounted for by modifying the cloudless sky value by a non-linear cloud term [Oke 1992] such as:

$$\Delta T^*_{lw}(t) = \Delta T_{lw}(t) (1 - b c) \quad (4.15)$$

where c is the fraction of sky covered with cloud (on a scale from zero to unity) and b is a coefficient used for decreasing cloud temperature with

heights. If the type of clouds is not known a value of 0.8, taken as the average for different cloud types, can be used.

4.2.3 Turbulent Heat Transport

The convective heat transfer coefficient is dependent primarily on wind velocity. Urban areas experience lower average wind speeds as compared to wind speeds over open areas. Reduction of wind speed and in turn the heat transfer coefficient helps to develop higher urban air temperatures. However, the effect of urbanisation is reduced as wind velocity increases. During the day sensible heat flux to the air is the dominant means of the canyon heat dissipation. At night turbulent heat transfer becomes of minor importance in the canyon energy balance. When the wind is weak at night, cold air descends from roof level to the ground level and accelerates cooling air near the ground, that is *nocturnal cold air drainage*.

The contribution of net solar and long-wave radiation to the air temperature is dependent upon the heat exchange of the urban canopy layer (UCL). Wind speed substantially reduces the effect of solar radiation on the thermal conditions of UCL surfaces for wind speeds not greater than 10 m/s [Kobysheva 1992]. The mean overall heat transfer coefficient (h) at the UCL surfaces can be calculated after the IHVE Guide [1970] as:

$$h = \varepsilon h_r + h_c \quad (4.16)$$

where

$$h_c = 5.8 + 4.1 U(t) \quad (4.17)$$

ε is low temperature emittance of the surface ($\cong 0.9$). h_r and h_c are radiation and convection transfer coefficients respectively (W/m^2K). At a mean surface temperature of 20°C, h_r has a value of 5.7. $U(t)$ is wind speed along the surface (m/s). Meteorological wind speed should be modified to account for terrain and height, which can be done using velocity multipliers proposed by AS 1170-2 [1989], as outlined in the previous chapter.

Canyon advection is the heat transport into or out of the canyon air volume as a result of a mean flow from the external environment. The transport may be achieved in either or both of horizontal or/and vertical flow. The advective transports indicate that with air flow parallel to the

canyon sides the advective contribution depends on the wind speed [Nunez & Oke 1977]. As the urban sites being considered in this thesis are assumed to be surrounded by fairly uniform building density, advective heat transport can be considered negligible as remarked by Oke [1992].

4.2.4 Sensible Heat Storage

Cities have a higher thermal capacity than rural areas due to the mass and nature of the urban fabric. By day the high thermal capacity of urban areas (in some cases it is twice that of rural areas) means that they warm more slowly than the surrounding countryside. The thermal lag thereby induced into the urban thermal system as compared with that in rural areas contributes to the genesis of heat islands. This high thermal capacity moderates the diurnal fluctuation in urban temperature and delays the time of the peak temperature.

The large surface area of buildings also means a more rapid sensible heat flux between the buildings and their air envelope. Consequently, the urban fabric is able to store large amounts of solar and anthropogenic heat which is released to heat the night-time air. The urban materials can accept and store more heat energy in less time than an equal volume of soil. The predominantly rocklike materials of the urban areas can conduct heat about three times as fast as it is conducted by wet, sandy soil [Lowry 1967].

Ambient temperature is influenced by the covering materials of the ground surface. Temperatures over grass have been quoted as being about 5 - 8°C cooler than those over bare soil [Beazley 1990] and around 15 - 18°C cooler than those over asphalt. However, Katayama *et al.* [1988] reported no difference in simulated air temperatures above different ground covering materials (asphalt, lawn and bare soil) in the temperate region of Japan. They hypothesised that this could be because the net-radiation might be similar above those covering materials. The reflected solar radiation from the lawn or the bare soil is larger than that from the asphalt. However, the long-wave radiation emitted from the lawn or the bare soil is smaller than that from the asphalt. As a result, there may be no significant difference among the net-radiation above them.

One of the main parameters of the microclimate differences is the thermal condition of the ground surface and surrounding walls. In this thesis, the cluster thermal time constant (CTTC) parameter is used to express the heat energy stored in the participating ground layer per unit change in the heat flux through it [Swaid & Hoffman 1990a]. An interesting feature of the heat storage rate is that it leads the maximum surface temperature by 1/8 of a period (3 hours) for periodic diurnal cycles. The CTTC parameter is proved to be constant (8 hours) irrespective of the thermal properties of the substrate material, assuming that the ground surface is impervious.

The CTTC parameter, which represents the local thermal inertia, is estimated as being proportional to the urban surface area within the UCL relative to the plot area of the neighbourhood. An increase of the CTTC parameter results in increasing the sensible heat storage and in turn the urban heat island. Swaid and Hoffman [1990a] give the method of estimating the CTTC parameter for a built environment as:

$$CTTC = (1 - (FA/S)) (CTTC_{ground}) + WA/S (CTTC_{walls}) \quad (4.18)$$

where FA/S = urban building density, WA/S = external wall area relative to plot area = $2 (H/W) ((1 - FA/S))$. $CTTC_{ground}$ = 8 hr for dry ground cover, and $CTTC_{walls}$ = 6 hr for hollow bricks and 8 hr for solid bricks and stone. For calculating the thermal constant for other building elements refer to Hoffman and Feldman [1981].

4.2.5 Evapotranspiration

Rosenberg defines evapotranspiration as:

"Evaporation is defined...as the physical process by which a liquid or solid is transferred to the gaseous state...The evaporation of water into the atmosphere occurs from the immediate surfaces of water bodies...from soils and from wet vegetation... The process of evaporation of water that has passed through the plant is called transpiration. Soil evaporation and plant transpiration occur simultaneously in nature, and there is no easy way to distinguish between the two processes. Therefore, the term evapotranspiration (ET) is used to describe the total process of water transfer into the atmosphere from vegetated land surfaces." [Rosenberg 1974: 159].

The concept of potential evapotranspiration (ETP) is widely used to describe the process. ETP is the evaporation from an extended surface of short greenery which fully shades the ground, exerts negligible resistance to the flow of water, and is always well watered. This kind of evapotranspiration is determined mainly by meteorological conditions rather than soil or plant factors. On the other hand, real evapotranspiration differs from the potential under most circumstances. The reasons for these differences are best explained by reference to the conditions imposed by the definition of ETP and an analysis of the reality of these conditions.

Evaporation is in any case one of the notoriously difficult meteorological processes to monitor in the field, and the difficulties are compound in urban areas. Therefore, it is advisable to rely on theoretical estimates of the effect of cities upon evaporation rates [Chandler 1976]. Oke *et al.* [1972] simulated cooling rates in Montreal due to evapotranspiration. The results, which are likely to be representative of a variety of mid-latitude cities in summer, are shown in Figure 4.4. It appears that the greater reductions are for the first 20 - 30 % of the city covered by vegetation.

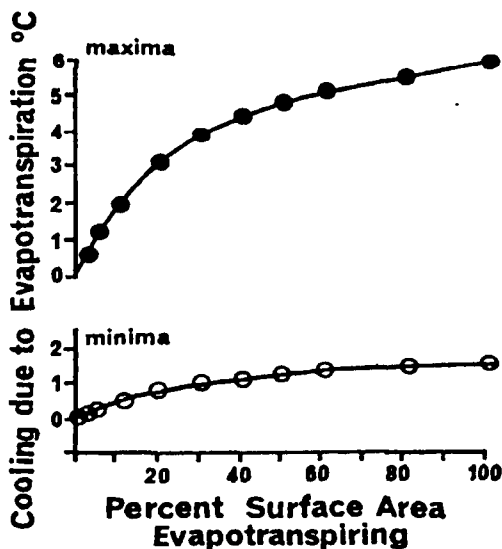


Figure 4.4 Simulated effects on cooling of varying the area of a city covered by evapotranspiring surfaces (Chandler 1976: 47)

Some empirical methods have been designed to estimate the potential evapotranspiration using climatic data only. These empirical methods can be used for simulating the urbanisation effects on the evapotranspiration

process. There is less opportunity for evaporation in urban areas; therefore, the heat energy that would have gone into the process is available for heating the air. Decreased evaporation is directly proportional to a reduction of vegetation areas and free-water surfaces. In addition, runoff is increased in urban areas in comparison with rural environments due to the extensive areas of impervious surfaces quickly leading to storm-water drains. This contrasts with the absorbent soils and ground water flow of rural areas.

Jensen and Haise [1963] derived a regression equation from the study of about 1000 reported measurements for various sampling periods with various crops in the western United States. The Jensen-Haise method was tested against measurements of daily water use by alfalfa and soybeans at Mead, Nebraska [Rosenberg 1974]. The method gave good results when the advection is minor, and serious underestimation with high advection. As a function of air temperature and solar radiation, the potential evapotranspiration is estimated by:

$$ETP = (0.014 T - 0.37) R_s \quad (4.19)$$

where ETP is potential evapotranspiration (in./day), T is ambient dry-bulb temperature (°F), and R_s is the evaporation equivalent of the solar radiation (in./day).

Huang *et al.* [1987] used this model to assess the cooling effects of vegetation in urban settings, but questioned its applicability for all climates and plant types and for predicting hourly evapotranspiration rates. Assuming a uniform canopy, the difference in evapotranspiration between two sites may be expressed as a function of the difference in vegetation ratio. Based on this model expressed in SI units, the variation in the heat content (W/m^2) due to a change in vegetation ratio as it were converted to either sensible or latent heat content can be estimated as:

$$\Delta ET = M_a (\Delta R_g) ((0.0252 T_a(t) + 0.078) I_G(t)) \quad (4.20)$$

where T_a is air temperature (°C), I_G is hourly mean global radiation on a horizontal plane (W/m^2), and ΔR_g is the change in vegetation ratio. M_a is moisture availability that expresses the ratio of actual to potential

evapotranspiration rate. A moisture availability of 0.3 can be adopted as a median value over residential areas [Lewis & Carlson 1989].

4.2.6 Anthropogenic Heat

There is limited literature, theoretical or observational, on the amount of anthropogenic (referred to as artificial or man-made) heat released in urban areas. Most of these studies are limited to North American and European cities where anthropogenic heat is substantially greater in winter than the net radiation balance. Some rates of man-made energy production in central Sydney in summer are given in Figure 4.5. If these rates are compared with the net radiation fluxes, man-made heat appears to be about 25% of incoming solar radiation. However, percentages are higher in winter and can be up to 50%. This heat results from industry, transport and other sources. The last includes about 4% due to heat from bodies of people and animals [Linacre & Hobbs 1977].

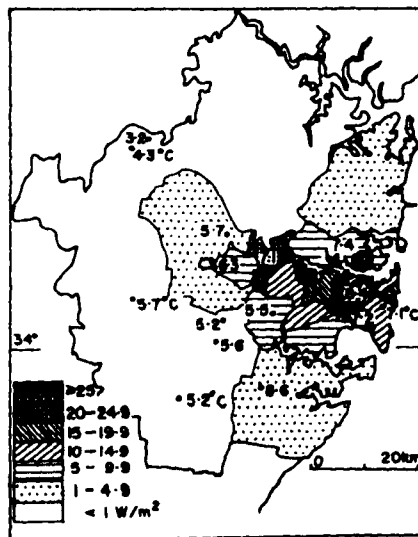


Figure 4.5 The man-made heating (W/m^2) and observed screen temperatures in Sydney at 8 am in July (Linacre & Hobbs 1977: 34)

Anthropogenic heat addition in an urban area is dependent upon different factors, such as geographical location, prevailing climate, population density, and industrial and commercial activities. It is difficult to specify the vertical distribution of this heat addition, or to break it down to sensible, latent, and radiative fractions. The average annual data covers important time and space variations. A city with a mild winter climate

exhibits a much smaller seasonal variation. Spatially, artificial heat varies greatly within a particular city, with the highest values usually found in the city core. The mean annual magnitude of this heat source depends upon the average energy use and the city's population density. For typical temperate climate cities, It is reported to be in the range 15 - 50 W/m² [Oke 1992].

The diurnal variation of anthropogenic heat addition is largely due to space heating, transportation, and electric usage [Torrance & Shum 1976]. There is relatively little information regarding daily variations of this artificial heat. However, in mild climates it seems that this heat addition is larger in the daytime with two peaks in morning and evening rush hours. A time-varying artificial heat flux ($H(t)_{urb}$) for capital Australian cities (Figure 4.6) is proposed by the researcher based on average additional heat flux observed in Sydney. These rates are attributable to domestic use and transportation only.

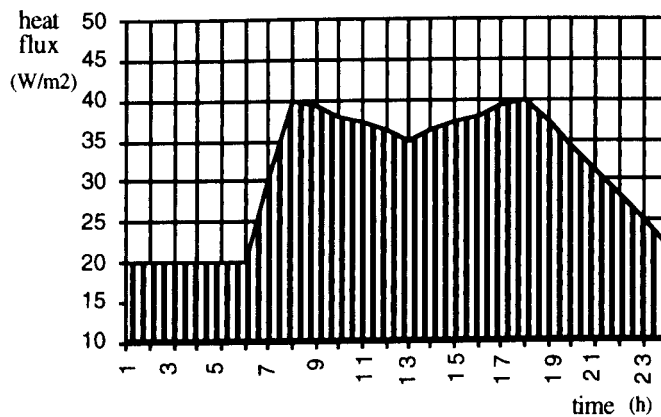


Figure 4.6 An assumed diurnal artificial heat flux $H(t)_{urb}$ for major Australian cities

Building density is known to influence the amount of artificial heat released. As increases in density are usually associated with decreasing vegetation areas, urban heat addition is maybe relative to vegetation ratio. The relationship between the vegetation ratio (R_g) and artificial heat flux (H) is proposed by Moriyama and Matsumoto [1988]:

$$H = (1 - R_g) H_0 \quad (4.21)$$

Where H_0 represents the density of artificial heat released when R_g is equal to 0. This relation can be re-formulated to express the variation in

artificial heat flux between the meteorological site and the urban site by varying the vegetation ratio.

$$\Delta H = H(t)_{urb} (\Delta R_g / (1 - R_{g\ urb})) \quad (4.22)$$

where $R_{g\ urb}$ is vegetation ratio at the urban site.

4.3 TEMPERATURE PREDICTION MODEL

Urban temperature models are reviewed to select an appropriate model for the purposes of this research. The model should be able to modify meteorological temperature to be urban site representative. The cluster thermal time constant CTTC model is selected for predicting air temperature variations in the urban canopy layer (UCL). The original model was developed by Swaid and Hoffman [1990a]. They presented evidence of experimental verification of the model against measurements done in Jerusalem and Tel-Aviv (32°N), Israel. The model was also corroborated with published measurements from Essen (52°N), Germany.

The CTTC model predicts the urban air temperature at time t ($T_a(t)$) calculated from the individual contributions of:

- the prevailing mesoscale background weather conditions expressed in the form of a base temperature (T_b),
- the contribution to air temperature variations of absorbed solar radiation by the urban canopy layer surfaces ($\Delta T_{sol}(t)$), and
- the contribution to air cooling of the net outgoing long-wave radiation flux from the urban canopy surfaces to outer space ($\Delta T_{lw}(t)$).

The general form of the urban air temperature prediction equation is:

$$T_a(t) = T_b + \Delta T_{sol}(t) - \Delta T_{lw}(t) \quad (4.23)$$

The use of the original model is restricted to fair-weather conditions (cloud cover < 2 oktas and mean diurnal wind speed < 2 m/sec). The model restriction to light winds conditions is to avoid consideration of advective effects. Restricting the model to use in almost clear sky conditions means that solar radiation is predominately from direct beam radiation and that for long-wave radiation the sky emissivity factor can be

considered constant. A further development of the model is undertaken as part of the work for this thesis.

4.3.1 The Developed CTTC Model

The original formulation of the model is based on predicting the contribution to air temperature variations of the solar and long-wave radiation and adding these to a base temperature which is described as the mean diurnal rural air temperature. On the other hand, the development of the model uses as input temperatures hourly air temperatures recorded at a weather station located usually in suburban area in the Australian major cities. The restriction imposed by the original formulation of fair weather conditions is relaxed so that it might be applicable in all fine weather conditions. The implications of this relaxation are discussed below.

The developed model uses the original basic equations for predicting the contribution to air temperature variations of solar and long-wave radiation at the weather station site and at the urban site being considered. Base temperatures for predicting urban air temperatures ($T_a(t)_{urb}$) are theoretically substituted by meteorological air temperatures ($T_a(t)_{met}$) minus the predicted contribution to $T_a(t)_{met}$ of solar and long-wave radiation. Thus, $T_a(t)_{urb}$ is expressed by $T_a(t)_{met}$ plus the differences in the contribution to air temperature variations of solar and long-wave radiation at the two sites. Equations 4.24 through 4.26 express this procedure.

$$T_a(t)_{urb} = T_b + \Delta T_{sol}(t)_{urb} - \Delta T_{lw}(t)_{urb} \quad (4.24)$$

$$T_a(t)_{met} = T_b + \Delta T_{sol}(t)_{met} - \Delta T_{lw}(t)_{met} \quad (4.25)$$

then

$$T_a(t)_{urb} = T_a(t)_{met} + (\Delta T_{sol}(t)_{urb} - \Delta T_{sol}(t)_{met}) - (\Delta T_{lw}(t)_{urb} - \Delta T_{lw}(t)_{met}) \quad (4.26)$$

The developed version of the CTTC model represents a simple and time-saving tool for considering the urban heat island effect. This model follows a different approach from that of the conventional energy balance models. The model deals with micro-scale processes operating in a building-air volume beneath roof-level. It accounts for the contribution of different and independent factors to the development of the urban heat island. The contribution to air temperature variations of solar and long-

wave radiation can be estimated using equations 4.6 through 4.18. The contribution of evapotranspiration and anthropogenic heat can be estimated by adding the heat that is available from lower evapotranspiration estimated by equation 4.20, plus the artificial heat calculated from equation 4.22 to the net surface radiative flux input in equation 4.6.

Limitations

The underlying physical assumptions and constraints of the model as developed for this thesis are:

- Spatial homogeneity of building and surface characteristics in the locality.
- Well-mixed UCL air volume with no temperature differentials in it.
- Solar radiation absorption at roof surfaces and their thermal mass do not affect diurnal variations of the air temperature within the UCL.
- The applicability of Jensen-Haise evapotranspiration model to predicting *hourly* evapotranspiration rates in urban areas is uncertain.
- Topography, water bodies and downwind effects of the urban area itself are eliminated.

4.3.2 Verifying the Model

A computer program CONSECTTC incorporating the developed CTTC model has been written, in Fortran, for personal computers (appendix 1). The results of the program were then compared to field measurements conducted to verify the developed model. The verification exercise involved measuring the climatic variables relating to two differently oriented canyons. The two canyons were assumed to have the same above-roof climate as they were about 200m apart. The ambient and canyon air temperature, global and diffuse radiation, and wind speed were measured continuously at the street- and roof-level. The hourly averaged measurements of air temperature, wind speed and cloud cover at the weather station (*Kent Town*) were obtained for the same period.

Measurement Site and Period

The field measurements were carried out in two canyons located at the Adelaide, North Terrace campus of The University of Adelaide. There were several buildings of almost the same height on the campus. The canyons were formed by buildings of approximately the same height and were of a length sufficient to be considered as semi-infinite. One canyon

had its long axis in an east-west direction and the other in a north-south direction. The E-W axis canyon was symmetrical, formed by 3-storey buildings each 15m high and a bitumen street 17m wide. The building facades were of red brick and glazing area of 35%. The N-S axis canyon was slightly asymmetrical, formed by two buildings of average height 12m and a brick-paved street 12m wide. In this case the building facades were of stone. The measurement period was December, 1993. A variety of synoptic conditions were experienced during this month.

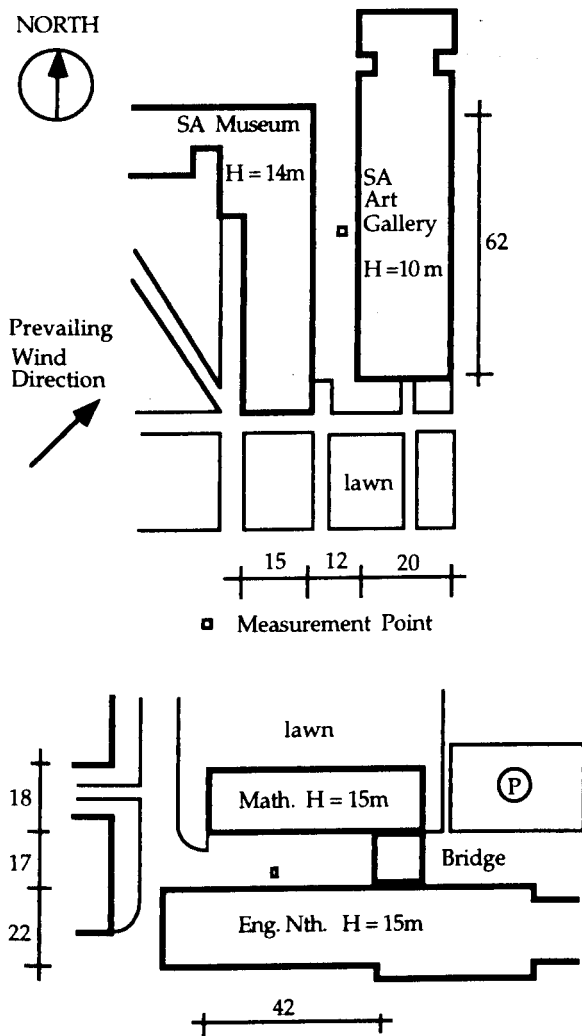


Figure 4.7 The experimental urban canyons at the University of Adelaide (Dimensions shown in meters)

Measurement Method and Set-up

Measuring instruments were set up on the roof of the Engineering Building (Figure 4.7). A 3-cup anemometer was placed 3m above the roof to measure wind speed. The global solar radiation was measured by a pyranometer at 2m above the roof. The diffuse radiation was measured

by a pyranometer with shadow band. The ambient air temperature was measured, 1.5m above the roof, by using a shielded resistance temperature device. In order to measure air temperature in the two canyons, temperature devices of the same type were hung 1.5m away from the north and west facades, and 2.5m above the street. All signals were recorded on a data logger at 1 minute intervals, and then hourly averaged.

Table 4.1
Input Data Requirements for the CTTC Model

Input parameters	Units
Urban Characteristics	
Mean surface absorptivity (α)	
Street canyon aspect ratio (H/W)	
Building density (FA/S)	
External walls area to plot area ratio (WA/S)	
Cluster thermal time constant of external walls (CTTC _{wall})	hr
Orientation (ORI)	deg
Climatic Data	
Direct radiation (I_{dir})	W/m ²
Diffuse radiation (I_{dif})	W/m ²
Solar Azimuth (AZI)	deg
Solar altitude (ALT)	deg
Air temperature (T_a)	°C
Vapour pressure (e_a)	mb
Cloud cover (c)	tenth
Wind speed (U)	m/s
Artificial heat density (H)	W/m ²

Table 4.1 shows input data requirements for the model. Table 4.2 shows the values assigned to urban characteristics relating to both canyon sites and the weather station site. Also shown is the mean solar absorptivities and the CTTC factors calculated according to equation 4.18. Because of the suburban nature of the urban development around the Meteorological site, the SVF was estimated from the skyline diagram shown in Figure 4.8. For the test canyons the SVF was estimated by a simplified method described by Oke [1992 : 352].

Table 4.2
Urban characteristics of the weather station and University sites

Site	FA/S	WA/S	H/W	SVF	m	CTTC
Met.	0.20	0.3	0.20	0.93	0.75	8.2
E-W	0.35	0.8	0.85	0.53	0.85	10.2
N-S	0.35	0.8	1.00	0.45	0.75	10.2

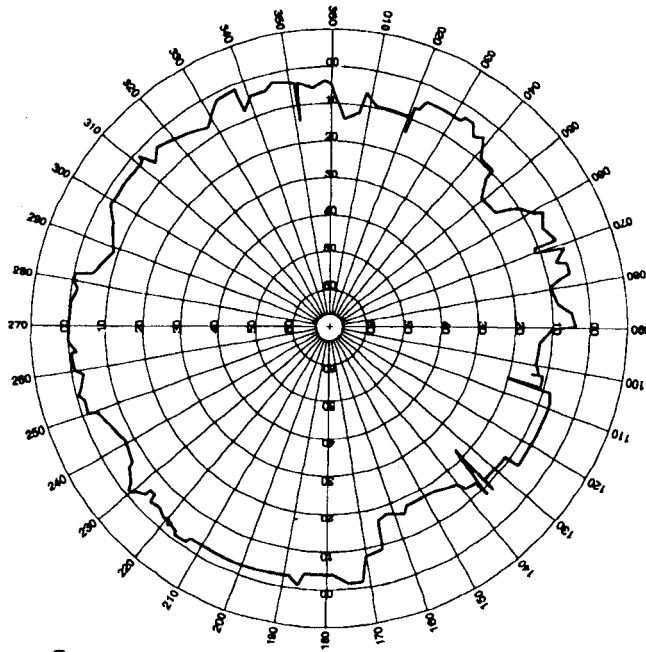


Figure 4.8 Skyline diagram (Kent Town Weather Station)

Performance of the developed model

The developed model was run for each of the two urban canyons. The results of measured and predicted air temperatures for a ten day period during the monitoring period are shown in Figures 4.9 (a & b) and 4.10 (a & b). Figures 4.9a and 4.10a comparing the meteorological and canyon air temperatures show the heat island effect. The heat island intensity varies typically through the course of the clear days. This intensity grows in the late afternoon to reach its climax often before sunrise, and decays rapidly thereafter. The heat island intensity on cloudy days is less variable, because of the clouds that act as a barrier to the flow of heat from the boundary layer to upper atmospheric layers. The average heat island intensity for the E-W canyon was higher than that for the N-S canyon (1.7 and 1.0°C respectively). The difference can be explained in terms of varying rates of solar radiation absorption due to the difference in aspect ratio and absorptivity. The comparisons of the predicted and measured air temperatures shown in Figures 4.9b and 4.10b appear to show good agreement. A comparison of mean values and correlational statistics calculated over the whole month supports the close fit between measured and predicted air temperatures giving some confidence in the validity of the developed model.

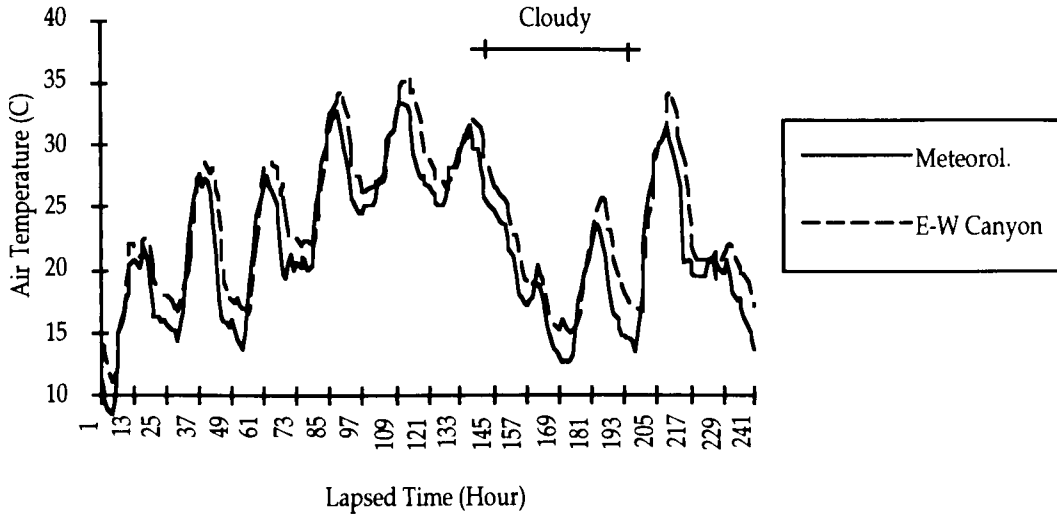


Figure 4.9a Meteorological versus measured air temperature in E-W axis canyon (5-14 Dec. 1993)

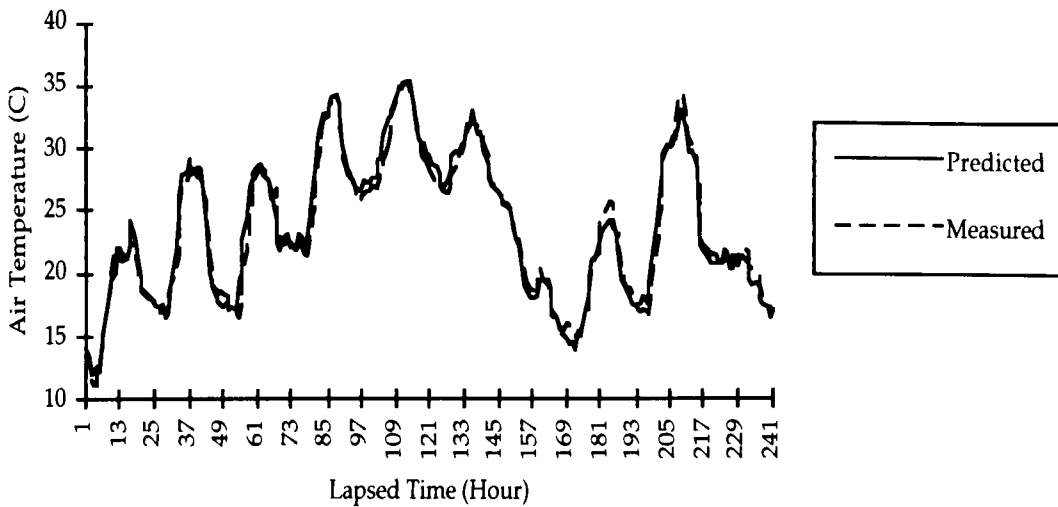


Figure 4.9 b Predicted versus measured air temperature in E-W axis canyon (5-14 Dec. 1993)

Regression Analysis

	<i>Measured</i>	<i>Predicted</i>
Maximum Mean	25.9	25.9
Mean Temperature	21.4	21.4
Minimum Mean	16.7	16.5
Correlation Coefficient	0.98	
Standard Error	1.15	
Slope	1.00	

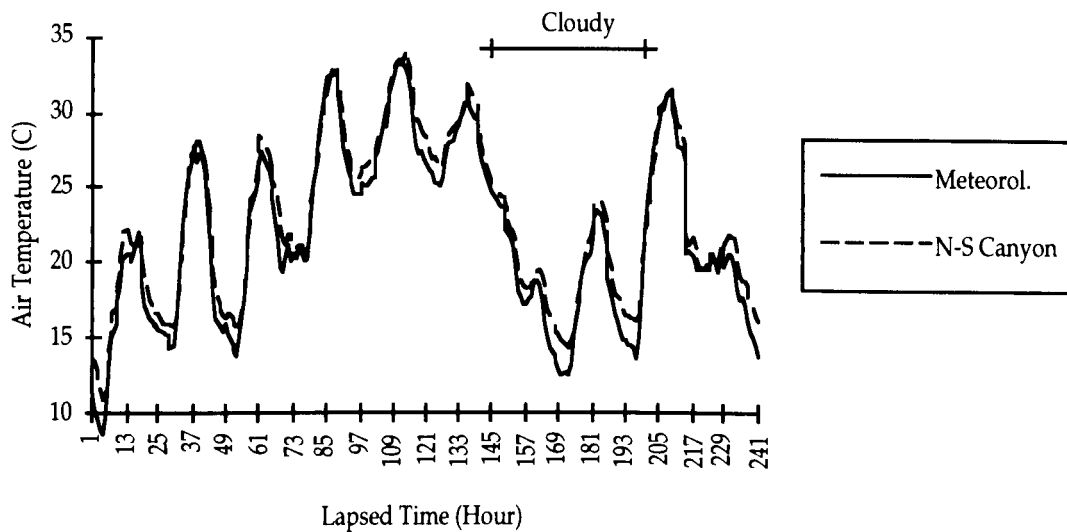


Figure 4.10 a Meteorological versus measured air temperature in N-S axis canyon (5-14 Dec.1993)

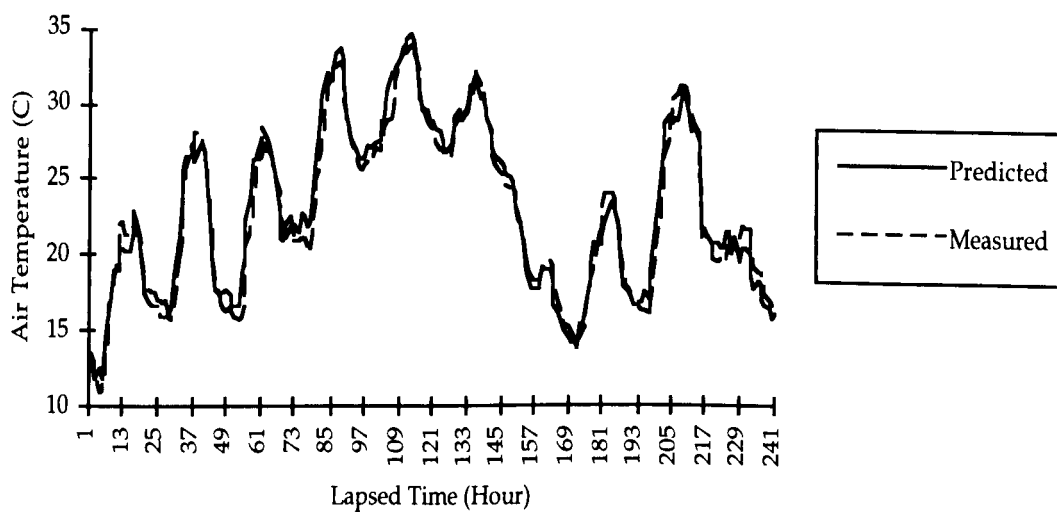


Figure 4.10 b Predicted versus measured air temperatures in N-S axis canyon (5-14 Dec. 1993)

Regression Analysis

	<i>Measured</i>	<i>Predicted</i>
Maximum Mean	25.1	24.9
Mean Temperature	20.7	20.6
Minimum Mean	16.1	16.1
Correlation Coefficient		0.98
Standard Error		1.10
Slope		1.02

Table 4.3
Effect of excluding the new features on mean temperature values

Features	ΔT Max. Mean	ΔT Mean	ΔT Min. Mean
Total solar radiation	- 1.3	- 0.9	- 0.6
cloud cover	+0.2	+0.2	+0.3
Evapotranspiration	- 0.5	- 0.3	- 0.2
Anthropogenic heat	- 0.2	- 0.2	- 0.1

New features incorporated into the developed model include the following: the dependence of solar radiation absorption on total radiation instead of direct radiation in the original model; the modification of outgoing long-wave radiation loss by the inclusion of average cloud cover; the thermal effect of vegetation in urban areas; and the contribution of anthropogenic heat to the air temperature. Effect of each of these new features on mean temperature values is investigated. Table 4.3 presents the temperature change (ΔT) in mean values, which would result by not including the new features in the model. The presented statistics are for the E-W axis canyon and similar results were obtained for the other canyon (not presented here). The exclusion of the new features other than cloud cover result in lower temperatures than those predicted by the full model. The use of only direct solar radiation rather than total solar radiation has the largest impact on mean temperatures, particularly on the maximum mean. Using direct radiation only the model resulted in a mean maximum temperature 1.3°C lower than that predicted by the full model, that is, including direct and diffuse radiation. Latent heat resulting from evapotranspiration has a similar influence but less than total solar radiation effect. However, the exclusion of cloud cover and anthropogenic heat have a minor effect.

Simulation and Modelling

- 5.1 SIMULATION PROCEDURE 80**
 - 5.1.1 Assumptions and Restrictions 80
 - 5.1.2 Simulation Approach 81
- 5.2 SIMULATION MODELS 82**
 - 5.2.1 The Building Energy Simulation Program 82
 - 5.2.2 Climate Modifier Models 84
- 5.3 DATA INPUT 85**
 - 5.3.1 Climatic Data 85
 - 5.3.2 Urban Configurations 87
- 5.4 BUILDING ANALYSIS 91**
 - 5.4.1 Heating/Cooling Model 92
 - 5.4.2 Building Construction 100

Climate interactions with land use and urban form on human health, environmental quality and energy use in urban areas need to be considered in urban and architectural design processes. The interaction between urban forms and climatic elements affects urban thermal environments. Urban designers and architects attempt to achieve certain objectives that are relevant to climate-adapted design (see the thesis Introduction). To propose urban forms that comply with these objectives, their thermal performance should be simulated and analysed. This chapter aims to give a concise description of the simulation procedure, models and data input as well as an analysis of the modelled dwellings and dwellers' modes of using energy.

5.1 SIMULATION PROCEDURE

Available techniques for evaluating urban thermal environments cover a wide range in terms of capability and cost. A basic and frequently used technique is computer modelling and simulation. Such a technique is inexpensive if compared with the cost of extensive monitoring of an existing environment. Computers have increased in speed and capacity rapidly, and this fact that has enhanced modelling and simulation. The use of this technique has enabled the microclimate around buildings as well as the indoor climate to be simulated. In this research, this technique will be used to investigate the effects of particular urban characteristics on particular climatic elements. However, built environments are very complex systems, and this may limit the simulation of various processes happening within them. The following section discusses the simulation assumptions for this study.

5.1.1 Assumptions and Restrictions

For this study, certain assumptions are made to simplify the situation to be manageable; they are:

Assumptions related to tested urban forms

The urban forms being tested are considered to be of uniform building density and height. The basic form unit is an urban canyon, with no open spaces or squares considered. The length of the urban canyon is assumed to be semi-infinite, in order to eliminate the corners effect. The street facades are presumed to be plain without protrusions, with no nearby

trees. The number of differently oriented dwellings are evenly distributed among the cardinal orientations.

Assumptions linked to chosen dwellings

The selected type of dwelling is a multi-unit (town-house), to form urban canyons that have continuous street facades, with no spacing in between. The heat flow from adjacent dwellings is assumed to be negligible, as all dwellings in a row are of the same building materials and are exposed to same climatic circumstances. The dwelling is assumed to have a building description that is considered as a representative of an average building description in the Australian temperate climates (refer to Section 5.3.2).

It is important to recognise that the dwelling types and urban forms used in this research constitute hypothetical case studies. The results of the research should be understood only in the context of the particular case studies at hand. They depend on the conditions and assumptions made about the nature of the dwelling's internal and external order, and how they interact with the conditions of the urban context. Provided then, that designers understand these assumptions and restrictions, they are able to estimate the significance of differences disclosed between alternative designs in a given location.

5.1.2 Simulation Approach

In general, for simulating building thermal performance, very little attention has been paid to having site specific weather data for design purposes. There are some exceptions in other design applications, main examples being wind engineers involved in structural design and air pollution meteorologists concerned with plant siting. Generally, the difficulties inherent in obtaining site specific weather data have caused designers and/or simulators to avoid the issue and adopt climatic data from the closest weather station [Arens *et al.* 1985].

Basically, there are two different approaches to simulating the climate at a building site.

- A dynamic model of both mesoscale and microscale atmospheric processes. This approach is infeasible for normal building design applications as it is a costly time-consuming process and requires an extensive input of weather data and physical characteristics of the

region, besides the complexity in linking the mesoscale to microscale (for example URMICLEM model as proposed by Taha 1990).

- Transformation of the meteorological data to approximate a nearby site's climate using generalised relationships linking site physical characteristics to site climate. The advantages of this approach are: reduced information about the site's physical characteristics; available weather data from hourly surface observations; and reasonably inexpensive application on one or several years of weather tapes (for example SITECLIMATE model as proposed by Arens *et al.* 1985).

This research follows the latter approach because of the large number of case studies to be dealt with (over 100) and the reasonably long period (one year) for which the micro-climate of these case studies will be simulated. Given that the former dynamic model approach is considered infeasible for multi-runs for long periods, it would be almost impossible to follow it in this case. This research uses various computer models to adjust climatic elements such as wind speed and air temperature. The energy use for internal climate control is estimated using the site-specific climatic data as an input into the building energy simulation program.

5.2 SIMULATION MODELS

The main reasons for simulation of building-climate interactions are the economical and practical problems involved in full-scale measurements and to evaluate yet-to-be built environments. These models may include, for example, physical scale models, analytical mathematical models and numerical computer-based models [Taesler 1984]. In this research, the procedure for quantitative assessments is to use computer models incorporating both the urban climate and the urban system affected by this climate. Weather data and urban configuration are used as an input to the modifier models. The site-specific weather data is used together with the building description as an input to the building energy simulation program.

5.2.1 The Building Energy Simulation Program (see also Appendix 2)

TEMPAL is one of the widely used thermal performance computer programs in Australia. It was originally developed at the University of Melbourne by A.B. and E.B. Coldicutt. An advanced version by T.J.

Williamson is used in this research (version 3.2). TEMPAL is used in this study to simulate the differences in the building energy consumption as a function of the site-specific climatic data derived from the microclimate modifiers. TEMPAL includes the immediate effects of the surroundings, such as shading from adjacent structures, allows for obstructed diffuse radiation and adjusts infiltration/ventilation rates. With the exception of the allowance for a 'terrain category' wind speed factor, it does adjust either external air temperature or airflow around buildings.

Coldicutt [1985] explains that TEMPAL is able to predict the thermal performance of a specified dwelling using actual weather data or design data. It predicts hourly internal environmental temperatures, sensible heating and cooling loads and the total energy added to or extracted from spaces for any nominated period—from 3 days to several years. TEMPAL uses a method of calculating heat gains and losses through opaque elements which is based on modified response factors termed *advancing mean*. This method approximates realistic time delays of the heat flow through all elements. The program tests hourly for the direction of the heat flow and then uses factors appropriate to the direction. The external stimulus is calculated as a sol-air temperature.

The thermal properties of the building elements are described in terms of their U-value and 24 hour transfer modulus and internal admittance, as well as corresponding lag and lead times where appropriate. Williamson *et al.* describe how the program models solar radiation on building surfaces

"The altitude and azimuth of the sun are calculated for given latitude and time of the year. Solar radiation is read from the climatic data file and then used to determine direct and diffuse irradiation. Radiation transmission through glass and blinds is calculated by a method based on the *ASHRAE Handbook of Fundamentals*. Air-to-air glass gain is calculated for the design U-value of the glazing assembly and the program varies the transfer characteristics to allow for changing external film resistance due to wind." [Williamson 1993a].

Limitations

TEMPAL as a building energy simulation program does not consider urbanisation effects on external air temperature, nor the effects of variation in wind direction or local shelter effects on air flow around

buildings. Therefore, the use of other models (modifiers) is necessary to overcome these limitations. This is dealt with in a following section.

Validation

Coldicutt [1985] reported that matching of predictions with measured conditions of eight dwellings has been undertaken in various situations and that simulations using variations in the thermal properties for the materials of construction and variations in infiltration rates indicate that the behaviour of the envelope is being accurately simulated. The correlations achieved justify confidence in the ability of the TEMPAL package to predict the energy required in buildings to achieve defined levels of internal temperatures. Examples of validation of TEMPAL program can be found in Williamson [1984].

5.2.2 Climate Modifier Models

The key issue of investigating the impact of urban form on heating/cooling energy use is to modify the weather data to represent the microclimatic data of each specific urban form. TEMPAL can account only for immediate effects of the micro-level urbanisation rather than the effects on external air temperature and airflow. Application of climate-modifiers is needed to consider these urbanisation effects. A local wind model is introduced to estimate the air change rate in the proposed dwellings taking into account the shelter effects of opposite buildings (see Section 3.4). The developed CTTC model is used to modify meteorological air temperatures in order to account for the urban heat island (see Section 4.3). A schematic illustration of the simulation models is shown in Figure 5.1.

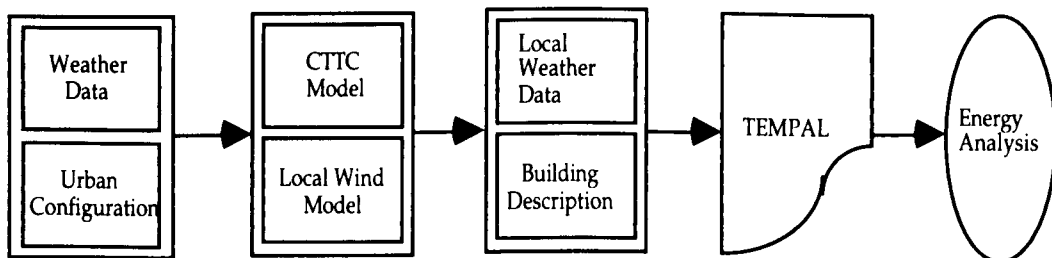


Figure 5.1 Schematic illustration of simulation models

5.3 DATA INPUT

Weather data files are derived from the Australian Climatic Data Bank which contains climate information measured by the Bureau of Meteorology and compiled by the CSIRO Division of Building Research [Walsh *et al.* 1983]. Full summer and winter periods representing typical meteorological seasons are selected from the weather tapes available for each city studied (Table 5.1). Each period is chosen by comparing average temperatures, wind speed, radiation data and so on for each month of each year with the overall average for that month for the number of years available. Then, the data are checked in terms of the amount of absolute variation of any month from the average for that month [Williamson 1993a]. For the purpose of this research, months with average temperatures less than 18°C are considered to be the winter season.

Table 5.1:
Selected representative periods as typical meteorological seasons

City	Summer season	Winter season
Perth	Nov. 1978 - Apr. 1979	May - Oct. 1974
Adelaide	Nov. 1983 - Mar. 1984	Apr. - Oct. 1986
Melbourne	Dec. 1976 - Mar. 1977	Apr. - Nov. 1974

5.3.1 Climatic Data

In temperate climates the weather conditions are not so extreme; this fact complicates rather than simplifies design requirements. There is a problem of cold in winter and a problem of heat in summer. In addition, there are intermediate periods when hot and cold spells may be experienced consecutively. None of these weather conditions alone would lead to any particular difficulties. When all occur within the same climate, however, the assignment of climate-adapted design in such climates becomes perhaps more difficult than that in more severe climates [Serra 1988]. This is attributed to the conflicting nature of climate-adapted design objectives in different seasons.

Locations are selected to represent three climatic categories: they are Perth (warm temperate), Adelaide (temperate) and Melbourne (cool temperate). Table 5.2 shows key average climatic data for these three cities. Presented mean maximum temperatures do not give a good idea about hot spells

that might be experienced in the Australian summer. In this case, 86%ile maximum temperatures in January might give a better idea; they are 28.3, 27.5 and 25.3°C for Perth, Adelaide and Melbourne respectively.

Table 5.2:
Average annual climatic data for Perth, Adelaide and Melbourne
[Data from Szokolay 1988]

	Perth	Adelaide	Melbourne
Sunshine hours	7.9	6.9	5.7
Cloud cover (octas)	4.4	5.0	5.9
Solar irradiation (Wh/m ²)	5186	5037	3973
Relative humidity (%) 9 hr	63	59	68
Relative humidity (%) 15 hr	50	47	52
Wind speed (Km/h)	15.6	11.3	12.3
Maximum gust	156	148	119
Mean max. temperature	23.5	21.5	19.9
Mean temperature (°C)	18.5	17.0	15.2
Mean min. temperature	13.5	12.4	10.2
Frost days	0	3	10
Heating degree hours	22166	29930	41345
Cooling degree hours (T _{base} = 18°C)	6722	3217	1343

Table 5.3:
Urban characteristics of urban weather stations

Site	FA/S	WA/S	SVF	m
Perth	0.20	0.50	0.86	0.75
Adelaide	0.20	0.33	0.93	0.75
Melbourne	0.20	0.60	0.83	0.75

FA/S = built up area, WA/S = wall area/plot area, SVF = sky view factor and m = absorptivity.

In order to simulate the microclimate for tested urban configurations the weather data from urban weather stations should be obtained. The method for modifying these climatic data to be representative of the sites being considered needs the site characteristics at those stations to be quantified. Information about the immediate surroundings around the stations is obtained by private communication with the staff working at these stations. All the weather stations are located in green areas surrounded by streets and/or buildings. Skyline diagrams are obtained

for quantifying building heights and distances away from the measurement sites. Table 5.3 presents urban characteristics of the urban weather stations in Perth, Adelaide and Melbourne.

5.3.2 Urban Configurations

A helpful starting point for choosing energy conscious urban forms could be to determine a practicable range that is consistent with climate-adapted design objectives. This study attempts to provide a practicable range of urban design variables that are readily understood, and easily controlled by urban designers and architects. General guidelines can be, and have been, formulated for the siting and layout of human settlements. Yet, with the exception of air pollution and high wind speed control, it is difficult to find cases where climatological advice has played a significant role in urban planning [Taesler 1984].

Urban climatologists attempt to establish quantitative guidelines that might assist urban planners and designers in developing climate sensitive urban settlements. Oke [1988] proposed an optimal zone of compatibility for a hypothetical mid-latitude city that would satisfy some design objectives to at least a minimal extent. These design objectives are related only to winter considerations such as solar access and wind shelter. This zone is determined by a range of aspect ratios (building height/street width) between 0.4 and 0.6 and a range of building densities between 0.2 and 0.4. In this study, objectives that are related to summer and winter considerations may make a wider range appropriate.

Assuming that everything about the urban area is fixed, apart from the building density and spacing, this presents just two design variables which can be manipulated. Different values of building density can be combined with different values of building spacing to give a variety of urban forms. In a representation of the design space, two axes are used to show the values of these two design variables. If any values were allowed for them (from zero to infinity), infinitely long axes should be required. However, in practice there are constraints operating which limit the practicable values [Radford et al. 1984]. These constraints together define a practicable zone within which climate interactions would be evident, and design variables to be tested must lie (Figure 5.2).

Aspect ratio limits that individually achieve climate-adapted design objectives can be determined for latitude 35° South as follows. An aspect ratio of 0.5 provides north wall solar access in mid-winter. An aspect ratio greater than 1.5 dramatically reduces insolation in winter relative to the reduced insolation in summer (see Figure 2.3). A minimum street aspect ratio of 0.4 is necessary for acceptable wind shelter (refer to Section 3.2.1). This is based on fully open streets where there is no additional protection like trees or awnings. An aspect ratio greater than unity has no potential for providing cross-ventilation through the building due to the strong sheltering effect of the opposite buildings [see Section 3.2.2]. Therefore, a range of aspect ratios to be consistent with these objectives can be between 0.5 and 1.25.

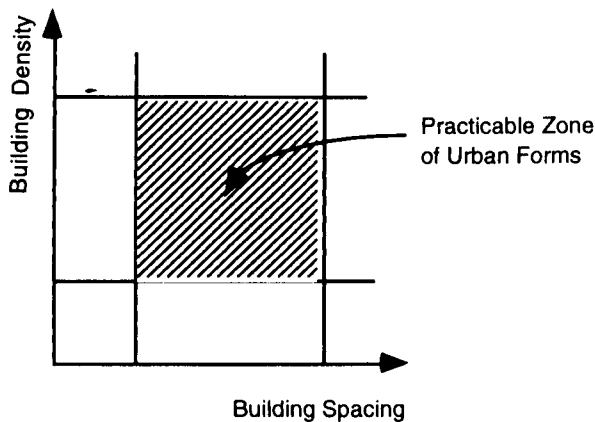


Figure 5.2 A practicable zone of urban forms defined by two urban design variables

Hypothetical layout positions to be tested are parallel block layouts (row buildings). Layout configurations are to be varied by:

- aspect ratio [spacing between blocks (W) 2, 1.4, 0.8 H , height (H) of building being held constant], and
- density (built-up area) using different dwelling shapes (narrow, medium and wide frontage).

Figure 5.3 shows cross-sections through the different tested configurations. To make comparison easy these densities are initially calculated on the net living area only. In other words, they are expressions of the ratio between ground area occupied by the dwelling and the total ground area including local roads and private open spaces, but excluding the land required for local centres and the usual allowances made for public open space [Hawkes 1977].

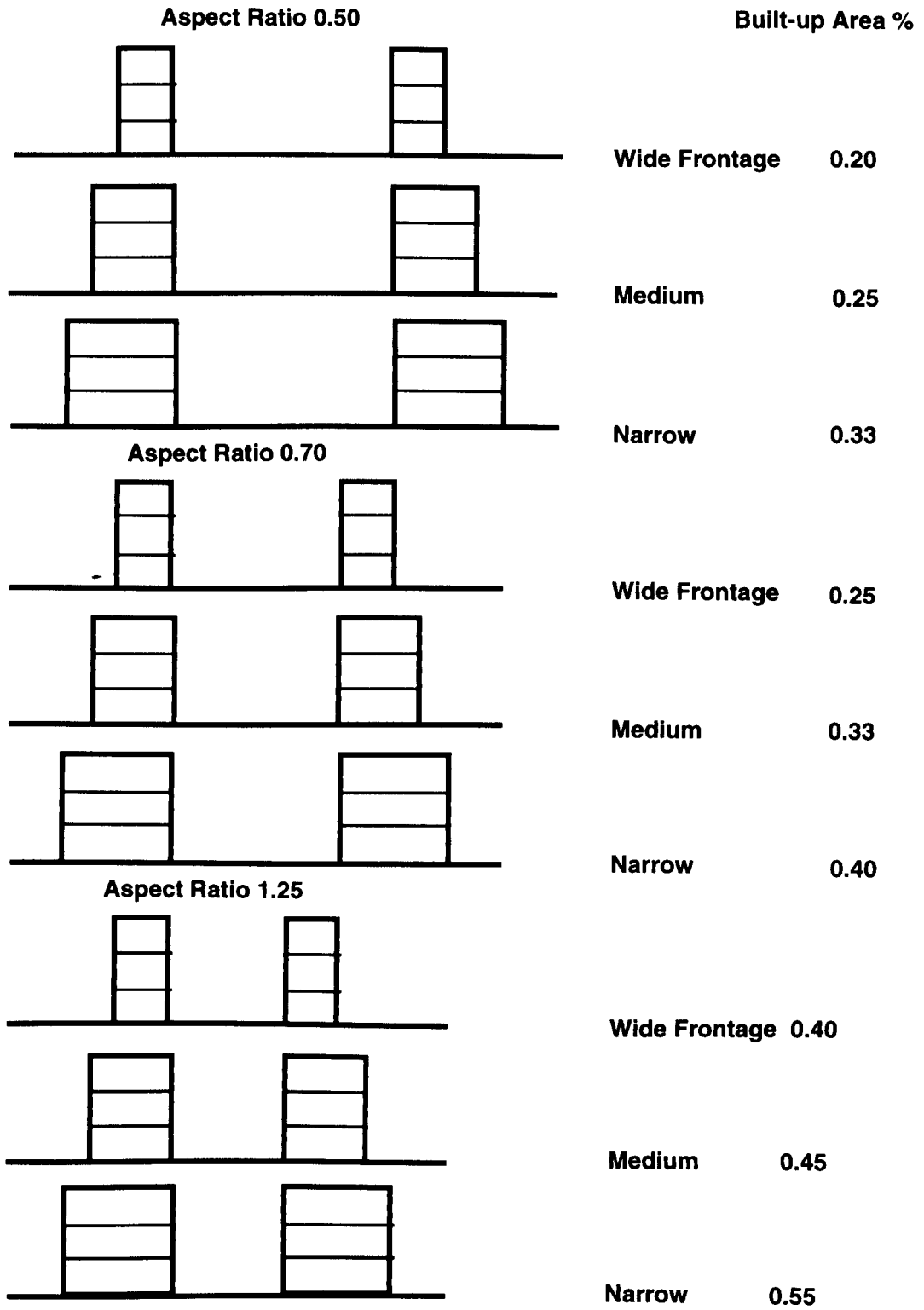


Figure 5.3 Cross-section through urban configurations

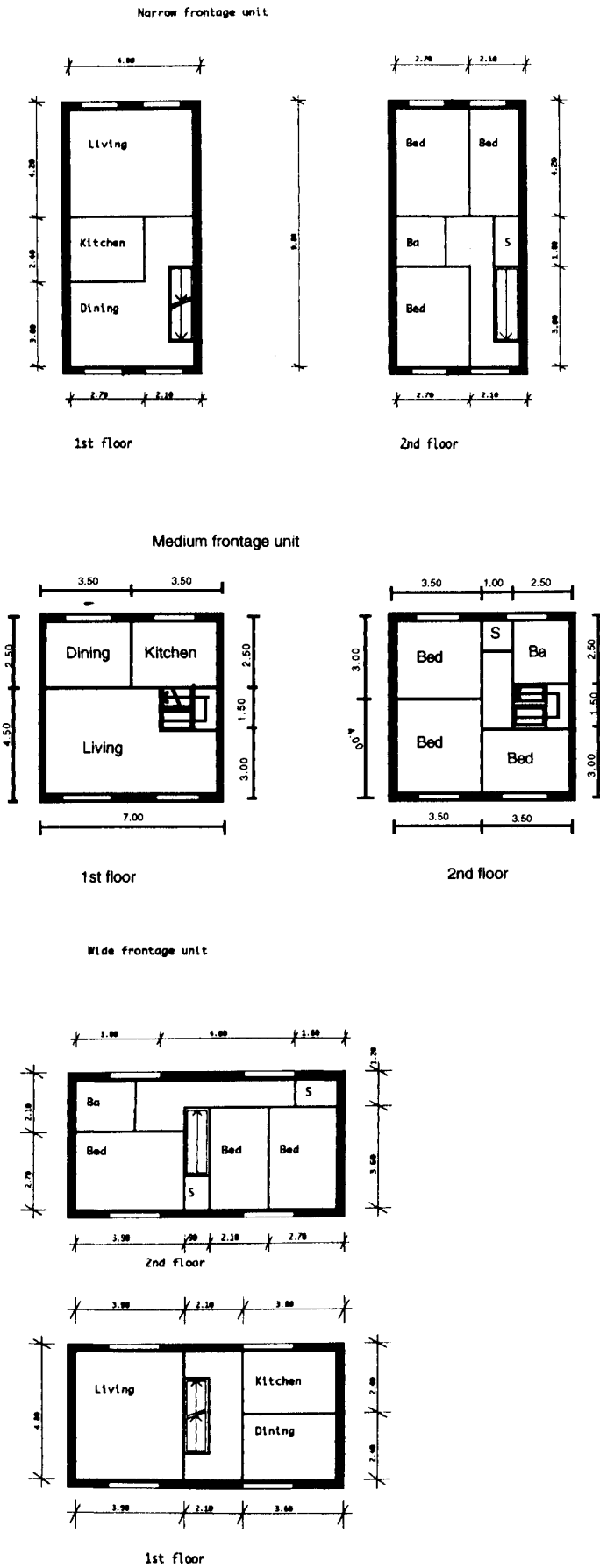


Figure 5.4 Diagrammatic plans of the design options

Building Description

The simulated dwelling is a three-storey attached unit (town house-type). The ground floor is non-habitable space, used as garage and parking. The first and second floors are living and sleeping zones respectively. The total habitable floor area of the dwelling = 100 m², and there is a total of glazing area = 20% of the wall area. There is no external shading device and curtains are drawn at night. Figure 5.4 shows architectural plans of the design options (narrow, medium and wide frontage). Aside from being better insulated than on average, the construction of the dwelling is typical to standard houses in Adelaide. The typical construction of external walls is from outside to inside: brick 110mm, insulation R2 and plaster-board 12mm. Inside walls are of plaster-board on studs. The roof (pitch 22.5°) consists of clay tiles, attic space, insulation (R 2.0) and plaster board. The floor construction is of concrete slab (100 mm) with carpet. Window frames are single pane with clear 3 mm glass. Thermal properties of these construction elements are shown in Table 5.4.

Table 5.4:

Thermal properties of construction elements used in the simulations (Williamson et al. 1993a)

	U-Value (W/m ² K)	T (W/m ² K)	Lag (hrs)	Y (W/m ² K)	Lead (hrs)
Wall	0.4	0.26	4.9	0.82	3.6
Roof (heat flow in)	4.63	3.71	0.4	4.65	0.1
(heat flow out)	5.66	4.58	0.3	5.68	0.2
Ceiling (heat flow in)	0.42	0.37	1.0	0.95	3.7
(heat flow out)	0.44	0.39	0.8	0.98	3.8
Floor (heat flow in)	2.07	1.21	4.3	2.73	2.4
(heat flow out)	1.69	0.79		2.47	
Internal Partitions	1.94	1.69	0.5	2.01	0.8
Contents	1.8	1.78	0.8	1.94	1.1

T = Transfer modulus Y = Internal admittance

The simulated dwelling has a 6 kW reverse cycle air conditioner (CoP 2.5) and a 4 kW electric heater (efficiency 100%). The ventilation control strategy is described in Section 3.4. Internal loads are based on two adults and two children allowing an average loads of 70 W/person sensible, 60 W/person latent plus 10 W/m² for equipment and 12 W/m² lighting. Use-patterns of heaters and coolers are described in the next section.

5.4 BUILDING ANALYSIS

It is important to gain some understanding of the extent to which the predicted effects of urban configuration on heating/cooling energy use might be dependent upon assumptions regarding the buildings that are modelled.

Therefore, a building analysis is required to indicate the significance of these assumptions to the energy simulations. Several variations to be considered are particularly linked to the construction elements and heating/cooling strategy. A heating/cooling model is to be proposed as a simplified description of use-patterns of heaters and coolers.

5.4.1 Heating/Cooling Model

Heating and cooling plant in Australian housing is usually under the occupants' control. The control exercised is influenced by the occupants' attitude and life style. As a result, a difference between predicted and actual energy consumption could occur if predictions are based on invalid models of people's heating/cooling routine. If predictions of energy consumption are based on a better understanding of building occupant behaviour, mismatches between predicted and actual outcomes would be minimised. This would enable better optimisation of design, especially where trade-offs between summer and winter performance are essential.

A model of heating and cooling routine is needed for predicting the building occupants' modes of using energy to ameliorate their thermal environment. The model should approximate real occupancy and use patterns of heating and cooling. An investigation was conducted to set up a heating/cooling model to be incorporated into the building energy simulation program TEMPAL. The investigation was based on energy simulations of a typical Adelaide house using TEMPAL program, and was performed to match predicted energy use to actual average energy use. Adelaide is selected due to the availability of more comprehensive information on using energy for heating/cooling reported in Coldicutt *et al.* [1988].

Neutral temperatures have been used in the design of heating and air-conditioning systems, and in determining thermostat settings for comfort and minimisation of discomfort complaints. The neutral temperatures are defined as the temperatures averaged for a large sample at which individuals feel neither cold nor hot. A literature review of comfort studies to research and determine neutral temperatures for Adelaide was undertaken. Most research into the subject has dealt with the temperate (moderate) climates of Europe and the United States. The following is a review of some comfort studies that are relevant to architectural design and energy use.

The first attempt to systematise incorporation of climatic conditioning into building design, and to define a comfort zone for architectural purposes was pioneered by Olgyay [1963]. Olgyay's bioclimatic chart depicts the comfort zone of the temperate climate of the United States (40°N) to be between (21 - 27.8°C) for summer conditions and between (20 - 24.5°C) for winter conditions which was determined in terms of the interaction of environmental variables for the climate in question. Olgyay suggested a correction factor of 0.42°C for the lower and upper perimeters of the comfort zone for every 5° latitude change toward the equator with an absolute upper limit of 29.5°C.

Koenigsberger *et al.* [1973] published a table in which thermal comfort limits are given as a function of relative humidity (RH) and annual mean temperature (AMT) to be applied to each month of the year. They stated that comfort limits for AMT = 15 - 20 °C and RH = 50 - 70% (conditions of temperate climates) are between (21 - 28°C) during the day and between (14 - 21°C) at night.

Based on the work of Koenigsberger, Evans [1980] produced tables giving day and night comfort limits for sedentary activities. Evans stated that, for relative humidity (50 - 70%), the comfort range for light summer clothing with a negligible air movement of (0.1 m/s) is between (22.5 - 27.5°C) day temperature and (20 - 26°C) night temperature. When warmer clothes are worn (winter conditions), the lower limit of the comfort range is between (18 - 22.5°C) day temperature and between (16 - 20°C) night temperature.

The ASHRAE comfort envelope is specified by effective temperature (ET*) in *ASHRAE Standard 55 - 1992*. The comfort zones for summer and winter are intended to provide acceptable conditions for occupants wearing typical indoor clothing and at or near sedentary activity. In accordance with the notion that no single environment is judged satisfactory by everybody, the ASHRAE comfort zone is based on 90% acceptance. The lower and upper temperature limits for comfort in winter are 20 - 23.5 ET*, and in summer 23 - 26 ET*.

Table 5.5:
Range of comfort with normal clothes as suggested by some researchers

	Winter	Summer
Olgyay 1963	20 - 24.5°C	21 - 27.8°C
Koenigsberger 1973		21 - 28°C
Evans 1980	18 - 22.5°C	22.5 - 27.5°C
ASHRAE 1992	20 - 23.5 ET*	23 - 26 ET*

Table 5.5 is a summary of the above studies, which shows that the lower limit of comfort ranges between 18°C to 20°C in winter, and the upper limit of comfort ranges between 26°C to 28°C in summer. The above studies give comfort ranges, however, the following gives neutrals. Humphreys [1978] proposed an approach for estimating the neutral temperature (T_n) as a function of the average monthly air temperature (T_m). The regression equation for free-running buildings is:

$$T_n = 11.9 + 0.534 T_m \quad (5.1)$$

Another equation is given by Humphreys for climate-controlled buildings, bearing in mind that the equation is based on data limited by lack of information regarding hot climates.

Auliciems [1986] developed an empirical correlation function as an improved version of the function earlier proposed by Humphreys. Neutrality (T_n) is expressed as a function of outdoor mean temperature (T_m):

$$T_n = 17.6 + 0.31 T_m \quad (5.2)$$

This correlation is based on field studies in Australia. Thus, it might be suitable for the purposes of this thesis. Two values are calculated for Adelaide, one based on the mean temperature of the seven month heating season, and the other on the mean temperature of the five month cooling season; they are: (21.9 - 24.1°C).

As a product of an extensive field study, Coldicutt *et al.* [1991] suggested a range of neutral temperatures in summer for living areas of the Adelaide house, in afternoons and evenings. They reported that the 50%ile neutral temperature was 21.5°C, and actual mean temperature, which was some 2K above this, was 23.5°C. This neutral temperature was associated with average humidity (45%), low air speeds (< 0.1m/s), average clothing levels (0.6 clo) and applies to people sitting or doing light work. It can be noticed that their neutral temperature is close to that of Auliciems.

The target of comfort studies, which are relevant to energy use, may simply be the thermal conditions that cause people to start using energy. The proposed heating/cooling model is a simplified description of when and where to operate heating or cooling and which set of temperature settings and fluctuations to choose to minimise mismatches between predicted and actual energy

consumption. Model parameters, which are relevant to people's modes of operating heating/cooling, are determined. These parameters are: design temperatures (thermostat set point), temperature fluctuations (thermostat swing), design times (plant operation period), and spaces concerned by heating and cooling.

Design temperatures

Until very recently, air-conditioning engineers had advocated a single universal neutral temperature near 25°C for people wearing very light-weight clothing, although in the interests of economy, some concessions have been made to seasonal flexibility in thermostat settings [Auliciems & Dear 1986]. A method of thermobile controls introduced by Auliciems [1990] indicates possible reductions in heating from all but the four warmest months in Adelaide, with May to September each showing savings > 20%. Design temperature has a significant impact on the effective building energy consumption. Faist [1988] has reported that, in the climate of Lausanne (46.5°N), fluctuations of set point temperature by $\pm 2^\circ\text{C}$ result in fluctuations of building energy consumption by $\pm 25\%$.

Temperature fluctuations

The lowest internal temperature at which no more than 50% of the thermal sensation votes are above neutral could be regarded as the mean cooling commencement temperature. Similarly, the highest temperature at which no more than 50% of the votes are below neutral could be regarded as the mean heating commencement temperature. Coldicutt *et al.* [1991] reported the upper limit of 50 %ile acceptable temperature for Adelaide in summer to be 27.5°C. Lowest and highest acceptable temperatures of 12.8 and 26.8°C are indicated for the heating and cooling seasons respectively [Riordan 1992]. These temperatures could be assumed as the average *tolerance* limits of indoor thermal environment for Adelaide. As it is difficult to anticipate what will happen after cooling or heating has commenced, for this research it will be assumed that temperatures are kept at thermostat set points.

Design times

Designers need to know about people's thermal preferences to apprehend what are the most important design times. A study of thermal preferences in South and Central Australia investigated priorities for thermal comfort in housing in a variety of climates [Coldicutt *et al.* 1988]. For Adelaide, design times are mentioned to be hot summer afternoons, evenings and nights in bed, with cold

winter evenings and mornings at getting-up time. Therefore, it might be presumed that design times in winter are evenings until bedtime (5-10 pm) with mornings next (7-9 am), and in summer are afternoons until bedtime (3-10 pm).

Spaces concerned

Coldicutt *et al.* [1988] reported that Adelaide houses had a great variety of coolers, particularly refrigerative coolers and fans. Mean days of reported use of main coolers were only 40 per annum. The most common area cooled with main coolers was one living room, but there was a variety of other use patterns, including one or more bedrooms, and living half of the house. For winter, the study reported various types of heaters, mainly portable electric. The mean number of days per year on which heaters were usually used was 104. The rooms most commonly heated were in the living zone of the house, ranging from one room to about half of the house.

Design times and spaces are identified, but there is little available information on set point temperatures and swings. Nevertheless, it is possible to infer such information using the following simulation method. The method for determining such temperatures is based on adjusting the set point on a particular temperature, which represents a base line for the investigation, and on monitoring the impact of changing the set point temperature by one degree at a time below or above this temperature. A base temperature for the simulations may be neutrality as calculated from equation 5.2 to be about 22 and 24°C for winter and summer respectively. A range of acceptable conditions can be taken as $\pm 2 - 4^\circ\text{C}$ about these neutralities (refer to the comfort studies pp. 93 - 95).

The simulation is guided by recorded average internal temperatures and total energy consumption. Riordan [1992] showed that mean internal temperatures in buildings are related to mean external temperatures. A group of linear regressions was inferred, which represents the relationships between mean internal (T_{int}) and external (T_{ext}) temperatures for selected Australian cities. The linear regression equation, which is given by Riordan, for Adelaide is:

$$T_{int} = 9.5695 + 0.6616 T_{ext} \quad (5.3)$$

The mean external temperatures, for the two seasons in question, are 14.1 and 21°C in winter and summer respectively. Equation 5.3 gives mean internal temperatures to be 18.9 and 23.5°C, which could be guidelines for actual average internal temperatures in Adelaide houses.

The average annual energy consumption (electricity and gas but excluding other fuels like wood) for two years (1989-1990) was recorded in Adelaide^{as} 44.3 GJ for standard houses, but it was not possible to apportion energy consumption to end-use categories [Williamson *et al.* 1993b]. An estimated one third of the total energy is used for space heating and cooling (14.6 GJ). An annual averaged heating loads for standard houses in Adelaide is estimated 10 GJ (EIC 1993). No figure is available for cooling loads, however, it can be inferred from the previous figures.

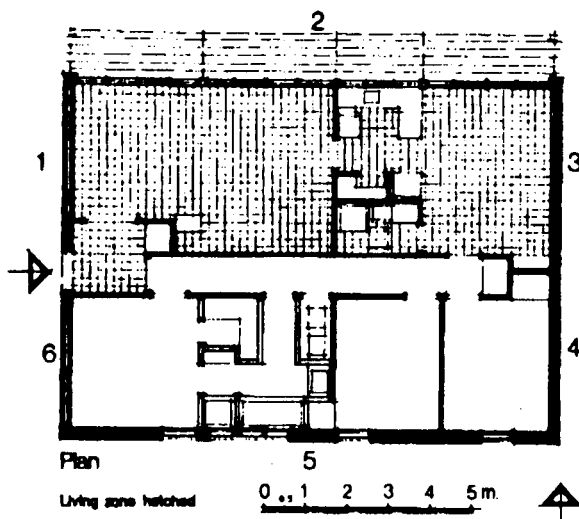


Figure 5.5 House plan

Building description

The simulated dwelling used to check the heating/cooling routine assumptions is a one-storey detached house of floor area $\cong 150 \text{ m}^2$. The plan of the house is rectangular and is aligned on the east-west axis, with a living zone facing north and a sleeping zone facing south (Figure 5.5). Windows are single pane with clear 3 mm glass and of total area 27 m^2 . There is no external shading devices and curtains are drawn at night. The construction of the external and inside walls and the roof is similar to the description in Section 5.3.2. The floor construction is of a concrete slab on ground (100 mm) with carpet. The house has a 8 kW cooling capacity reverse cycle air conditioner and a 6 kW heating capacity electric heater. Internal loads are also identical to the figures given in the aforementioned description. Generally, the house is as close to average as possible in order to simulate conditions that could give average energy use.

Energy Use Discussion

Many separate TEMPAL runs are required over full heating season (Apr. - Oct.) and cooling season (Nov. - Mar.) in order to check assumptions about thermostat set points and swings. The results indicate that the specified mean internal temperatures and energy use could be achieved with set point temperatures 21 and 25°C for heating and cooling seasons respectively. These temperatures lie within the comfort envelope proposed by the *ASHRAE Standard 55 - 92*. If these temperatures are compared with Auliciems' neutral temperatures, it would be observed that they are close to their neutral counterparts. Therefore, the use of neutral temperatures as thermostat set points could be applicable.

Sensitivity analysis is performed to explore the impact of the different parameters mentioned above. The following is only a small sample of data selected to be presented. The results show that all specified parameters except the thermostat swing have a significant effect upon the energy use for heating and cooling. A range of swings, commencing from 1 to 3 degrees below and above the thermostat setting, is employed. The impact on energy use was insignificant, within $\pm 2\%$ in all those cases.

Table 5.6 shows the effect of fluctuation of the thermostat setting by $\pm 1^\circ\text{C}$, normalised to the base temperatures selected above. This small change in the thermostat setting produces a fluctuation in the energy use by an average $\pm 25\%$ in both winter and summer. Therefore, the set point temperature, as a mean internal temperature maintained in the house during heating/cooling operation, has a crucial influence upon energy consumption. In other words, the effect of the temperature at which heating/cooling cuts in/out is trifling compared to that of the thermostat setting.

Table 5.6:
The effect of thermostat setting on predicted energy use

Set point temperature (°C)	Heating energy use (GJ)	Difference normalised to the base case	Set point temperature (°C)	Cooling energy use (GJ)	Difference normalised to the base case
22	12.6	+ 26%	26	3.4	- 20%
21	10.0	—	25	4.3	—
20	7.6	- 24%	24	5.7	+ 32%

The striking effect of hypothetical times and spaces results in an over-estimation of the predicted energy use. Tables 5.7 a, b indicate the surplus of energy use when the design time is assumed to be for the whole period of occupancy of the living zone (7 am - 10 pm). The figures point out an increase in the energy use by 45 and 51% in winter and summer respectively. The large increase in predicted energy use based on the presumption of heating/cooling the whole house for a nominated period of occupancy of the living zone (7 am - 10 pm), and of the sleeping zone (11 pm - 6 am) is shown in tables 5.7 a, b. The increase in energy use due to heating the sleeping zone is 83%, however, the increase due to cooling in summer is minor (about 2%).

Table 5.7a:

The impact of hypothetical times and spaces on predicted heating energy use

Nominated time and space (Heating)	Heating energy use (GJ)	Excess of predicted heating
living zone (7 - 9 am & 5 - 10 pm)	10.0	—
living zone (7 am- 10 pm)	14.5	45%
living zone (7 am- 10 pm) & sleeping zone (11 pm- 6 am)	26.5	165%

Table 5.7b:

The impact of hypothetical times and spaces on predicted cooling energy use

Nominated time and space (Cooling)	Cooling energy use (GJ)	Excess of predicted cooling
living zone (3 - 10 pm)	4.3	—
living zone (7 am- 10 pm)	6.5	51%
living zone (7 am- 10 pm) & sleeping zone (11 pm- 6 am)	6.6	53%

As an alternative cooler, evaporative cooling might be used instead of the refrigerative cooling. Coldicutt and Williamson [1988 : 31] reported on the effectiveness and performance of evaporative cooling: "On average, evaporative cooling in Adelaide dwellings uses roughly 40% of the energy used by refrigerative cooling to achieve equivalent comfort conditions."

Finally, it is not claimed that the temperatures, aforementioned as recommended temperatures for predicting the energy use, represent the

actual preferred temperatures in the typical Adelaide house. However, it is an attempt to explore the influence of people's heating/cooling routine on the predicted energy consumption. The investigation shows that the thermostat setting could be adjusted on the neutrality, with swing of 1 - 2 degrees below and above the set point. This setting would give reasonably accurate predicted energy use if it is associated with the times and spaces outlined above.

5.4.2 Building Construction

An investigation is performed on the thermal efficacy of building elements on energy use. The thermal performance of widely used alternatives are compared with that of construction elements one at a time. This is to show the deviations in performance of the alternatives from the base case (the prototype building). In this sense, an idea about variations in energy use that follow alterations in the building description might be inferred. This investigation is conducted using TEMPAL program on the narrow-frontage unit (see Figure 5.4) in free-standing N-S and E-W oriented blocks in the climate of Adelaide. The following is a discussion of the building elements selected for this phase of the investigation.

Ceiling Insulation

The effect of insulation is directly proportional to the difference between indoor and outdoor temperatures. In winter, insulation is most beneficial particularly in houses with low air change rates and high solar gains [Coldicutt & Williamson 1988]. In summer, the effect of insulation is not so beneficial as it is in winter especially in unconditioned buildings with very high temperatures and solar gains. The thermal insulation level used in the ceilings of prototype buildings is R 2.0. The predicted energy use increases by as much as 20% when no ceiling insulation is used.

Exterior Walls

One function of exterior walls is to minimise internal daily temperature swings; therefore, comfort conditions may be achieved without or with limited use of heating/cooling. The thermal performance of a wall can be described partly by its admittance factors. The building internal admittance can significantly influence both fluctuations in internal temperature and energy use. A high internal admittance might be



beneficial in summer whether cooling is required or not. However, winter low internal admittance is preferred if intermittent heating is employed [Coldicutt *et al* 1989]. Brick veneer + R 2.0 is replaced with brick cavity + R 1.0 whose internal admittance is sixfold the former. Heating energy use increases by about 20% and cooling energy use reduces by 15 - 30%.

Floor Cover

The distribution of solar radiation input to an enclosure is a complex mechanism. Part of the solar radiation is lost out of the enclosure due to reflection and transmission, another part is absorbed in materials of the enclosure, and the remaining part in the enclosure, termed "solar used" [Coldicutt 1985], contributes to a change in internal thermal conditions. The floor mass has a critical effect on controlling indoor temperature fluctuations. With a concrete slab there is a very slow response to temperature change as there is large heat storage in the slab. A sharp increase in heating energy use (100%) is predicted when a carpeted concrete slab, selected for the prototype buildings, is replaced by a slab with hard finish. However, cooling energy reduces by about 15%, which highlights the insulating properties of carpeted slabs in cold weather.

Internal Partitions

Internal mass contributes to reduce the fluctuation of indoor temperatures about the mean which may be beneficial if it brings temperatures closer to comfort levels. The highest degree of internal wall mass is provided by full masonry construction. Brick veneer dwellings may be thermally improved by the use of masonry walls between rooms. However, dwellings with heating/cooling tend to use more heating and less cooling if the internal lightweight partitions, used in the prototype buildings, are replaced by masonry cores. An increase in heating energy use by about 20% is predicted due to the slow response of the masonry core in terms of temperature rise when heating is employed. Nevertheless, a reduction in cooling energy use by 25 - 30% is predicted which is based on the ability of internal mass to absorb and store heat during the day and release it at night.

Window/Wall Area

A major source of heat gain and loss in buildings is diathermic materials, such as glazing. Heat passes through glazing by conduction depending

on the temperature differences between the indoor and outdoor. When solar radiation falls on a clear glass window some is reflected, some is absorbed, while most transmits into the building. Windows for housing should be designed to admit the sun's warmth in the cold season and to minimise overheating in the hot season. A bigger glazing area admits more solar heat, but loses/gains more air-to-air heat due to the glazing poor insulating properties. The prototype buildings have window/wall area ratio = 20%. When this ratio is reduced to 10%, heating energy use slightly increases by up to 10%. Cooling energy use for N-S oriented dwelling reduces by 25%, but for E-W oriented dwelling the reduction is more noticeable, about 40%.

Glazing Material

Many factors affect Solar-Optical properties of glass, such as the Sun's angle of incidence, reflective treatments, chemicals in glass, and so on. The properties of glass with various treatments are experimentally determined for normal incidence by CSIRO [Hassall 1973]. 3mm soda lime sheet is used as a reference STANDARD as described in the ASHRAE Handbook of Fundamentals [1989]. Solar transmittance and absorptance of 6mm heat absorbing glass are almost half and tenfold that of standard 3mm clear sheet glass respectively [ASHRAE 1989]. When the standard 3mm glass used in the prototype building is replaced by 6mm heat absorbing glass, predicted energy use slightly changes by less than $\pm 10\%$.

Table 5.8:
Heating/cooling energy use (GJ) with various building elements

Building Elements	N-S oriented Dwelling			E-W oriented Dwelling		
	Heating	Cooling	Total	Heating	Cooling	Total
Base Case	5.0	1.3	6.3	5.3	2.6	7.9
No Ceiling Insulation	6.0	1.7	7.7	6.2	3.2	9.4
Exterior Walls (brick cavity)	5.9	0.9	6.8	6.3	2.2	8.5
Floor Cover (hard finish)	10.0	1.1	11.1	10.4	2.1	12.5
Internal Partitions (masonry)	5.9	0.9	6.8	6.4	2.0	8.4
Window/Wall Area (10%)	5.5	1.0	6.5	5.7	1.6	7.3
Glazing Material (heat absorb.)	5.4	1.2	6.6	5.6	2.4	8.0

Predicted heating/cooling energy use in GJ with various building elements for both N-S and E-W oriented dwelling are presented in Table 5.8. The foregoing investigation shows that slight variations in some

Predicted heating/cooling energy use in GJ with various building elements for both N-S and E-W oriented dwelling are presented in Table 5.6. The foregoing investigation shows that slight variations in some construction elements have a noticeable impact on energy use. It is concluded that the large variations in heating/cooling routine and building construction, which occur in practice, are likely to result in large variations in heating/cooling energy use. This suggests that the relative effects of urban configuration on heating/cooling energy use might be different if very different heating/cooling routine or building construction was used. A full support to this suggestion could not easily be achieved.

Simulation assumptions for Melbourne and Perth are the same as that for Adelaide. There could be some differences in assumptions regarding building construction and people's modes of using energy in these two cities; however, the Adelaide simulation assumptions are adopted for the three cities. To make the comparison among the three cities feasible, climatic data is the only variable for the various case studies simulated in the three cities to test the impact of climatic variations. Actual likely considerations in these two cities may result in some differences in energy use figures. For example, the use of brick cavity walls in Perth and longer periods of plant operation in Melbourne may result in lower energy use in the case of Perth but higher energy use in the Melbourne case.

Results and Discussion

6.1 DESIGN OBJECTIVES 106

6.1.1 Solar Access 106

6.1.2 Wind Shelter 108

6.1.3 Urban Warmth 110

6.1.1 Isolated Analysis 111

6.2 DESIGN VARIABLES 113

6.2.1 Building Density 114

6.2.2 Building Spacing 115

6.2.3 Building Orientation 117

6.3 ENERGY ANALYSIS 118

The investigation of climate modifications by buildings can be undertaken by studying isolated effects of a specific urban design variable on a specific element of urban climate. A preliminary building energy analysis is performed to separately consider the effects of an urban design variable on each climatic element affected by this variable. In order to complete the building energy analysis, however, all of these effects must be analysed in an integrated form. Arumi [1979: 157] states that "Integrated analysis is needed because some of the results of isolated analysis may be altered significantly when specific variables are considered in context of the total design.". Later in this chapter, an integrated energy analysis is performed, that is, an analysis of the building energy use in urban context. In this analysis, effects of selected urban design variables on climatic elements affected by these variables are all considered.

6.1 DESIGN OBJECTIVES

The impact of applying the climate-adapted design objectives on energy use is investigated with the climate of Adelaide. The climate of this city is selected as a midpoint between the extremes of the three temperate climates that are studied. The dwelling selected for the simulation is the narrow-frontage design option (see Figure 5.4). The energy simulations are performed for a range of street aspect ratios selected to comply with the climate-adapted design objectives. In the following sections, the isolated effects on energy use of solar access, wind shelter and urban warmth are presented. In performing the simulations on a particular climatic element, this climatic element is only considered in the simulations. However, when the analysis requires the impact of some other climatic elements, they are considered in this case.

6.1.1 Solar Access

Passive space heating requires appropriate access to the sun in the cold season. Studies that have investigated the issue of solar access are based on protecting a building from shading by other buildings and vegetation at certain times. Often, solar access is defined in terms of maintaining direct-beam irradiation over the equator-facing wall on the day of lowest solar altitude for a stated number of hours. Consideration of solar access may be adequate in cold climates where there is no problem of excess heat

in the hot season. However, protection of solar access should not be compulsorily applied in temperate climates, where there are problems of both heat and cold, until the effect of urban shading on solar heat gains in summer and winter is investigated.

An investigation is carried out to evaluate the effect of street aspect ratio and window orientation on total solar gains through glass. The solar radiation is only obstructed by buildings flanking the street without any other obstructions like shading devices or trees. External shading devices as passive solar design techniques can reduce solar heat gains. However, an appropriate shading device should be designed on an individual basis and cannot be generalised in all urban forms. Therefore, to simplify the situation shading devices will not be considered in this investigation. The simulation is performed using the energy-based shading design program SHADING (see Section 2.2.2).

Solar Gains Discussion

Total solar heat gains through glass for urban dwellings are predicted for a range of aspect ratios between 0.5 and 1.5. Table 6.1 shows total solar heat gains in GJ/m² of glass area by street aspect ratio for N-S and E-W oriented dwellings. As expected, solar heat gains are significantly affected by street aspect ratio. Solar heat gains are reduced by 30% and 50% in summer and winter respectively when the aspect ratio is changed from 0.5 to 1.5. In summer, the solar gains of the N-S oriented dwelling are less than half that of the E-W oriented dwelling. In winter, the N-S oriented dwelling receives solar gains less than one and a half times that of the other dwelling for aspect ratios less than unity. However, for aspect ratios greater than unity the difference between solar gains of the two dwellings is minor.

Table 6.1
Total solar heat gains (GJ/m² of glass area) by street aspect ratio in Adelaide

Aspect ratio H/W	N-S oriented dwelling		E-W oriented dwelling	
	Summer	Winter	Summer	Winter
0.50	0.75	1.20	1.33	1.03
0.75	0.68	1.10	1.16	0.94
1.00	0.66	0.95	1.02	0.81
1.25	0.61	0.65	0.91	0.71
1.50	0.55	0.53	0.85	0.61

Table 6.2 shows total solar heat gains in GJ/m² of glass area for differently oriented dwellings with aspect ratio equals unity. It is shown that the N-S oriented dwelling receives the highest and lowest solar gains in winter and summer respectively. Broadly, the average winter solar heat gains of NW-SE and NE-SW oriented dwellings (orthogonal 45°) seem to be almost the same as that of N-S and E-W oriented dwellings (orthogonal 90°). But, the average summer solar heat gains of NW-SE and NE-SW oriented dwellings are significantly more than that of N-S and E-W oriented dwellings. This might be inconsistent with Knowles' suggestion [1981 : 21] that Spanish grid (orthogonal 45°) is preferable in mid-latitude cities. One possible reason for this discrepancy is that Knowles' suggestion was based on shadow distribution studies for evaluating ground solar access, which may lead to a different result to what is proposed here based on wall solar access.

Table 6.2
Total solar heat gains (GJ/m² of glass area) by orientation in Adelaide

Orientation	Heat gain Summer	Heat gain Winter
NW-SE	1.00	0.90
NE-SW	0.96	0.85
N-S	0.66	0.95
E-W	1.02	0.81

6.1.2 Wind Shelter

An investigation is carried out to test whether the heat loss due to ventilation offsets an increase in passive solar heat gain due to the building's exposure to the sun. The effect of street aspect ratio on ventilation heat losses is tested using the TEMPAL program in conjunction with a local wind model. The mean pressure differences between the windward and leeward facade are calculated using the UCB model (see Section 3.3.1). The ventilation rate is based on hourly averaged wind speed corrected to the local roughness, and ventilation heat loss is computed for the dwelling according to the ventilation control strategy (see Section 3.4).

Ventilation Loss Discussion

Ventilation heat losses in GJ are shown in Table 6.3 side by side with solar heat gains in GJ. The results indicate that the additional solar heat gains

due to an open geometry could be offset by the concomitant increase in ventilation heat losses. The ventilation heat losses are affected by ventilation rate in buildings and the difference between the external and internal temperatures. The difference between the internal and external temperature is affected by the solar energy gains and the ventilation rate. Therefore, this increase in ventilation heat losses results from an increase in solar energy gains and in air change rate. The airflow caused by wind is affected by the wind pressure differences that are controlled by street aspect ratio.

The E-W oriented dwelling is warmer in summer and cooler in winter than the N-S dwelling. In Summer, the E-W dwelling has solar heat gains less than twice that of the N-S dwelling. However, the ventilation heat loss for the E-W dwelling is not doubled which results in a warmer interior. In winter, the opposite happens as the N-S dwelling has solar heat gains less than one and a quarter times that of the E-W dwelling. However, the infiltration heat loss for the N-S dwelling is slightly more than that of the E-W dwelling. Consequently, the mean internal temperature of the N-S dwelling is warmer than that of the E-W dwelling.

Table 6.3

Solar heat gain and ventilation heat loss (GJ) by street aspect ratio for the narrow-frontage dwelling in Adelaide

Aspect ratio H/W	Solar heat gain Summer		Vent. heat loss Summer		Solar heat gain Winter		Vent. heat loss Winter	
	N-S	E-W	N-S	E-W	N-S	E-W	N-S	E-W
0.50	5.1	8.9	8.4	10.6	6.3	5.6	5.0	4.6
0.70	5.1	8.6	8.2	10.2	6.2	5.5	4.7	4.4
1.25	5.0	7.4	7.7	9.5	5.4	4.6	4.1	4.1

The preliminary investigations show that the effects of the apparently conflicting design objectives may offset each other. Consequently, the total energy demand for heating and cooling of buildings within a certain zone of urban forms could be roughly similar. This has been tested for some design objectives disregarding the modification of urban air temperature. The inclusion of urban air temperature modifications might have either a positive or negative effect on these results. A study is presented in the following section to incorporate the urban warmth (heat island effect) into the results.

6.1.3 Urban Warmth

Elevated air temperatures in urban 'heat islands' highlight the significance of considering the urban warmth in building performance simulation processes. Most building simulation models have adopted, as site specific, climatic data from weather stations that may be several kilometres away from the site being considered. This fact, which represents an inaccurate input, influences the output of the simulation models, which may under- or over-estimate the internal air temperature and required energy use for heating and cooling. The CTTC model in its developed form is used for incorporating the heat island effect into building simulation models.

Computer simulations are performed to test the significance of incorporating the heat island effect to external air temperatures. Two sets of air temperature are used: one is the temperature recorded in the weather station and the other is the modified temperature by the developed CTTC model for a hypothetical urban site. Other effects of surroundings are included in both runs, such as shading from adjacent structures, obstructed diffuse radiation, and wind shelter effects on infiltration and ventilation rates. The TEMPAL program is used to predict internal temperature and energy use for heating/cooling. The urban site selected for the purpose of this test has a built-up area = 0.33 and a street aspect ratio = 0.5. The street canyon runs in two directions; they are N-S and E-W. The simulated dwelling is the narrow-frontage unit facing E-W (along N-S axis street) and N-S (along E-W axis street).

In the heating season, mean modified external temperatures in E-W and N-S axis street were about 0.6 and 0.4°C warmer than the mean meteorological temperature respectively. Similarly, in the cooling season mean modified external temperatures were 0.6 and 1.5°C warmer than the mean meteorological temperature. The percentage frequency of external temperatures within ranges for both cases is shown in Tables 6.4 a and b. It can be noticed that in the heating season modified external temperatures < 12°C occur less frequently than the equivalent meteorological temperatures. However, in the cooling season modified external temperatures > 18°C occur more frequently than the equivalent meteorological temperatures. These elevated temperatures have

beneficial and detrimental effects on reducing heating and increasing cooling energy requirements respectively.

As a result of accounting for the urban heat island effect, the results indicate about 10% saving in space heating of both dwelling orientations, and about 15 and 60% increase in space cooling requirements for N-S and E-W oriented dwellings respectively. The total predicted energy use of a N-S oriented dwelling was almost the same in both runs. This does not mean that the urban heat island could be ignored due to its cancelling-out effect. Disregarding the heat island effect could imply that cooling loads are being under-estimated and heating loads are being over-estimated. However, the total predicted energy use of E-W oriented dwelling was greater when the external temperature is modified. This is attributed to an increase in the cooling energy resulted from the heat island effect.

Table 6.4 a

Percentage frequency of air temperature within range for both runs in the heating season

Air temperature range (°C)	< 9	9 < 12	12 < 15	15 < 18	18 < 21	21 < 24	24 < 27
Meteorological	11.1	27.7	36.1	16.1	5.3	1.7	1.3
E-W axis street	7.6	25.2	36.0	19.7	6.6	2.5	1.4
N-S axis street	8.8	26.0	36.5	18.4	5.9	2.2	1.3

Table 6.4 b

Percentage frequency of air temperature within range for both runs in the cooling season

Air temperature range (°C)	18 < 21	21 < 24	24 < 27	27 < 30	30 < 33	33 < 36	>36
Meteorological	21.2	18.1	10.4	5.3	3.6	1.8	0.2
E-W axis street	22.0	19.2	11.2	6.4	3.6	2.0	0.4
N-S axis street	20.3	20.3	13.7	7.6	4.1	3.0	0.9

6.1.4 Isolated Analysis

Isolated energy analysis is performed to provide an objective assessment of how the climate-adapted design objectives separately affect building energy use. Three simulation sets are conducted in the climate of Adelaide to single out the effects of solar shading, wind shelter and heat island. The first set involves only the shading effect (commonly considered in most building energy simulation programs). The second set includes both shading and shelter effects. The third set encompasses the

previous two together with the heat island effect. Tables 6.5 shows the predicted heating/cooling energy use (GJ) in various urban configurations for the three simulation sets.

Table 6.5

Predicted heating/cooling energy use (GJ) in various urban configurations for three simulation sets

Street Aspect Ratio (H/W)	0.50			0.70			1.25		
Built-up Area (%)	0.20	0.25	0.33	0.25	0.33	0.40	0.40	0.45	0.55
predicted heating energy use in N-S oriented dwellings									
Shading Only	6.2	5.5	4.9	6.5	5.6	5.0	7.2	6.3	5.5
Shading + Shelter (No Heat Island)	5.9	5.2	4.7	6.0	5.2	4.7	6.4	5.6	5.1
Shading + Shelter + Heat Island	5.2	4.7	4.3	5.3	4.8	4.3	6.7	5.9	5.4
predicted heating energy use in E-W oriented dwellings									
Shading Only	6.8	5.9	5.2	6.8	6.0	5.4	7.4	6.4	5.8
Shading + Shelter (No Heat Island)	6.4	5.6	5.1	6.4	5.6	5.0	6.7	5.9	5.2
Shading + Shelter + Heat Island	6.0	5.3	4.7	6.1	5.3	4.7	7.1	6.3	5.7
predicted cooling energy use in N-S oriented dwellings									
Shading Only	2.1	1.7	1.4	2.1	1.7	1.4	2.1	1.7	1.4
Shading + Shelter (No Heat Island)	2.1	1.7	1.4	2.1	1.7	1.4	2.1	1.7	1.4
Shading + Shelter + Heat Island	2.1	1.8	1.6	1.9	1.6	1.5	1.3	1.2	1.1
predicted cooling energy use in E-W oriented dwellings									
Shading Only	4.1	2.8	2.3	3.8	2.7	2.2	3.1	2.3	1.9
Shading + Shelter (No Heat Island)	4.2	2.8	2.3	3.8	2.7	2.2	3.1	2.3	1.9
Shading + Shelter + Heat Island	4.9	4.2	3.5	4.0	3.6	3.1	2.3	2.0	1.8

In the heating season, it is quite clear that wind shelter contributes to an energy saving in all urban configurations. The heat island results in even further saving in low and medium density developments. However, in high density developments the heat island offsets a considerable part of the energy saving resulted from wind shelter. One possible reason is that higher densities and deeper canyons cause cooler daytime temperatures (as presented in the following section). Given that there is no heating applied at night, any potential energy saving does not appear in these simulations. It can be concluded that the heat island impact on heating energy use is most beneficial in lower densities and shallower canyons.

In the cooling season, wind shelter results surprisingly in no increase in energy use in higher densities and deeper canyons. Given that deep canyons have less potential for providing cross-ventilation through dwellings, the strong sheltering effect should have caused an increase in cooling energy use. It is possible that reduced ventilation rates did not influence the cooling energy use because the ventilation heat loss was not reduced as much. In addition, reduced ventilation heat losses result in slightly warmer indoor temperatures, which promote air-to-air heat losses. The additional air-to-air heat losses almost offset the reduction in ventilation heat losses.

Elevated external temperature due to the heat island causes a slight increase in cooling energy use in lower densities and shallower canyons running east-west. However, it produces a notable energy increase in shallower canyons running north-south. This could be attributed to the great difference in solar radiation availability between the two cases. The heat island has a beneficial effect on cooling energy use in higher densities and deeper canyons, where it reduces the energy use in the afternoon until evening due to cooler air temperatures in this period. However, warmer air temperatures due to the heat island are experienced at night; this affects indoor comfort but not energy use. Again, energy use was not affected because there was no cooling applied at night.

6.2 DESIGN VARIABLES

An integrated analysis is performed on the hypothetical urban configurations determined in Section 5.3.2. Three locations are used to test the impact of latitude-related and other variations in climate; Perth (c. 32°S), Adelaide (c. 35°S) and Melbourne (c. 38°S). A range of simulations are conducted—a total of 108 simulations—to investigate the effects of building density, spacing and orientation. For each location the N-S and E-W orientations, three dwelling shapes (narrow, medium and wide frontage) and three building spacing (street aspect ratio 0.5, 0.7 and 1.25) are simulated each for both heating and cooling seasons. These combinations result in various building densities ranging between 0.2 to 0.55. The following sections discuss the impact of these parameters on urban air temperature and residential energy use simulated by the TEMPAL program in conjunction with the modifier models.

6.2.1 Building Density

As mentioned before, a range of building densities ($FA/S = 0.2 - 0.55$) is investigated to test its impact on external air temperature and building energy use. Building density has a rather complicated effect on external air temperature as it is linked to many other aspects. The diversity of the impact of these aspects makes it difficult to infer one universal relationship. The joint effect of all these aspects constitutes the final impact on external temperatures. Building density is a ratio connected to others like vegetation ratio and building surface/volume ratio. It has an inverse relationship with each of them. It is directly proportional to anthropogenic heat release.

Vegetation ratio affects the moisture available from evapotranspiration processes, which affects the daytime temperature response. This means that a reduction in the vegetation area causes warmer daytime temperatures. Increased building density usually means increased population density as well as activities that increase the anthropogenic heat and consequently the external air temperature. Building thermal mass affects the thermal inertia (heat storage), which affects the night-time temperature pattern. Increased thermal mass leads to more heat storage by day that is released at night to heat the air. This process is affected by the building surface/volume ratio that can express the building mass providing similar building materials and thicknesses are used.

Assuming that the other urban configuration parameters (building spacing and orientation) are kept constant, this leaves building density as the only variable to be tested. The building shapes selected for the investigation (wide, medium and narrow frontage) have surface/volume ratio 0.5, 0.4 and 0.3 respectively. If Figure 5.3 is recalled, it will be noticed that these ratios correspond to inversely ordered building densities. This means that increasing the building mass follows increased building surface/volume ratio not density. Increasing the building mass and inertia dampens the diurnal amplitude of air temperature, which causes warmer night time and cooler daytime temperatures.

Diurnal air temperature variation in two E-W axis canyons with the same street aspect ratio (0.5) and different densities (0.2 and 0.33) for the climate of Adelaide are simulated on two days. Figures 6.1 a and b present

simulated air temperature profiles at these hypothetical sites with that at the weather station on 10 January 1984 and 15 July 1986. The temperature profiles reflect the effect of heat storage, as the higher density experiences warmer temperatures during the afternoon until early morning. As this period is mainly the critical time for heating/cooling, the energy use is expected to be lower in the case of heating and higher with cooling.

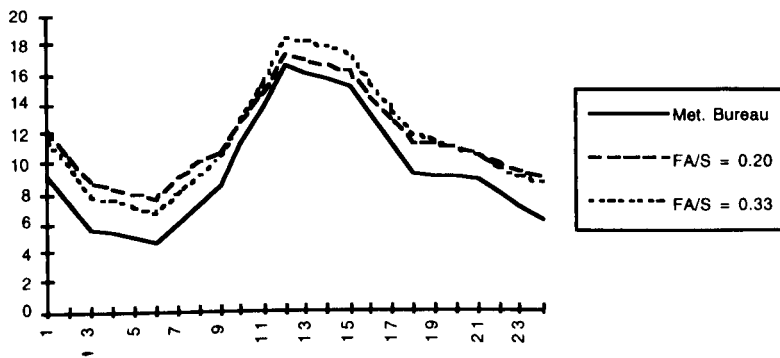


Figure 6.1 a Simulated air temperature profiles for two different building density's sites compared with that at the weather station in Adelaide (15 July, 1986)

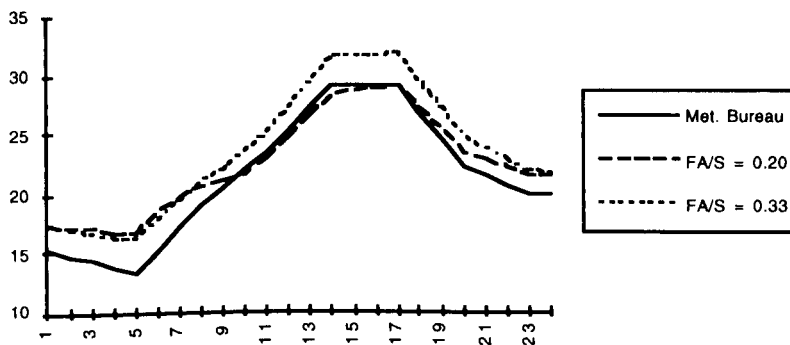


Figure 6.1 b Simulated air temperature profiles for two different building density's sites compared with that at the weather station in Adelaide (10 January, 1984)

6.2.2 Building Spacing

Building spacing is expressed in this thesis with a ratio between building height and spacing—the aspect ratio (H/W). This aspect ratio has an effect on both solar access and wind shelter. For example, a shallow aspect ratio, which is preferable in mid-latitude cities, ensures reasonable solar access and urban ventilation. However, it is not of much help for either urban shading or wind shelter. Aspect ratios as a function of obstruction geometry affect short-wave and long-wave radiative fluxes at

the surfaces of urban canyons. Solar radiation input to the canyon is greatly influenced by the extent to which the canyon surfaces are shaded. Long-wave radiation loss from the canyon is affected by the obstruction of the canyon surfaces from the sky temperature sink. Therefore, aspect ratio has a significant impact on air temperature variations.

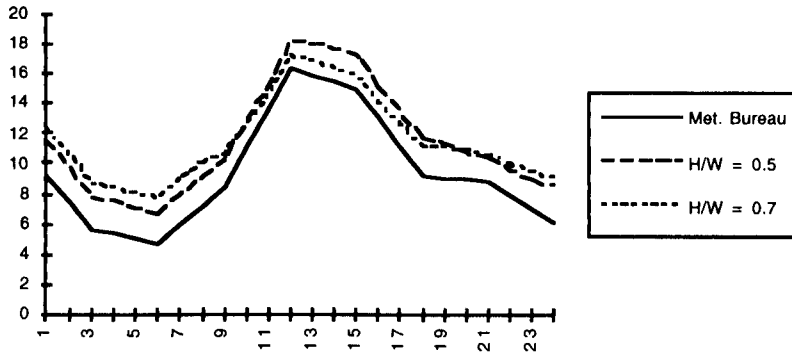


Figure 6.2 a Simulated air temperature profiles for two sites with different aspect ratios compared with that at the weather station in Adelaide (15 July, 1986)

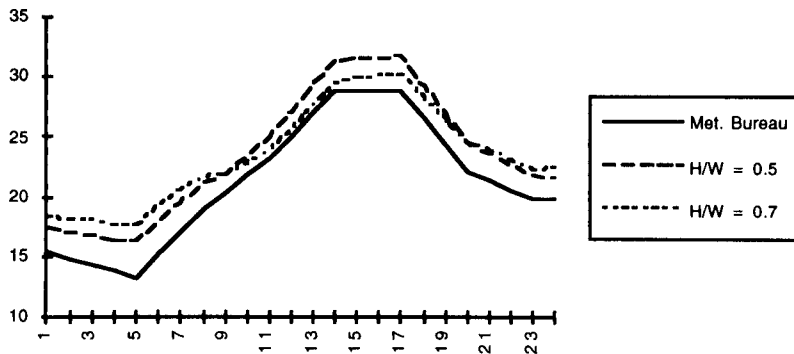


Figure 6.2 b Simulated air temperature profiles for two sites with different aspect ratios compared with that at the weather station in Adelaide (10 January, 1984)

The impact of aspect ratio on the temperature pattern comprises three interrelated but opposing effects. Deeper canyons increase both thermal inertia and shaded areas, but decrease the sky view factors of canyon's facets. A decreasing sky view factor results in a roughly steady temperature increase over the course of the day [Swaid & Hoffman 1990 b]. Nevertheless, increasing shaded areas causes a more noticeable temperature decline at the maxima than at any other time. The effect of aspect ratio on thermal inertia follows its relationship with building surface/volume ratio. Urban configurations of the same building density

and different aspect ratios have different wall areas that affect building surface/volume ratio.

The empirical relationship between street aspect ratio and the maximum heat island intensity is logarithmic [Oke 1988 : 109], therefore, small changes in canyon geometry at low values of aspect ratio result in a considerable heat island intensity. To investigate the effect of aspect ratio on air temperature variation, the air temperature is simulated for two urban hypothetical sites of building density 0.33 and aspect ratios 0.5 and 0.7 in Adelaide. Air temperature profiles on two days (the same as in the previous section) are presented along with that at the weather station in Figures 6.2 a and b. The daytime temperatures for the deeper canyon ($H/W = 0.7$) are cooler, but night time temperatures are warmer.

6.2.3 Building Orientation

A desirable orientation varies according to the climate and to the need for sun or shade and a cool breeze or wind shelter. The choice of a preferable orientation is not an easy task, especially, where a trade-off between hot and cold season performance is required. This is the case in temperate climates, where winter and summer considerations may be of roughly equal strength. The orientation with respect to the sun affects solar heat gains and ambient air temperatures. The orientation with due regard to wind affects ventilation heat losses. It is less predictable if compared to that of the sun since the path of sun is known all year round, but the direction of even the prevailing wind is likely to fluctuate either side of its principal and from year to year.

The issue of orientation may have two levels to be considered in urban design. The first level, probably the most important in low-density urban areas, is the orientation of the building. The second is the orientation of streets and open spaces, which could affect the siting of buildings along the street. In medium- and high-density urban areas, orientation of urban street canyons, which represent the basic urban form unit, definitely affects the overall orientation of buildings flanking the street. In this case, the issue has another dimension which should be considered—the whole urban pattern is a blend of at least four different orientations. For the purposes of this research, the street facades are assumed to be evenly distributed among the four cardinal orientations.

The impact of street canyon orientation on building solar heat gains is discussed in an earlier section (Section 6.1.1). It is inferred that an east-west axis street is preferable in mid-latitude cities. Orientation also affects the duration and intensity of the direct solar radiation input to urban canyons. Therefore, it has a considerable effect on the shape and intensity of intra-urban thermal anomalies. Figures 6.3 a and b present simulated external air temperature for differently oriented canyons of the same urban configurations ($FA/S = 0.33$ and $H/W = 0.7$) in Adelaide on two days (the same as in the previous two sections). Again, east-west axis street proved to be of preferable temperatures in both solstice seasons.

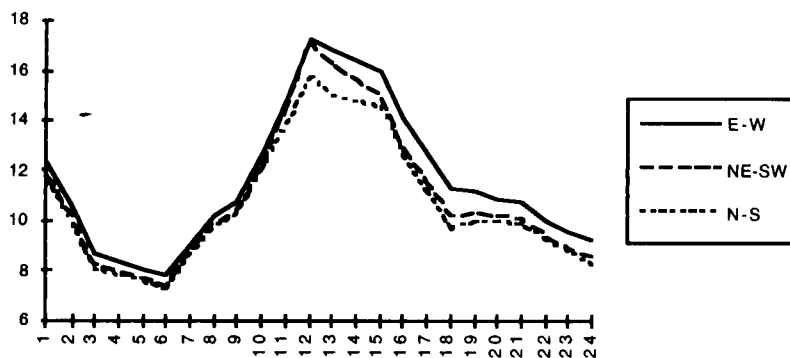


Figure 6.3 a Simulated air temperature profiles for differently-oriented urban street canyons in Adelaide (15 July, 1986)

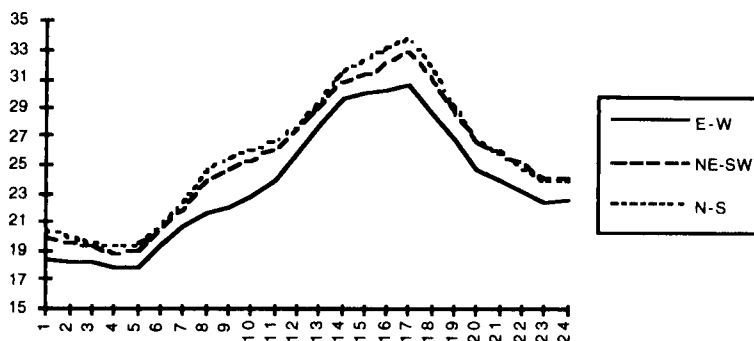


Figure 6.3 b Simulated air temperature profiles for differently-oriented urban street canyons in Adelaide (10 January, 1984)

6.3 ENERGY ANALYSIS

It was early hypothesised that total energy use (heating and cooling) of dwellings in urban areas whose configuration is compatible with the climate-adapted design objectives could be similar. Energy use of

dwelling at hypothetical urban sites is estimated in three different climates. Total energy use figures of N-S and E-W oriented dwellings are averaged. Tables 6.6 through 6.8 present heating and cooling energy use of both N-S and E-W oriented dwellings in various urban configurations together with total and average figures. Average energy use figures for the three cities are consistent with the climate, where Perth and Melbourne have the lowest and the highest energy use respectively.

Average energy use figures of each dwelling shape (narrow, medium and wide frontage) are compared to the energy use of the same dwellings as they were in a free standing block (base cases). The energy use of base cases is estimated using weather data with no modifications whatsoever. Average energy use figures are relatively close to their base cases in each city. This suggests that the ultimate impact on energy use of modification of weather data to be site-specific could be insignificant. Given that these figures are for the terrace housing adopted for the purposes of this research, other housing types may produce different results.

It can be noticed that average figures of each dwelling shape in all tested configurations are reasonably close in Adelaide and Melbourne. However, the average figures in Perth for deep canyons and high densities are less than their counterparts for shallow canyons and low densities. It is possible that shading had an advantageous and influential impact on energy use in this case. The findings support the original hypothesis and suggest that energy use figures were similar due to the cancelling-out effects of applying the climate-adapted design objectives. These findings quantify the heat island as a counterbalance to reduced solar access in medium-density developments.

Despite the wide range of urban configurations dealt with, the difference between average energy use of a particular dwelling shape in various urban configurations is remarkably little. This may suggest that within this adequate range of urban forms, any change in the urban configuration has a minor effect on the heating/cooling energy use. This conclusion is extremely useful for designers as it is so simple and hence easy to apply. If the building analysis (Section 5.4) is recalled, a comparison can be made between the effects on energy use of changes in the urban configuration on one side and the building construction and use-patterns of heating/cooling on the other side. Any slight change in the latter would

result in a noticeable change in the energy use. In this particular case, this conclusion gives the building description and energy use patterns priority in thermal design.

Surprisingly, heating energy use figures for the narrow-frontage dwelling are less than that of the wide-frontage dwelling. What was expected in these cases is the reverse of this relation. The assumption is based on the fact that the latter has a glazing area twice as great as the former's. In this particular case, the additional solar heat gains for the wide-frontage dwelling are counteracted by the concomitant increase in air-to-air heat losses. This conclusion is not based on glazing/wall area ratio; since they all possess the same ratio (20%). Nonetheless, cooling energy use figures are as expected, that is, cooling energy use figures for the narrow-frontage dwelling are less than that of the wide-frontage dwelling. These findings place the narrow-frontage dwelling as an energy-saving design option.

For all cases, energy use figures for E-W oriented dwellings are greater than their counterparts for N-S oriented dwellings. The difference between those figures is greatest in the case of cooling; this highlights the importance of solar shading to east and west facing windows in summer. This difference is reduced with deep canyons; this can be attributed to the minor difference between solar gains of the two differently-oriented dwellings (recall Table 6.1). Total energy use figures for east-west and north-south oriented dwellings are reasonably close with deep canyons in Melbourne. However, there is a noticeable difference in Perth even with deep canyons (up to 45%). One possible explanation is that cooling energy use is a significant constituent of the total energy use in Perth.

Table 6.6
Heating and cooling energy use (GJ) for various urban configurations in Perth

H/W	Frontage	Heating		Cooling		Total		Average N-S+E-W
		N-S	E-W	N-S	E-W	N-S	E-W	
Base case	Wide	1.2	1.6	4.4	8.7	5.6	10.3	8.0
	Medium	1.1	1.4	3.6	6.6	4.7	8.0	6.4
	Narrow	1.1	1.3	3.1	5.1	4.2	6.4	5.3
0.5	Wide	1.2	1.8	5.0	10.3	6.2	12.1	9.2
	Medium	1.0	1.7	4.4	8.8	5.4	10.5	8.0
	Narrow	0.9	1.5	4.1	7.6	5.0	9.1	7.1
0.7	Wide	1.1	1.8	4.6	9.0	5.7	10.8	8.3
	Medium	1.0	1.7	4.2	7.8	5.2	8.5	6.9
	Narrow	0.9	1.5	3.8	6.7	4.7	8.2	6.5
1.25	Wide	1.8	2.4	4.1	6.2	5.9	8.6	7.3
	Medium	1.6	2.1	3.5	5.2	5.1	7.3	6.2
	Narrow	1.6	1.9	3.2	4.7	4.8	6.6	5.7

Table 6.7
Heating and cooling energy use (GJ) for various urban configurations in Adelaide

H/W	Frontage	Heating		Cooling		Total		Average N-S+E-W
		N-S	E-W	N-S	E-W	N-S	E-W	
Base case	Wide	6.0	6.3	2.1	4.5	8.1	10.8	9.5
	Medium	5.2	5.6	1.7	3.6	6.8	9.2	8.0
	Narrow	5.0	5.3	1.3	2.6	6.3	7.9	7.1
0.5	Wide	5.2	6.0	2.1	4.9	7.3	10.9	9.1
	Medium	4.7	5.3	1.8	4.2	6.5	9.5	8.0
	Narrow	4.3	4.7	1.6	3.5	5.9	8.2	7.1
0.7	Wide	5.3	6.1	1.9	4.0	7.2	10.1	8.7
	Medium	4.8	5.3	1.6	3.6	6.4	8.9	7.7
	Narrow	4.3	4.7	1.5	3.1	5.8	7.8	6.8
1.25	Wide	6.7	7.1	1.3	2.3	8.0	9.4	8.7
	Medium	5.9	6.3	1.2	2.0	7.1	8.3	7.7
	Narrow	5.4	5.7	1.1	1.8	6.5	7.5	7.0

Table 6.8
Heating and cooling energy use (GJ) for various urban configurations in Melbourne

H/W	Frontage	Heating		Cooling		Total		Average N-S+E-W
		N-S	E-W	N-S	E-W	N-S	E-W	
Base case	Wide	6.9	7.1	0.8	2.7	7.7	9.8	8.8
	Medium	6.4	6.6	0.6	1.8	7.0	8.4	7.7
	Narrow	6.0	6.3	0.5	1.3	6.5	7.6	7.1
0.5	Wide	6.8	7.5	1.1	3.3	7.9	10.8	9.4
	Medium	6.0	6.6	0.9	2.6	6.9	9.2	8.1
	Narrow	5.3	5.9	0.8	2.2	6.1	8.1	7.1
0.7	Wide	6.8	7.6	1.0	2.8	7.8	10.4	9.1
	Medium	6.1	6.7	0.8	2.1	6.9	8.8	7.9
	Narrow	5.4	6.0	0.7	1.8	6.1	7.8	7.0
1.25	Wide	8.6	8.5	0.8	1.4	9.4	9.9	9.7
	Medium	7.5	7.6	0.6	1.1	8.1	8.7	8.4
	Narrow	6.9	6.9	0.5	0.9	7.4	7.8	7.6

Summary and Recommendations

This research is primarily intended to determine the importance of specific urban design variables as they might affect the energy demand for heating and cooling of an urban dwelling. This chapter aims to give a summary of the research, and then general statements about it. The following sections give a review of the methods and materials used to carry out the research, the most important findings, and limitations of the research that restrict the extent to which the findings can be generalised. Later, urban design guidelines are proposed as generalisations from the results, which are followed by some recommendations for future research and practical applications.

ELEMENTS OF CLIMATE

Urban forms affect main climatic elements, such as solar radiation, wind speed and air temperature. As such, urban forms formulate a microclimate as distinct from the general climate. They are claimed to be the major cause of intra-urban climatic variations. These effects on the climate needed an investigation, particularly, in temperate climates where these effects are of a conflicting nature in different seasons. For example, a shallow canyon has the advantage of an appropriate solar access and ventilation on one hand. On the other hand, it does not help much in providing urban shading or wind shelter. The following deals with urban effects on solar radiation, wind field and air temperature.

Solar Radiation

Solar radiation availability in urban areas can be categorised, based on the access level required, into three categories; they are ground, wall and roof. These levels are categorised from the most conservative to the most liberal. The first level can be used in mixed-use areas to provide two hours solar access to streets and parks in lunchtime. The second level allows the sun to penetrate buildings for about five hours during the day. The third level aims to protect roof solar collectors and allows maximum density to be achieved. This thesis was concerned with the second level, which is required for investigating the urban configuration effects on building solar heat gains.

There are two main solar access techniques for protecting solar access; they are shadowing and total radiation. The former is a very commonly

used technique and has various applications like solar envelope and fence. These concepts define the limiting heights of a particular development in order not to shade an adjacent site in certain times. Concepts of that kind consider only the direct radiation and ignore the diffuse and reflected components. Conversely, the latter considers all the radiation components in a way that estimates the real effect of any obstruction. In addition, it can be programmed for personal computers for rapid and relatively accurate calculations. This technique was used in this thesis to estimate the obstruction effects on solar radiation availability to a particular building.

Wind Field

The wind field can be characterised by two parameters; they are the vertical profile of wind speed and the turbulence spectrum. These parameters are required for an adequate representation of the wind effects. As turbulence intensity was not available in weather data used in this research, wind speed has not been adjusted to account for turbulence. An estimate of the perception of windiness as well as the other climatic elements helps assessing shelter requirements. Urban wind is affected by building density, height and spacing. The wind speed in urban canyons is smaller than that above the canyon; the difference between them increases as building density or height increases.

One of the common techniques for estimating airflow through building is mathematical predictive models. They make use of wind pressure differences across a building and size and airflow discharge characteristics of building openings. The natural ventilation flow is partly wind-driven and partly temperature-driven. Thus, the volumetric flow rate is mainly affected by the pressure and temperature difference between the outdoor and the indoor. The relative effect of either of them to the other depends on the climate and building characteristics. In this thesis, a predictive airflow model was used to estimate only airflow caused by wind, which was influenced by the test urban configurations.

Air Temperature

The heat island is a phenomenon expressed as warmer temperatures in urban areas than that in suburban and rural areas. The temperature increases with building density and energy consuming activities. The effect of the heat island on energy use for heating and cooling is

significant and is contingent upon the geographic location and weather conditions. This thesis researched some statistical models that have been developed to express the intensity of the heat island in terms of various climatic elements. An analytical model for predicting urban air temperatures was developed for the purposes of this research. This model accounts for the urbanisation effects on intra-urban variation of air temperatures.

The city itself is the cause of the climatic differences from the surrounding open country. Expanded urban surface area and multiple reflections increase the absorption of short-wave radiation. Reduction of sky view factors reduces the long-wave radiation loss. Reduction of urban wind speed leads to decreased total turbulent heat transport. Increased thermal admittance of construction materials increases sensible heat storage. The additional sources of heat and dust provided by human activity contribute to the generation of the heat island. The city's lack of water and vegetation over many areas causes slower evaporation from soil and vegetation as compared to a rural area, and this reduces latent heat losses.

MICROCLIMATE MODEL

Most thermal performance simulation models do not modify the weather data to be site-specific. The site could be several kilometres away from the weather station which means that the weather data could be different from that at this site. A computer model was developed to incorporate microclimatic effects into building energy simulations. Modifier models were integrated to create a microclimate model that was then linked to the building energy analysis program TEMPAL. This model allows the user to simulate building thermal performance with more accuracy than with the conventional method of using weather tapes. The development of this model was the key to investigating the effects of urban design variables on building energy use.

Some input parameters into building energy simulation programs are identified as very sensitive and unpredictable. Small variations of these parameters could have a significant impact on building energy simulations. It was shown that they affect indoor climate and energy use for heating and cooling when they are considered separately. These input parameters are outdoor temperature, air change rate and indoor set point

temperature. Various models were adopted and/or developed for better prediction of those parameters. These models are the local wind model, the urban temperature model, and a model of heating/cooling routine.

Local Wind Model

A model for predicting air change rate was incorporated to the thermal performance simulation program replacing the original empirical formulae. These formulae allow for simulating the effect of neither specific building characteristics nor wind direction. However, the proposed model calculates wind-driven ventilation rates modified for the effects of urban and building characteristics. This model incorporated the UCB local wind model into an airflow model developed to simulate the internal space volume and total openings area. A ventilation control strategy was adopted to simulate the opening of windows in such a way that reflects the behaviour of dwellers. This strategy is controlled by indoor and outdoor air temperature, internal relative humidity and wind speed.

Urban Temperature Model

The urban temperature model is a developed version of the original CTTC model for predicting urban air temperature variations. The model modifies the meteorological temperature to be urban site-specific. It takes into account the urban heat island effect that is attributable to features of urbanisation underlying energy balance changes. The developed model was experimentally verified against field measurements done at the University of Adelaide. The heat island effect proved to have a crucial impact on simulated energy use for heating/cooling. It contributes to a saving in space heating and an increase in cooling energy.

Heating/Cooling Model

A difference between predicted and actual energy consumption could occur if the prediction is based on a unrealistic model of dwellers' heating/cooling routine. A model of heating/cooling routine was developed based on better understanding of occupants' behaviour. Using this model, mismatch between predicted and actual energy use was minimised. Neutral temperatures were adopted as set point temperatures for the heating/cooling plant with 2 degrees swing. They were inferred to be 21°C and 25°C in winter and summer respectively. Only the living area was heated or cooled for nominated periods of occupancy. Plant

operation times were evenings until bedtime (5 - 10pm) with mornings next (7 - 9am) in winter and afternoons until bedtime (3 - 10pm) in summer.

FINDINGS & SPECULATIONS

Energy use for climate control was predicted in urban configurations that are compatible with the following climate-adapted design objectives: solar access and wind shelter in winter and urban shading and ventilation in summer. It is shown that these urban configurations have roughly the same total heating/cooling energy use. One possible explanation is that the effects of applying design objectives of conflicting nature might cancel out each other. It should be noted that net urbanisation effects on total heating/cooling energy use predicted in the following urban configurations were relatively small; therefore, urban designers might reasonably use any of the options considered.

It is suggested in this research that higher urban densities and deeper canyons than those based on solar access criteria will not result in a noticeable increase in the residential heating/cooling energy use in moderate and cool-temperate climates. In addition, the advantageous shading effects of higher densities and deeper canyons result in notable energy savings in warm-temperate climates. However, the impact of higher urban densities and deeper canyons on total energy demand in cities is complex and conflicting [Givoni 1989]. On one hand, higher densities reduce transportation energy use by shortening the length of trips travelled by cars, and reduce the heat loss from buildings by reducing the overall area of building envelope. On the other hand, they increase the need for electricity for the elevators of high-rise buildings and for artificial lighting, and increase the load on air-conditioning to remove the heat concomitant to the artificial lighting.

The results are limited to the assumptions made below regarding the simulation models, the urban configurations and other assumptions. Therefore, these results must be cautiously interpreted in the light of the assumptions at hand. They are meant to show the relative thermal performance of urban design parameters rather than to predict actual building thermal performance. The isolated effects of each parameter (building density, spacing and orientation) on microclimate and/or

energy use could be researched before. Nevertheless, the integrated effects of these parameters have not been investigated (to the best of the author's knowledge) for reasons such as the lack of suitable simulation models. For example, there is no simple model available for testing the impact of these parameters on air temperature variations.

LIMITATIONS

Limitations of this research and the models used in the simulations are mainly due to the complexity of the situation dealt with. Urban forms being simulated were simplified to urban canyons with no open spaces or squares. The urban canyon was assumed to have a semi-infinite length thus eliminating the corners effects. The geometry of the modelled canyon was simply symmetrical flanked by continuous facades with no spaces in between. The simulated dwelling type was a town-house which does not represent the major dwelling type in Australia. Furthermore, possible shading effects of trees or awnings were not considered in the simulations.

Modifier models used in the energy simulations have some limitations. The merit of the new features added to the CTTC model is limited to the applicability of the proposed evapotranspiration method to predicting *hourly* rates and the uncertainty of the assumed diurnal artificial heat profile. Water bodies, topography and downwind effects of urban areas were not included. The ventilation model does not consider pressure fluctuations arising from either wind turbulence or buoyancy. Distribution of openings on one wall is uniform and between walls is fixed. No pressure drop inside building, negligible effects due to partitions.

Energy saving, considered in this research, was oriented to residential energy use for internal climate control. Other relevant energy such as solar water heating and day-lighting has not been considered. Input data to simulation models were averages. This represents a simplification that does not consider the huge variations in some items such as energy use patterns and building construction. It is believed that using very different building description (see Section 5.3.2) may result in differences in the heating/cooling energy balance. Therefore, the results of the simulations

should be understood only in the context of the particular case studies at hand; this may limit any generalisations from them.

URBAN DESIGN GUIDELINES

The notion of climate-adapted design was researched in this thesis in terms of the applicability of some urban design guidelines. These guidelines were meant to improve the indoor thermal environment and hence to reduce the reliance on generated energy. Some urban design guidelines in mid-latitude cities can be generalised from the research results. These guidelines involve recommended building densities, spacings and orientations. They define a practicable zone of urban configurations within which climate-adapted urban design objectives could be fulfilled. The guidelines have the special merits of being quantitative and only depending on simple measures that are easily understood and potentially helpful to urban designers.

A range of building densities between 0.25 - 0.5 is recommended in which very low or high densities are avoided (compare with the range proposed earlier by Oke [1988 : 111] to be 0.2 - 0.4). This range is compatible with urban consolidation strategies that attempt to stem the unsustainable sprawl of Australian cities. The range allows higher densities to be placed which may help to balance the cost of infrastructure (code comparison: maximum site coverage is 0.5 - 0.6 [AMCORD 1992]). As higher densities add to the urban warmth, they can contribute to a reasonable saving in heating energy use. However, this might be affected by the average height of the buildings. Therefore, the heat island intensity in an urban area with buildings of the same height (the case dealt with in this research) could be different from that in an urban area with the same average height but with a combination of low and high buildings in close proximity.

Street aspect ratio limits between 0.5 - 1.25 are proposed to achieve climate-adapted design objectives in temperate climates. The proposed range is consistent with the urban design guidelines for Adelaide city, which limit aspect ratio between 0.5 and 1.5 [CCA 1988 : 17]. When this range is tested for various temperate climate categories, certain aspect ratios appear to be better than the others. Deeper canyons (aspect ratio 1 - 1.25) could be superior in warm-temperate climates, as they are much

cooler in summer. However, in cool-temperate climates, shallower canyons (aspect ratio 0.5 - 0.75) might be preferable as they augment solar access to the street and buildings flanking the street.

Recommended favourite orientations are solar energy-based, as they are selected with solar access in mind. These orientations influence solar gains in the same manner as they affect air temperature. Orientations with due regard to prevailing wind cannot be generalised, as each and every case is unique in itself. East-west axis street is the best of all orientations; where it provides the highest insolation in winter and the lowest in summer. This street orientation has also been recommended by Givoni [1989 : 3-28]. The main facades of buildings tend to be oriented parallel to the street, thereby streets running in this direction promote buildings facing north and south.

FUTURE RESEARCH

Suggestions for future research and practical applications imply the simulation approach and the modelled urban configurations. The simulation approach followed in this thesis was based on transformation of weather data to approximate a site climate. The other approach of simulation, which is a dynamic model of both mesoscale and microscale atmospheric process, could be more reliable in terms of accuracy. Therefore, it is suggested in a future work to use this approach of simulation and/or actual measurements in order to test the accuracy of the thesis simulation approach. In the case of positive results, this simulation approach will be recommended for its simplicity and accuracy.

The basic form unit of urban configurations, used in the simulations, was the urban street canyon. This unit is of uniform building height, semi-infinite length and no open spaces. In spite of being commonly used in research of this kind, an urban canyon with these characteristics does not represent the real conditions. In addition, the terrace housing—selected for the purposes of the simulations—does not always represent the only type of dwellings that formulate urban canyons. It is suggested to seek other urban forms that approximate the reality without the crude assumptions linked to the previous form. In other words, it is hinted at overcoming the simplicity inherent to this form by modelling more complex urban forms.

Bibliography

- Abdou, O. 1987, *The Impact of Passive Solar Energy Utilization on Multi-Storey Apartment Houses in Hot Dry Climates*, Doctoral Dissertation, The University, Michigan.
- Aida, M. 1981, Urban albedo as a function of the urban structure, *Boundary Layer Meteorol.*, Vol. 23, pp. 405-413.
- Aida, M. and Gotoh 1981, Urban albedo as a function of the urban structure - A two-dimensional numerical simulation, *Boundary Layer Meteorol.*, Vol. 23, pp. 414-424.
- AIRAH 1989, *The Australian Institute of Refrigeration, Air Conditioning and Heating Handbook*, Victoria.
- Al-Megren, K. 1987, *Wind Towers for Passive Ventilation Cooling in Hot-Arid Regions*, Doctoral Dissertation, The University, Michigan.
- AMCORD 1992, *Australian Model Code for Residential Development; Guidelines for Urban Housing*, Australian Government Publishing Service, Canberra.
- Arens, E. Lee, E. Bauman, F. and Flynn, L. 1985, *SITECLIMATE: A program to create hourly site-specific weather data*, Proceedings of the ASHRAE/DOE/BTECC conference, thermal performance of exterior envelopes of buildings III, Florida.
- Arens, E. 1989, Predicting the thermal comfort of people in outdoor spaces, *Building and Environment*, Vol. 24, pp. 315-320.
- Arnfield, A. 1982, An approach to the estimation of the surface radiative properties and radiation budgets of cities, *Physical Geography*, Vol. 3, No. 2, pp. 97-122.
- Arnfield, A. 1990, Street design and urban canyon solar access, *Energy and Buildings*, Vol. 14, pp. 117-131.
- Arumi, F. 1979, Computer-Aided Energy Design for Buildings, in *Energy Conservation through Building Design*, ed D. Watson, McGraw-Hill Inc., USA
- AS 1170.2 1989, *Australia Standard 1170, SAA loading code, part 2 - wind forces*, Standards Association of Australia, Sydney.
- ASHRAE 1992, *ASHRAE Handbook of Fundamentals*, American Society of Heating, Refrigeration and Air-Conditioning Engineers, NY.
- Auliciems, A. and Dear, R. 1986, Airconditioning in Australia I-Human thermal factors, *Architectural Science Review*, Vol. 29, pp. 67-75.
- Auliciems, A. 1990, Airconditioning in Australia III - Thermobile Controls, *Building and Energy*, Vol. 33, pp. 43-48.

- Australian Draft Standard DR 92022 March 1992 Design Guide Part 1, thermal insulation of roof/ceiling and walls in dwellings which require heating, the Standards Association of Australia.
- Aynsley, R. Melbourne, W. and Vickery, B. 1977, *Architectural Aerodynamics*, Applied Science Publishers LTD, London.
- Ballinger, J. Samuels, R. Coldicutt, S. and Williamson, T. 1991, *A National Evaluation of Energy Efficient Houses: attitudes and experiences, thermal and environmental comfort, and energy consumption*, Final report to the Energy Research and Development Corporation, Project No. 1274, Sydney.
- Ballinger, J. 1992, *Energy Efficient Australian Housing*, 2nd edn, Australian Government Publishing Service, Canberra.
- Bansal, N. Garg, S. and Kothari, S. 1992, Effect of Exterior Surface Colour on the Thermal Performance of Buildings, *Building and Environment*, Vol. 27, No.1, pp. 31-37.
- Beazley, E. 1990, Sun, Shade and Shelter, *Landscape Design*, pp 194-7
- Bauman, F. Ernest, D. and Arens, E. 1988, The effects of surrounding buildings on wind pressure distributions and natural ventilation in long building rows, *ASHRAE Transactions* , Vol. 94, Pt. 2.
- Bornstein, R. 1986, Urban climate models: nature, limitations and applications, in T.R.Oke (ed.), *Urban climatology and its applications with special regard to tropical areas*, Report 652, WMO Geneva, pp. 235-49.
- Bosselmann, P. and Arens, E. 1991, *Sun, Wind, and Pedestrian Comfort; A Study of Toronto's Central Area*, no. 25, City of Toronto; Planning and Development Department, Toronto.
- Boutet, T. 1987, *Controlling Air Movement; A Manual for Architects and Builders*, McGraw-Hill, NY.
- Brunt, D. 1932, Notes on radiation in the atmosphere, *Quart. J. Royal Meteorol. Soc.*, Vol. 58, PP. 389-420.
- Casabianca, G. Evans, J. and de Schiller, S. 1991, Solar Rights and Planning Codes, Proceedings of PLEA; *Architecture and Urban Space*, Kluwer Academic Publishers, London, pp. 61-66.
- CCA 1988, Urban Design Guidelines, Corporation of the city of Adelaide, Adelaide.
- Chand, I. Bhargava, P. Sharma, V. and Krishak, N. 1992, Studies on the effect of mean wind speed profile on rate of airflow through cross-ventilated enclosures, *Architectural Science Review*, Vol. 35, pp. 83-88.

- Chandler, T.J. 1976, *Urban climatology and its relevance to urban design*, Technical note 149, WMO, Geneva.
- Clarke, J. A. 1985, *Energy Simulation in Building Design*, Adam Hilger Ltd, Bristol and Boston.
- Coldicutt, A. and E. 1985, *Reference Manual TEMPAL; Computer Prediction of Thermal Performance of Buildings*, The University, Melbourne.
- Coldicutt, S. and Williamson, T. 1988, *Design Guide for Energy Efficient Housing Adelaide*, Energy Information Centre and Department of Architecture, University of Adelaide, Adelaide.
- Coldicutt, S. Williamson, T. and Penny, R. 1988, Attitudes and Compromises affecting Design for Thermal Performance of South Australian Housing, *Proceedings of Healthy Buildings Conference*, Stockholm, pp. 621-30.
- Coldicutt, A. Williamson, T. Coldicutt, S. 1989, *Thermal Properties of Construction Elements*, Department of Architecture, University of Adelaide, Adelaide.
- Coldicutt, S. Williamson, T. and Penny, R. 1991, Thermal Preference Methodology Information for Designers, *Architectural Science Review*, Vol 34, pp 85-94.
- County Council of Essex 1973, *A Guide for Residential Areas*, England.
- Danielson, L. 1982, Drafting a Solar Access Ordinance: One City's Experience, *Solar Law Reporter*, Vol. 3, No. 6, pp. 911-965.
- Davenport, A. 1960, *Winds Loads on Structures*, Technical Paper No. 88, National Research Council, Ottawa.
- De Gids, W. Ton, J. and van Schijndel, L. 1977, Natural Ventilation of Dwellings, *Proceedings of CIB conference in Holzkirchen, Germany*, pp. 94-122.
- Drysdale, J. 1975, *Designing Houses for Australian Climates*, Australian Government Publishing Service, Canberra.
- EBCC, 1984, *Solar access legislation for South Australia*, Energy in Building Consultative Committee, Adelaide.
- EIC, 1993, Energy Information Centre in Adelaide, Personal Communication.
- El Diasty, R. 1986, Prediction of illumination using radiation measurements, *Building and Environment*, Vol. 21, pp. 3-10.
- Eliasson, I. 1991, Urban Geometry, Surface Temperature and Air Temperature, *Energy and Buildings*, Vol. 15, pp 141-5.

- Emmerson, R. 1980, *Microclimate*, in *Building Design for Energy Economy*, The Construction Press, Lancaster.
- Etheridge, D. and Britain, P. 1977, The Prediction of Ventilation Rates in Houses and the Implications for Energy Conservation, *Proceedings of CIB; Ventilation and Infiltration in Dwellings, Germany*, pp. 46-67.
- Etheridge, D. 1988, Modelling of air infiltration in single- and multi-cell buildings, *Energy and Buildings*, Vol. 10, pp. 185-192.
- Evans, M. 1980, *Housing, Climate and Comfort*, The Architectural Press, London.
- Faist, A. 1988, Design Aids: Presect and Future, *Proceedings of PLEA; Energy and Buildings for Temperate Climates*, eds E. Frenandes and S. Yannas, Pergamon Press, Oxford, pp. 609-19.
- Fathy, H. 1986, *Vernacular Architecture: Principles Examples with Reference to Hot Arid Climates*, The University of Chicago Press, Chicago.
- Fisk, D. 1981, Comfort and Energy Consumption, in *The Architecture of Energy*, eds D. Hawkes and J. Owers, Construction Press, UK.
- Geiger, R. 1959, *The climate near the ground*, Translated by Scripta Technica, Inc., Harvard press, Cambridge.
- Gibbs, P. Gani, R. and Symons, J. 1988, Heat Transfer from building Surfaces due to Wind Effects, *Proceedings of ANZAScA; People and Technology: Sun, Climate and Building*, Brisbane, pp. 79-84.
- Givoni, B. 1981, *Man, Climate and Architecture*, 2 nd edn, Applied Science Publishers LTD, London.
- Givoni, B. 1989, *Urban design in different climates*, WCAP-10,WMO , Geneva.
- Glaumann, M. and Westerberg, U. 1988, Climatic Planning - Wind, *Byggtjaenst*, pp. 1-10.
- Glaumann, M. and Westerberg, U. 1991, Design Criteria for Solar Access and Wind Shelter in the Outdoor Environment, *Energy and Buildings*, Vol. 15, pp. 425-31.
- Harris, J. and Pollock, P. 1986, Solar access in Boulder, Colorado five years after, *Proceedings of 11th National Passive Solar Conference*, Colorado.
- Hassall, D. 1973, *Reflective Insulation and the Control of Thermal Environments*, metric edition, ST REGIS-ACI PTY LTD, Sydney.
- Hawkes, D. 1973, Density, Build Form and Environment, in *Housing Markets Density Policy Project Organisation*, University of Sussex, UK.

Hawkes, D. 1981, Building Shape and Energy Use, in *The Architecture of Energy*, Construction Press, UK.

Hayman, S. 1988, Height Zoning for Urban Solar Access, Proceedings of ANZAScA; *People and Technology: Sun, Climate and Building*, Brisbane, pp. 135-8.

Hayman, S. 1989, Limits of Accuracy of Graphical Solar Access and Shadow Studies, *Architectural Science Review*, Vol. 32, pp. 15-20.

Hoglund, B. Mitalas, G. and Stephenson, D. 1967, Surface temperatures and heat fluxes for flat roofs, *Building Science*, Vol. 2, pp. 29-36.

Hoffman, M. and Feldman, M 1981, Calculation of the Thermal Response of Buildings by the Total Thermal Time Constant Method, *Building and Environment*, Vol. 16, pp. 71-85.

Honjo, T. and Takakura, T. 1990, Simulation of Thermal Effects of Urban Green Areas on their Surrounding Areas, *Energy and Buildings*, Vol. 15-16, pp. 443-446.

Huang, Y. Akbari, H. Taha, H. and Rosenfeld, A. 1987, The Potential of Vegetation in Reducing Summer Cooling Loads in Residential Building, *American Meteorological Society*, Vol. 26, pp. 1103-1116.

Humphreys, M. 1975, Field Studies of Thermal Comfort; Compared and Applied, *UK Building Research Establishment, Current Paper*, Vol 76.

Humphreys, M. 1978, Outdoor temperatures and comfort indoors, *Building Research and practice*, pp. 92-104.

Hunter, L. Watson, I. and Johnson, G. 1991, Modelling Air Flow Regimes in Urban Canyons, *Energy and Buildings*, Vol. 15, pp. 315-24.

Hussain, M. and Lee, B. 1980, An investigation of wind forces on three-dimensional roughness elements in a simulated atmospheric boundary layer flow, *Department of Building Science, University of Sheffield, Report No. BS 56*.

IHVE 1970, Institution of Heating and Ventilating Engineers, *IVHE Guide Book A*, The Curwen Press, London.

Indicative Planning Council for the Housing Industry 1980, *Report on Multi-Unit Dwelling Development in Australia*, Canberra.

Jensen, R. and Haise, H. 1963, Estimating evapotranspiration from solar radiation, *Irrigation Drainage Div. Amer. Soc. Civil Eng.*, Vol. 89, pp. 15-41.

Johnson, G. Hunter, L. and Arnfield, A. 1991, Preliminary field test of an urban canyon wind flow model, *Energy and Buildings*, Vol. 15-16, pp. 325-332.

- Kay, M. Hora, U. Ballinger, J. and Harris, S. 1982, *Energy-Efficient Site Planning Handbook*, The Housing Commission of NSW, Sydney.
- Katayama, T. Ishii, A. Nishida, M. and Sakakibara, N. 1988, Optimum site planning of apartment houses for complex use of natural energy, *Proceedings Healthy Buildings*, Stockholm, pp. 653-662.
- Keeble, E. Collins M. and Ryser, J. 1991, The potential of land-use planning and development control to help achieve favourable microclimates around buildings, *Building and Energy*, Vol. 15-16, pp 823-36.
- Kenworthy, A. 1985, Wind as an Influential Factor in the Orientation of the Orthogonal Street Grid, *Building and Environment*, Vol. 20, pp 33-38.
- Knowles, R. 1974, *Energy and Form: An Ecological Approach to Urban Growth*, MIT Press, Cambridge, MA.
- Knowles, R. 1981, *Sun Rhythm Form*, The MIT Press, Cambridge, MA.
- Kobysheva, N. 1992, *Guidance material on the calculation of climatic parameters used for building purposes*, Technical Note No. 187, WMO- No. 665, Geneva.
- Koenigsberger, O. Ingersoll, T. Mayhew, A. Szokolay, S. 1973, *Manual of tropical housing and building; Part one: Climatic design*, Longman, London.
- Landsberg, H. 1981, The Urban Climate, *Int. Geophys. Ser.*, Vol. 28, Academic Press, NY, p. 275.
- Letherman, K. and Al-Azawi, M. 1986, Prediction of the Heating And Cooling Energy Requirements in Buildings using the Degree Hours Method, *Building and Environment*, Vol. 21, pp 171-6.
- Lewis, J. and Carlson, T. 1989, Spatial variations in regional surface energy exchange patterns for Montreal, Quebec, *Canadian Geographer*, Vol. 33, pp. 194-203.
- Lim, B. and Rao, K. 1984, An Integrated Approach to Environmental Comfort with Low Energy, in *Energy Conservation in the Design of Multi-Storey Buildings*, ed H. Cowan, Pergamon Press, Sydney.
- Linacre, E. and Hobbs, J. 1977, *The Australian Climatic Environment*, John Wiley and Sons, Brisbane.
- Lowry, W. 1967, The climate of cities, *Scientific American*, Vol.217 , pp. 15-23.
- Ludwig, F. 1970, Urban temperature fields in urban climates, *WMO Technical Note No. 108*, pp. 80-107.

- Marcus, T. and Morris, E. 1980, *Buildings, Climate and Energy*, Pitman Publishing LTD, London.
- McBoyle, G. 1970, Observations on the effect of city's form and functions on temperature patterns, *NZ Geographer*, Vol.26 , pp.145-150.
- Meier, A. 1990, Strategic Landscaping and Air-conditioning Saving: A Literature Review, *Energy and Buildings*, Vol. 15-16, pp. 479-486.
- Moriyama, M. and Mutsumoto, M. 1988, Control of urban night temperature in semi-tropical regions during summer, *Energy and Buildings*, Vol. 11, pp. 213-219.
- Murakami, S. Mochida, A. and Hayashi, Y. 1991, Numerical simulation of velocity field and diffusion field in an urban area, *Energy and Buildings*, Vol. 15-16, pp. 345-356.
- Nantka, M. 1990, Comparison of Different Methods for Airtightness and Air Change Rate Determination, ASTM STP 1067, ed M. Sherman, *American Society for Testing and Materials*, Philadelphia.
- Nevala, D. and Etheridge, D. 1978, Natural Ventilation in Well-insulated Houses, in *Energy Conservation in Heating, Cooling, and Ventilating Buildings*, eds C. Hoogendoorn & N. Afgan, Hemisphere Publishing Corp., London.
- Nunez, M. and Oke, T. 1977, The Energy Balance of an Urban Canyon, *Applied Meteorol.*, Vol.16 , pp. 11-19.
- Oke, T. Yap., D. and Fuggle, R. 1972, Determination of urban sensible heat fluxes, *International Geography*, Ed. Adams, W. and Helleiner, F., University of Toronto Press, pp. 176-8.
- Oke, T. 1981, Canyon Geometry and the Nocturnal Urban Heat Island: comparison of scale model and field observations, *Climatol.*, Vol. 1, pp. 237-54.
- Oke, T. 1988, Street design and urban canopy layer climate, *Energy and Buildings*, Vol.11 , pp. 103-113.
- Oke, T. 1992, *Boundary Layer Climates*, 2nd edn, Routledge, London.
- Olgay, V. 1963, *Design with climate : Bioclimatic approach to architectural regionalism*, Princeton University Press.
- Prior, M. and Keeble, E. 1991, Directional wind-chill data for planning sheltered microclimates around buildings, *Energy and Buildings*, Vol. 15-16, pp. 887-893.

- Procos, D. 1988, Does Street Orientation Have an Effect on Passive Solar Heating?, Proceedings of PLEA; *Energy and Buildings for Temperate Climates*, eds E. Fernandes and S. Yannas, Pergamon Press, Oxford, pp. 121-5.
- Radford, A. Gero, J. and D' Cruz, N. 1984, Energy-Conservation Design in Context; The Use of Multi-Criteria Decision Methods, in *Energy Conservation in the Design of Multi-Storey Buildings*, ed H. Cowan, Pergamon Press, Sydney.
- Riordan, P. 1992, *Context Relevance in Thermal Comfort Studies*, Honors Architectural Studies, The University of Adelaide.
- Rosenberg, N. 1974, *Microclimate: The Biological Environment*, John Wiley and Sons, Inc., New York.
- Rosنفeld, A. Akbari, H. Bretz, S. Fisher, B. Kurn, D. Sailor, D. and Taha, H. 1995, Mitigation of urban heat islands: materials, utility program, updates, *Energy and Buildings*, Vol. 22, pp. 255-265.
- Saini, B. 1970, *Architectural in Tropical Australia*, Melbourne University Press, VIC.
- Saini, B. 1980, *Building in Hot Dry Climates*, John Wiley and Sons, Brisbane.
- Sham , S. 1987, *Urbanization and the atmospheric environment*, Penerbit Universiti Kebangsaan Malaysia, Bangi.
- Sharlin, N. and Hoffman, M. 1984, The urban complex as a factor in the air temperature pattern in a Mediterranean coastal region, *Energy and Buildings*, Vol. 7, pp. 149-158.
- Sioufi, M.M. 1987, *Urban patterns for improved thermal performance*, (D.Arch) thesis, The University, Michigan.
- Stemers, K. 1991, Low Energy Design in Urban Context, Proc. of PLEA; *Architecture and Urban Space*, eds S. Alvarez et al., Kluwer Academic Publishers, London.
- Swaid, H. and Hoffman, M. 1990 a, Prediction of urban air temperature variations using the analytical CTTC model, *Energy and Buildings*, Vol. 14, pp. 313-324.
- Swaid, H. and Hoffman, M. 1990 b, Climatic Impacts of Urban Design Features for High- and Mid- Latitude Cities, *Energy and Buildings*, Vol. 14, pp. 325-336.
- Swaid, H. and Hoffman, M. 1991, Thermal Effects of Artificial Heat Sources and Shaded Ground Areas in the Urban Canopy Layer, *Energy and Buildings*, Vol. 15, pp. 253-61.

- Szokolay, S. 1987, *Thermal Design of Buildings*, RAI Education Division, Australia.
- Szokolay, S. 1988, *Climatic data and its use in design*, RAI education division, Canberra.
- Szokolay, S. 1991, *Climate, Comfort and Energy; Design Of Houses for Queensland Climates*, The University of Queensland, Brisbane.
- Tacken, M. 1989, A comfortable wind climate for outdoor relaxation in urban areas, *Building and Environment*, Vol. 24, No. 4, pp. 321-324.
- Taesler, R. 1986, Urban climatological methods and data, ed. T. Oke, *Urban climatology and its applications with special regard to tropical areas*, Report 652, WMO Geneva, pp. 199-236.
- Taesler, R. 1988, Calculation of Solar Radiation in Built-up Environments, *Proceedings of Healthy Buildings*, Stockholm, pp. 79-88.
- Taha, H. Akbari, H. Rosefeld, A. and Huang, J. 1988, Residential Cooling Loads and the Urban Heat Island—the Effects of Albedo, *Building and Environment*, Vol. 23, pp. 271-83.
- Taha, H. 1990, *An Urban Micro-Climate Model for Site-Specific Building Energy Simulation: Boundary Layers, Urban Canyon, and Building Conditions*, Ph.D. Dissertation, University of California, Berkeley.
- Tan, S. and Fwa, T. 1992, Influence of Pavement Materials on the Thermal Environment of Outdoor Spaces, *Building and Environment*, Vol. 27, No. 3, pp. 289-295.
- Terjung, W. and Louie, S. 1974, A Climatic Model of Urban Energy Budgets, *Geographical Analysis*, Vol. 6, pp. 341-367.
- Terjung, W. and O' Rourke, P. 1980a, Simulating the Casual Elements of Urban Heat Islands, *Boundary-Layer Meteorology*, Vol. 19, pp. 93-118.
- Terjung, W. and O' Rourke, P. 1980b, Influences of Physical Structures on Urban Energy Budgets, *Boundary-Layer Meteorology*, Vol. 19, pp. 412-39.
- Todhunter, P. and Terjung, W. 1988, Intercomparison of Three Urban Climatic Models, *Boundary-Layer Meteorology*, Vol. 42, pp. 181-205.
- Todhunter, p. 1990, Microclimate variations attributable to urban-canyon asymmetry and orientation, *Physical Geography*, Vol. 11, pp. 131-141.
- Torrance, K. and Shum, J. 1976, Time-varying energy consumption as a factor in urban climate, *Atmospheric Environment*, Vol. 10, pp. 329-337.

- Vitruvius, 1960, *The Ten Books of Architecture*, Dover, New York.
- Walker, I. and Wilson, D. 1993, Evaluating models for superposition of wind and stack effect in air infiltration, *Building and Environment*, Vol. 28, No. 2, pp. 201-210.
- Walsh, P. 1980, Energy Costs of Buildings and their Relationship to Urban Planning, *Proceedings of 50th ANZAAS Congress*, Adelaide.
- Walsh, P., Munro, M., and Spencer, J. 1983, An Australian climatic databank for use in the estimation of building energy use, *CSIRO Aust. Div. Build. Res.*, Tech. Paper.
- Watson, D. 1979, *Energy conservation through building design*, McGraw-Hill, Inc., USA.
- Watson, I. and Johnson, G. 1987, Graphical Estimation of Sky view Factors in Urban Environments, *Climatology*, Vol. 7, 193-197.
- Williams C. and Soligo M. 1992, A discussion of the components for a comprehensive pedestrian level comfort criteria, *Tenth Structures Congress*, ed. Jim Morgen, New York.
- Williamson, T. 1984, *An Evaluation of Thermal Performance Computer Programs*, Final Report, Australian Housing Research Council, AHRC Project 89.
- Williamson, T. 1986, *Solar access control*, Department of Architecture, University of Adelaide.
- Williamson, T. Coldicutt, S. Bennetts, H. and Riodan, P. 1993a, *Windows and Energy*, Department of Architecture, The University, Adelaide.
- Williamson, T. Coldicutt, S. Samuels, R. Ballinger, J. and D' Cruz, N. 1993b, Performance Analysis of Energy Efficient Houses in Australia, *Proceedings of CIB W67 Conference Energy Efficient Buildings*, Stuttgart.
- Wilson, A. 1976, Application of Computers to the Analysis of Buildings, *Proceedings CIB, Energy Conservation in the Built Environment*, Construction Press, UK, pp. 320-5.
- Wiltshire, J. and Warren, B. 1988, *Energy saving through landscape planning*, vol. 5, PSA, England.
- Wiren, B. 1983, Effects of surrounding buildings on wind pressure distributions and ventilative heat losses for a single-family house, *Wind Engineering and Industrial Aerodynamics*, Vol. 15, pp. 15-26.
- Wise, A. 1978, Ventilation of buildings: A Review with emphasis on the Effects of Wind, in *Energy Conservation in Heating, Cooling, and Ventilating*

Buildings, eds C. Hoogendoorn and N. Afgan, Hemisphere Publishing Corp., London.

Yoshida, A. Kazuhide, T. and Watatani, S. 1991, Field Measurements on Energy Balance of an Urban Canyon in the Summer Season, *Energy and Buildings*, Vol. 15, pp. 417-23.

Appendices

CONSECTTC Program 146

The TEMPAL Package (Summary Documentation) 159

TDINPUT (TEMPAL Data Input File) 165

CONSECTTC Program

- C Written by P. Riodan and T. Williamson based on algorithms supplied by the author.
 C modified march 1991 to use new format CSIRO data
 C and april 1993 to include option of CTTC heat island effects

```

CHARACTER LOCAT*20
real m_met,h_met,hRoof_met,HonW_met,FAonS_met,WAonS_met
real SVFh_met,SVFw_met,SVFh_urb,SVFw_urb
real m_urb,h_urb,hRoof_urb,HonW_urb,FAonS_urb,WAonS_urb
real SVFroof_met,Br_met,ori_met
real SVFroof_urb,Br_urb,ori_urb
real calmwind,CTTCWalls_met,CTTCWalls_urb
integer clearsky
integer IMS,IYS,IM,IY
print*,'*****'
print*,'THIS PROGRAM WRITES SELECTED DATA FROM FULL CSIRO
print*,'CLIMATIC DATA TAPE
print*,'FILES WRITTEN FOR TEMPAL USE CONSOLS & CONTEMS(d3 & d4)'
print*,'
print*,'IMS - START MONTH OF DATA ON TAPE
print*,'IYS - START YEAR OF DATA ON TAPE
print*,'IM - REQUIRED START MONTH FOR SELECTED DATA
print*,'IY - REQUIRED START YEAR FOR SELECTED DATA
print*,'
print*,'*****'

```

- c Note: Variable names dealing with variables required for urban heat
 c temperature calculations have been named to match the naming used
 c by Swaid and Hoffman in a series of papers published in 'Energy
 c and Buildings'.

```

OPEN(UNIT=1,FILE='TAPE1')
OPEN(UNIT=2,FILE='D3.DAT')
OPEN(UNIT=3,FILE='D4.DAT')
OPEN(UNIT=4,FILE='consecn.met')
OPEN(UNIT=7,FILE='consecn.urb')
PRINT 100
100 FORMAT(/,5X,' INPUT NAME OF LOCATION - ')
    read(5,fmt='(a)')locat
10  FORMAT(A20)
    print 11
11  format(/,5x,' input IMS, IYS, IM, IY, NO OF MONTHS - ')
    READ *, IMS,IYS,IM,IY,NMONTH
    print*,'Reading CTTC data for the weather data collection site.'

    call ctctdata(4,m_met,h_met,hRoof_met,HonW_met,FAonS_met
1,WAonS_met,SVFh_met,SVFw_met,SVFroof_met,Br_met
2,ORI_met,CTTCWalls_met)

    print*
    print*,'Reading CTTC data for the urban cluster site.'

    call ctctdata(7,m_urb,h_urb,hRoof_urb,HonW_urb,FAonS_urb
1,WAonS_urb,SVFh_urb,SVFw_urb,SVFroof_urb,Br_urb
2,ORI_urb,CTTCWalls_urb)

```

- C READ MONTHS PRIOR TO REQUIRED PERIOD

```

IFLG=1
MNUM=IM-IMS+(IY-IYS)*12
IF(MNUM.EQ.0) GOTO 20
CALL TREAD(IMS,IYS,MNUM,IFLG
1,m_met,h_met,hRoof_met,FAonS_met,WAonS_met,SVFh_met,SVFw_met
2,m_urb,h_urb,hRoof_urb,FAonS_urb,WAonS_urb,SVFh_urb,SVFw_urb
3,SVFroof_met,Br_met,ORI_met
4,SVFroof_urb,Br_urb,ORI_urb
5,calmwind,clearsky,HonW_met,HonW_urb
6,CTTCWalls_met,CTTCWalls_urb)

```

C READ REQUIRED DATA AND WRITE TO FILES D3 & D4

```

20 IFLG=2
CALL TREAD(IM,IY,NMONTH,IFLG
1,m_met,h_met,hRoof_met,FAonS_met,WAonS_met,SVFh_met,SVFw_met
2,m_urb,h_urb,hRoof_urb,FAonS_urb,WAonS_urb,SVFh_urb,SVFw_urb
3,SVFroof_met,Br_met,ORI_met
4,SVFroof_urb,Br_urb,ORI_urb
5,calmwind,clearsky,HonW_met,HonW_urb
6,CTTCWalls_met,CTTCWalls_urb)

```

```

CLOSE(UNIT=1)
CLOSE(UNIT=2)
CLOSE(UNIT=3)
CLOSE(UNIT=4)
CLOSE(UNIT=7)
STOP
END

```

```

C -----
SUBROUTINE TREAD(IMON,IYEAR,NMON,IFLG
1,m_met,h_met,hRoof_met,FAonS_met,WAonS_met,SVFh_met,SVFw_met
2,m_urb,h_urb,hRoof_urb,FAonS_urb,WAonS_urb,SVFh_urb,SVFw_urb
3,SVFroof_met,Br_met,ORI_met
4,SVFroof_urb,Br_urb,ORI_urb
5,calmwind,clearsky,HonW_met,HonW_urb
6,CTTCWalls_met,CTTCWalls_urb)

```

```

CHARACTER PLACE*2,MONTH(12)*1
real m_met,h_met,hRoof_met,FAonS_met,WAonS_met
real SVFh_met,SVFw_met,SVFh_urb,SVFw_urb
real m_urb,h_urb,hRoof_urb,FAonS_urb,WAonS_urb
real SVFroof_met,Br_met,ORI_met
real SVFroof_urb,Br_urb,ORI_urb
real calmwind,UrbanHeatingAtMetSite
real Ipen_urb(96),Ipen_met(96),HonW_met,HonW_urb
real BaseTemHist(96)
real CTTCWalls_met,CTTCWalls_urb
real WindTimesTen,WindmPerSec,WindKnots
integer clearsky,yy,mm,dd,hh
real TEMmet,TEMrur,TEMurb,HeatD(24)
real WTEMmet,WTEMrur,WTEMurb
real rur2metDiff,rur2urbDiff,rur2metWDiff,rur2urbWDiff
INTEGER TEMP,tenh2o,ATMP,WIND,WINDD,CLOUD,GIRad,DIFH,DCTN
integer IDHrflg(4)

```

```

DATA MONTH/'J','F','M','A','M','J','J','A','S','O','N','D'/

```

```

Data HeatD/20,20,20,20,20,20,30,40,39,38,37,36,
1      35,36,37,38,39,40,37,34,31,28,25,22/

mtempkount=0.

      DO 7 K=1,NMON
      M=0
      GOTO(10,20,10,30,10,30,10,10,30,10,30,10) IMON
10    IDAY=31
      GOTO 50
20    IDAY=28
      IF(IYEAR.EQ.68) IDAY=29
      IF(IYEAR.EQ.72) IDAY=29
      IF(IYEAR.EQ.76) IDAY=29
      IF(IYEAR.EQ.80) IDAY=29
      IF(IYEAR.EQ.84) IDAY=29
      IF(IYEAR.EQ.88) IDAY=29
      IF(IYEAR.EQ.92) IDAY=29
      IF(IYEAR.EQ.96) IDAY=29
      GOTO 50
30    IDAY=30
50    NF=IDAY*24

      IF(K.EQ.1.AND.IFLG.EQ.2) THEN
      READ(1,100) PLACE,NYR,MON
100   FORMAT(A2,I2,I2,34X)

140   FORMAT(1X,'CONSOLS',A1,I2,A2,I2)
142   FORMAT(1X,'CONTEMS',A1,I2,A2,I2)
      ELSE
      ENDIF

      iprevday=0
      GIRadLastHr=0
c     initial integration start time
      do 59 ih=1,4
      IDHrflg(ih)=6
59    continue

60    DO 3 Icount=1,NF

c     if first real day for reading data, must fill Ipen array with solar radiation data

      if(iflg.eq.2.and.Icount.eq.1) then

      do 121 i=1,95
      READ(1,110,END=90)yy,mm,dd,hh
1     ,TEMP,tenh2o,ATMP,WIND,WINDD,CLOUD,GIRad,DIFH,DCTN,ialt,iaz

      alt=float(ialt)/57.29578
      if(hh.eq.0) hh=24
      ii= 97-i
      Ipen_met(ii)= float(GLRAD)
      Ipen_urb(ii)= float(GLRAD)
121   continue

c     return to original position

```

```

do 14 i=1,95
  backspace(1)
14  continue
  endif

  GIRadLastHr= aGIRad
  READ(1,110,END=90)yy,mm,dd,hh
1  ,TEMP,tenh2o,ATMP,WIND,WINDD,CLOUD,GIRad,DIFH,DCTN,ialt,iaz
  alt=float(ialt)/57.29578
  azi=float(iaz)/57.29578
  aGIRad=float(GIRAd)
  if(hh.eq.0) hh=24
110  FORMAT(2x,4i2,I4,i3,i4,i3,i2,i1,6x,i4,i3,i4,i2,i3)

  If((GIRadLastHr.eq.0.).and.(aGIRad.gt.0.)) then
    do 115 ih=1,3
      ihp1=ih+1
      IDHrflg(ihp1)=IDHrflg(ih)
115  continue
      IDHrflg(1)=hh
      endif

      if(hh.eq.1) then
        iday=(icount/24)+1
        print*, 'Reading day ',iday
      endif

      IF(IFLG.EQ.1) GOTO 3
c  if iflg=1 then only stepping through unwanted months
c  so jump to end of subroutine.

c  TEMmet is dry bulb air temp at the met station
  TEMmet=FLOAT(TEMP)/10.0
c  next line changes abs. moisture content from 10**-1 g/kg to g/kg
  h2o=float(tenh2o)/10.0
c  call conversion(TEMmet,h2o,atmp,WTEMmet)
  DRAD=FLOAT(DCTN)

  DIFR=FLOAT(DIFH)
  WindTimesTen=FLOAT(WIND)
c  need to change 10**-1 ms-1 back ms-1 then to knots
  WindmPerSec=WindTimesTen/10.0

c  normalisation of wind speed to pressure

  theta_rad=22.5*WINDD*0.017453
  ORI_urb_rad=ORI_urb*0.017453
  HonWdummy=HonW_urb
  if (HonWdummy.gt.1.) HonWdummy=1.
  WonHdummy=1./HonWdummy
  Cpw=0.095-0.519*(cos(theta_rad-ORI_urb_rad))**2
1  +0.571*log(WonHdummy)*abs(cos(theta_rad-ORI_urb_rad))
  Cpl=-0.602*(cos(theta_rad-ORI_urb_rad))**2
  Cp = Cpw - Cpl
  WindmPerSec=WindmPerSec*sqrt(Cp)

c  reset Ipen array with current Dctn
  call solarhistory(Ipen_met,ORI_met,SVFh_met,SVFw_met,

```

```

1 hh,HonW_met,FAonS_met,WAonS_met,aGIRad,DIFR,DRAD,alt,azi)

      call solarhistory(Ipen_urb,ORI_urb,SVFh_urb,SVFw_urb,
1 hh,HonW_urb,FAonS_urb,WAonS_urb,aGIRad,DIFR,DRAD,alt,azi)
c *****
c   evapotranspiration calculation

      ETP=0.3*(0.0252*TEMmet+0.078)*aGLrad

      EvapoTrans = ETP*(FAonS_urb - FAonS_met)
Ipen_urb(1)=Ipen_urb(1) + EvapoTrans

c   anthropogenic heat

      DeltaH = (FAonS_urb - FAonS_met)*HeatD(hh)/(0.2+FAonS_met)
Ipen_urb(1)= Ipen_urb(1) + DeltaH

c   use wind speed in ms-1 direct from tape1
      if((WindmPerSec.le.calmwind).and.(cloud.le.clearsky))then

c   h=Ehr+Hc see IHVE Guide pA3-6, Hr=5.7, E=0.8, adjust wind
c   speed for urban situation * 0.7

      h_met= 10.9 + WindmPerSec*0.93*4.1
      hRoof_met= 10.9 + WindmPerSec*4.1
      h_urb= 10.9 + WindmPerSec*0.65*4.1
      hRoof_urb= 10.9 + WindmPerSec*0.7*4.1

      mtempkount=mtempkount+1
      TEMbaseMean=0.
      call basecalcs
1(TEMmet,TEMbase,CLOUD,m_met,h_met,hRoof_met,FAonS_met,WAonS_met
2,SVFh_met,SVFroof_met,Br_met,Ipen_met,HonW_met,CTTCWalls_met
3,DeltaTaSolar_Met,DeltaTNLWR_Met,hh,aGIRad,IDHrflg)
      call TempHistory(TEMbase,BaseTemHist)

      do 12 ib=1,48
          TEMbaseMean=TembaseMean + BaseTemHist(ib)
12 continue
          TEMbaseMean = TEMbaseMean/48.
c   print *,TEMbaseMean
          call clustcalcs
1(TEMmet,TEMbase,TEMurb,CLOUD,m_urb,h_urb,hRoof_urb,FAonS_urb,
2WAonS_urb,SVFh_urb,SVFroof_urb,Br_urb,Ipen_urb,HonW_urb,
3CTTCWalls_urb,DeltaTaSolar_Urb,DeltaTNLWR_Urb,hh,aGIRad,IDHrflg)
c   calculate corresponding wet bulb temps,
c   (assumes constant absolute water content and air pressure)
      call conversion(TEMbase,h2o,atmp,WTEMbase)
      call conversion(TEMurb,h2o,atmp,WTEMurb)
      else
          TEMurb=TEMmet
          TEMbase=TEMmet
          WTEMurb=WTEMmet
          WTEMbase=WTEMmet
      end if

```

```

        WRITE(2,120)DRAD,DIFR,WindmPerSec
120  FORMAT(3(F5.0,1X))
c    calculate temperature differences
        rur2metDiff = TEMmet- TEMbase
        base2urbDiff = TEMurb- TEMbase
        base2metWDiff=WTEMmet-WTEMbase
        base2urbWDiff=WTEMurb-WTEMbase
        Write(3,131)TEMurb,CLOUD,WTEMurb
1    ,TEMmet,DeltaTaSolar_Met,DeltaTNLWR_Met
2    ,DeltaTaSolar_urb,DeltaTNLWR_urb,DCTN,dd,hh

131  FORMAT(F5.1,2x,I3,2x,F5.1,5f5.1,i5,i3,i3)

3    CONTINUE
        IMON=IMON+1
        IF(IMON.GT.12) THEN
            IMON=1
            IYEAR=IYEAR+1
        ELSE
            ENDIF
        -
7    CONTINUE
        IF(IFLG.EQ.1) GOTO 99

C    WRITE REPEAT LAST HOUR
90   WRITE(2,120)DRAD,DIFR,WindKnots
        WRITE(3,131)TEMurb,CLOUD,WTEMurb
1    ,TEMmet,TEMbase,TEMbaseMean,DeltaTaSolar_Met,DeltaTNLWR_Met
2    ,WTEMmet,WTEMbase,DCTN
3    ,dd,hh,WindmPerSec,cloud
99   RETURN
        END

c -----
subroutine solarhistory(Ipen,ORI,SVFh,SVFw,hh,
1 HonW,FAonS,WAonS,gRad,Difr,Drad,alt,azi)
    real Ipenh,Ipenv1,Ipenv2,Ipenhr,Ipenv1r,Ipenv2r,Ipen(96),alt,azi
    integer hh
    PI=3.1415926
    ORIradi=ORI*0.017453
c    read most recent 24 hrs of direct solar radiation into an array

        WonH=1./HonW
        call PartialShadedArea(HonW,alt,azi,ORIradi,Grad,PSAh,
1PSAv1,PSAv2,PSAtot)
c    slope set to 90deg
        slp=PI/2.
C    AZ SURFACE1 AZIMUTH RELATIVE TO SUN (RADIANS)
        cosI=cos(azi-orirad)
C    CALC DIFFUSE RAD. ONLY IF NO DIRECT SUN ON SURFACE
        CTHETA1=cosI*COS(ALT)*SIN(SLP) + SIN(ALT)*COS(SLP)
        IF(CTHETA1 .LE. 0.) ctheta1=0.
C    AZ SURFACE2 AZIMUTH RELATIVE TO SUN (RADIANS)
        cosIc=cos(azi-(orirad+PI))
C    CALC DIFFUSE RAD. ONLY IF NO DIRECT SUN ON SURFACE
        CTHETA2=cosIc*COS(ALT)*SIN(SLP) + SIN(ALT)*COS(SLP)
        IF(CTHETA2 .LE. 0.) ctheta2=0.

```



```

      WonH=1/HonW

      do 10 ihrb=95,1,-1

          ihrbp1=ihrb+1
          Ipen(ihrbp1)=Ipen(ihrb)
10      continue
c      sum radiation in canyon W/m2
c      direct and diffuse on ground
          Ipenh=Drad*sin(alt)*(1.0-PSAh)+SVFh*Difr
c      direct and diffuse on wall 1
          Ipenv1=Drad*ctheta1*(1.0-PSAv1) + SVFw*Difr
c      direct and diffuse on wall 2
          Ipenv2=Drad*ctheta2*(1.0-PSAv2) + SVFw*Difr

c      reflected on ground wall reflection taken as 0.2
          Ipenhr=0.2*(Ipenv1+Ipenv2)*(1-SVFh)
c      reflected on wall 1
          Ipenv1r=0.2*(Ipenv2+Ipenh)*(1-SVFw)
c      reflected on wall 2
          Ipenv2r=0.2*(Ipenv1+Ipenh)*(1-SVFw)
c      TOTAL radiation/unit area in canyon
          Ipen(1)=(Ipenh+Ipenhr)/(2*HonW+1)
          1 + (Ipenv1+Ipenv2+Ipenv1r+Ipenv2r)/(1+0.5*WonH)
c      Print *, Ipen(1)
99      return
          end

c -----
      subroutine PartialShadedArea(HonW,alt,azi,ORIr,Grad,
1      PSAh,PSAv1,PSAv2,PSAtot)
          PI=3.1415926

c      calculate horizontal & vertical area partially shaded fraction
          WonH=1./HonW
c      Horizontal partially shaded area
          If((Grad.eq.0.0).or.(alt.eq.0.)) then
              PSAh=1.
              goto 25
          endif
          If(Grad.gt.0.0) then
              PSAh=abs(HonW*cos(azi-orirad)/tan(alt))
              if(PSAh.gt.1.0) PSAh=1.0
          endif

c      vertical partially shaded area
25      if(Grad.eq.0) then
          PSAv1=1.0
          PSAv2=1.0
          endif

          CosI=cos(azi-ORIr)
          cosIC=cos(azi-(ORIr+PI))
          if(cosi.gt.0.) then
              psav1=0.
              psav2=1.
          else if(cosic.gt.0.) then
              psav1=1.0
              psav2=0.
          endif

```

```

endif

IF(PSAh.ge.1.0) then
if((Grad.gt.0.0).and.(cosI.gt.0.0)) then
PSAv1=abs(1.0-(WonH*tan(alt)/cosI))
if(PSAv1.gt.1.0) PSAv1=1.0
endif
if((Grad.gt.0.0).and.(cosI.lt.0.0)) then

PSAv2=abs(1.0-(WonH*tan(alt)/cosIC))
if(PSAv2.gt.1.0) PSAv2=1.0
endif
endif

c total partially shaded area
If(Grad.eq.0.0) PSAtot=1.0
if((Grad.gt.0.0).and.(PSAh.le.1.0)) then
PSAtot=(HonW + PSAh)/(2*HonW + 1.0)
endif
if((Grad.gt.0.0).and.(PSAh.gt.1.0)) then
PSAtot=(1.0 + (HonW*(PSAv1+PSAv2))/(2.*HonW + 1.))
endif
return
end

c -----
subroutine TempHistory(TEMBase,BaseTem)
real BaseTem(96), tembase
do 10 ihrb=95,1,-1

    ihrbp1=ihrb+1
    BaseTem(ihrbp1)=BaseTem(ihrb)
10 continue
    BaseTem(1)= Tembase

99 return
end

c -----
Subroutine conversion(t,absh2o,ipa,twb)
real pvactual,pvtest,inc

c pressures are worked with in mb in this subroutine, mb=kpa*10
c the csiro tapes have atm. pres. in 10**-1 kpa which is mb
c so the tape value can be used directly below:-
c ipa = atomospheric pressure mb
c pv = vapor pressure mb
c ps = saturation pressure mb
c absh2o = absolute atomospheric moisture content g/kg
c t = dry bulb temp deg C

pvactual=float(ipa)/((621.97/absh2o)+1.)
twb=AINT(t+1)
inc=1
pvtest=-1
do while (inc.ge.(0.01))
pvtest=exp(1.8091+17.269425*twb/(237.3+twb))-
1 0.00078666*(t-twb)*(1+twb/610)*ipa
if(pvtest.gt.pvactual)twb=twb-inc

```

```

      if(pvtest.lt.pvactual)then
      twb=twb+inc
      inc=inc/10
      twb=twb-inc
      else
      end if
      if(pvtest.eq.pvactual)inc=0
c   no need to continue, value of inc assigned 0 to get out of loop
      end do
      return
      end
c-----
      SUBROUTINE cttcdata
      1(u,m,h,hRoof,HonW,FAonS,WAonS,SVFh,SVFw,SVFRoof,Br
      2,ORI,CTTCWalls)

      real m,h,hRoof,HonW,FAonS,WAonS
      real SVFh,SVFw,SVFRoof,Br,PSA(24),CTTCWalls
      integer u,ihr

c   read data required for cttc urban heat island effect calcs
c   from file cōnsec.dat

40  format(40x,f4.2)
60  format(60x,f5.2)
601 format(60x,f5.1)
c   read past header and star line
      read(u,*)
      read(u,*)
      read(u,*)

c   read urban cluster properties
c   m   :Mean surface absorptivity (m)
c   h   :Mean o/all heat trans coeff(Wm-2K-1),st level
c   hRoof:Mean o/all heat trans coeff(Wm-2K-1),roof level
c   HonW :Street canyon aspect ratio (H/W)
c   FAonS:Building density (FA/S)
c   WAonS:Massive external walls-to-plot-area ratio(WA/S)
c   Br   :Brunt number (Br)
c   CTTCWalls:Cluster thermal time constant of external walls

      read(u,60)m
      read(u,60)h
      read(u,60)hRoof
      read(u,60)HonW
      read(u,60)FAonS
      read(u,60)WAonS
      read(u,60)Br
      read(u,60)CTTCWalls
      read(u,601) ORI
c   calculate the sky view factor at street level(SVFh) from HonW
c   using equation given with Tab1,pp327,E&Bv14.
c   SVFh   :Mean sky view factor (SVFh)
      SVFh = cos(atan(HonW*2.0))
c   SVFw   :Mean sky view factor of walls
      SVFw = 0.5*(1.-cos(atan(2./HonW)))
c   SVFRoof:Mean sky view factor at roof-top level(SVFRoof),assume=1
      SVFRoof= 1.0

```

```

c  display data for checking
    write(6,61)m
61  format('Mean surface absorptivity (m)          ',f5.2)
    write(6,62)h
62  format('Mean o/all heat trans coeff(Wm-2K-1)st level ',f5.2)
    write(6,63)hRoof
63  format('Mean o/all heat trans coeff(Wm-2K-1)roof level ',f5.2)
    write(6,64)HonW
64  format('Street canyon aspect ratio (H/W)          ',f5.2)
    write(6,65)FAonS
65  format('Building density (FA/S)                  ',f5.2)
    write(6,66)WAonS
66  format('Massive external walls-to-plot-area ratio(WA/S)',f5.2)
    write(6,67)Br
67  format('Brunt number (Br)                        ',f5.2)
    write(6,675)CTTCWalls
675 format('CTTCWalls,Cluster thermal time const, ext walls',f5.2)
    write(6,68)SVFh
68  format('Mean sky view factor at street level (SVFh) ',f5.2)
    write(6,681)SVFw
681 format('Mean sky view factor from walls (SVFw)      ',f5.2)
    write(6,69)SVFroof
69  format('Mean sky view factor at roof-top level(SVFroof)',f5.2)

c  pause 'Check data, then press ENTER to continue.'
    return
    end

c -----
c  subroutine basecalcs
1(Ta,To,cc,m,h,hRoof,FAonS,WAonS,SVFh,SVFroof,Br,Ipen,HonW
2,CTTCwalls,DeltaTaSolar,DeltaTNLWR,t,GRad,IDflg)
    real To,Ta,m,h,hRoof,FAonS,WAonS,SVFh,SVFroof,Br
    real Ipen(96),DeltaTaSolar,DeltaTNLWR,CTTCWalls
    real sigma,TaK,HonW,lamdaHour

    integer lamda,t,u,cc,IDflg(4)
c  TaK=Ta in Kelvin, t = hour

c  To=Temp of air at the baseal base temp site.
c  Ta=Temp of air in the urban cluster, adjusted from rural air temp.
c  sigma = Stefan-Boltzmann Constant is 5.67 * 10-8 W/m2K4
    sigma = 5.67E-8
c  t, time, is tDeltaTNLWRhe number of hours to be integrated
c  t = 94
c  emmissivity ,Brunt No Br.

c  Equations 5 & 6 calc the net long wave radiation
c  temp effect(DeltaTNLWR). Eq 5 for day and eq.6 for night.
c  Different equations are needed for day and night.
c  Use the direct solar radiation as a test for day or night.

    TaK=Ta+273.15
    SVFm=SVFh*(1.-FAonS) + SVFroof*FAonS
    cldc=float(cc)/8.
    if(GRad.gt.0.0)then

```

```
DeltaTNLWR
```

```

1 =sigma*(TaK**4)*(1.-Br)*(1.-0.8*cldc**2)*SVFm/h

c *****Diagnostic output*****
c print',day ,DeltaTNLWR & 1= ',DeltaTNLWR,DeltaTNLWR1
c *****
c     else
c     DeltaTNLWR
1 =sigma*(TaK**4)*(1.-Br)*(1.-0.8*cldc**2)*(SVFh/h)*(1.0-FAonS)
2 +sigma*(TaK**4)*(1.-Br)*(1.-0.8*cldc**2)*(SVFRoof/hRoof)*(FAonS)

c *****Diagnostic output*****
c print',night ,DeltaTNLWR & 1= ',DeltaTNLWR,DeltaTNLWR1
c *****
c     end if

c Equation 3 calculates the cluster thermal time constant:
c this is from p254 in B&E Vol 15&16
c     CTTC=8.0*(1.0-FAonS)+WAonS*CTTCWalls

c *****Diagnostic output*****
c print',CTTC (Hrs)= ',CTTC
c *****

c Equation 2 integrates the solar contribution:
c     DeltaTaSolar=0.0

c     print', IDflg
c     if(t.lt.IDflg(3)) then
c     ibott=t+(24-IDflg(3)+1)+48
c     else
c     ibott=(t+1)-IDflg(3)+48
c     endif

c     ibott=72

c     do lamda = ibott,1,-1

c     lamdam1=lamda-1
c     lamdap1=lamda+1

c     DeltaTaSolar = DeltaTaSolar+(m*(Ipen(lamda)
1 -Ipen(lamdap1))/h)*(1-exp(-1.0*(lamdap1/CTTC)))

c *****Diagnostic output*****
c print',Ipen= ',ipen(lamda),'DeltaTaSolar= ',DeltaTaSolar
c *****
c     end do

c Equation 1 calculates overall effect:

c calculating base temp
c     To = Ta - DeltaTaSolar + DeltaTNLWR
c     print ',t,Ta,To,DeltaTaSolar,DeltaTNLWR

99 continue

return

```

```

end
c -----
  subroutine clustcalcs
1(Ta,To,Turb,cc,m,h,hRoof,FAonS,WAonS,SVFh,SVFroof,Br,Ipen
2,HonW,CTTCWalls,DeltaTaSolar,DeltaTNLWR,t,GRad,IDflg)
  real To,Ta,m,h,hRoof,FAonS,WAonS,SVFh,SVFroof,Br
  real Ipen(96),DeltaTaSolar,DeltaTNLWR,CTTCWalls
  real sigma,TaK,HonW,lamdaHour
  integer lamda,t,u,cc,IDflg(4)
c TaK=Ta in Kelvin, t = hour

c To=Temp of air at the rural base temp site.
c Ta=Temp of air in the urban cluster, adjusted from rural air temp.
c sigma = Stefan-Boltzmann Constant is 5.67 * 10-8 W/m2K4
  sigma = 5.67E-8

c Equation 3 calculates the cluster thermal time constant:
c this is from p254 in B&E Vol 15&16
  CTTC=8.0*(1.0-FAonS)+WAonS*CTTCWalls

c *****Diagnostic output*****
c print*,CTTC (Hrs)= ',CTTC
c *****

c Equation 2 integrates the solar contribution:
  DeltaTaSolar = 0.0

c print*, IDflg

  if(t.lt.IDflg(3)) then
  ibott=t+(24-IDflg(3)+1)+48
  else
  ibott=(t+1)-IDflg(3)+48
  endif

c ibott=72

  do lamda = ibott,1,-1

  lamdam1=lamda-1
  lamdap1=lamda+1

  DeltaTaSolar = DeltaTaSolar+(m*(Ipen(lamda)
1 -Ipen(lamdap1))/h)*(1-exp(-1.0*(lamdap1/CTTC)))

c *****Diagnostic output*****
c print*,Ipen= ',ipen(lamda),'DeltaTaSolar= ',DeltaTaSolar
c *****
  end do

c initial guess at Tg=Turb=Tmet
  Kount=0
  a=0.4
  Tg=Ta
  goto 10
5 Tg=Tg + A*(Turb-Tg)
  Kount=Kount+1
  If(Kount.eq.100) goto 100

```

- c Equations 5 & 6 calc the net long wave radiation
- c temp effect(DeltaTNLWR). Eq 5 for day and eq.6 for night.
- c Different equations are needed for day and night.
- c Use the direct solar radiation as a test for day or night.

```

10  TaK=Tg+273.15
    cldc=float(cc)/8.
    SVFm=SVFh*(1.-FAonS) + SVFroof*FAonS
    if(GRad.gt.0.0)then

        DeltaTNLWR
1  =sigma*(TaK**4)*(1.-Br)*(1.-0.8*cldc**2)*(SVFm/h)

c  *****Diagnostic output*****
c  print*, 'day ',DeltaTNLWR= ',DeltaTNLWR
c  *****

    else
        DeltaTNLWR
1  =sigma*(TaK**4)*(1.-Br)*(SVFh/h)*(1.0-FAonS)*(1.-0.8*cldc**2)
2  +sigma*(TaK**4)*(1.-Br)*(SVFroof/hRoof)*FAonS*(1.-0.8*cldc**2)

c  *****Diagnostic output*****
c  print*, 'night ',DeltaTNLWR= ',DeltaTNLWR
c  *****

    end if

    Turb=To+DeltaTaSolar-DeltaTNLWR
    If(abs(Tg-Turb).lt.0.05) then
c  print *,t,Ta,To,Turb ,DeltaTaSolar,DeltaTNLWR
    goto 99
    endif
    GoTo 5
99  Return
100 Stop ' Turb failed to converge in Clustcalcs'
    End
C *****

```

The TEMPAL Package (Summary Documentation)*(Data from Coldicutt 1985)***1. General Information**

Name of Package	TEMPAL
Brief description	Design/user oriented package. TEMPAL predicts the thermal performance of buildings. Using actual weather data suitable for the particular locality it predicts hourly environmental temperatures, loads and total energy added to or extracted from spaces for any nominated period - 3 days to year(s).
Computer system	CYBER 73 (BASIC or FORTRAN), VAX (FORTRAN)
Mode(s)	Usually interactive for data input, then batch for the balance of the package.
Input data changes	The package has been designed to facilitate new runs with data changes. Certain files can be retained so that the entire package need not to be re-run.
Languages	BASIC (Control Data corporation) and FORTRAN IV
Documentation	<p>A B COLDICUTT (1977) TEMPAL - A design oriented thermal performance computer package, updated(1978).</p> <p>TEMPAL REFERENCE MANUAL A B and E B COLDICUTT (1981) gives the theoretical basis, flow charts, data requirements and package details. SEPARATE CHAPTER ISSUE. Various Chapters and/or Appendices may be issued separately to suit the requirements of the particular user.</p> <p>Of importance are:</p> <p>Part A Chapters 3 and 4</p> <p>Part B Chapter 3</p> <p>Appendix, viz.</p> <p>"BUILDING INFORMATION SUBMISSION BY THE CLIENT"</p> <p>"DATA INPUT TO TEMPAL"</p> <p>"SPECIAL FEATURES OF TEMPAL"</p> <p>"The TEMPAL package ... SUMMARY DOCUMENTATION"</p> <p>(all issued by Department of Architecture and Building, University of Melbourne)</p>
Input data verification	Complete verification. Input data is read and written on scratch files for the use by program. In course of run, checks compatibility, prints out sample data and

gives error diagnostics, such that it is quite unusual to enter main programs with incompatible data.

2. Plant Capacity

Estimated by the program

Tables of loads allow required plant capacity to be decided.

Plant size

Program estimates hourly input to spaces (heating or cooling) to meet specified internal environmental temperatures for any period
 OR If limited capacity specified the program estimates hourly temperatures attained (if undersized).
 OR If no heating or cooling, hourly temperatures attained.

Start-up Demand

As specified by user, e.g. - hour of start and output capacity or it can be determined by the program.

3. Weather Data

Standard weather data

Weather data (hourly values for 6 or more years) supplied by Division of Building Research, CSIRO for most key places in Australia.

User weather data

Monitored weather data may be put in same format as standard weather data.

4. Load Profile Calculations

Calculation time intervals

Hourly, for any desired period.

Internal load profiles spaces (hourly).

Input by user - estimates of total sensible load in

Internal comfort

Comfort criteria are based on environmental temperature. Values may be specified at any range nominated by user. Humidity is not considered in standard package.

Infiltration

Empirical formulae are available for infiltration and ventilation (window openings) of form:

and $N = A + B \cdot V$ for infiltration
 $N = A + B \cdot V$ for ventilation
 $N = \text{No. of Airchanges/hour}$
 A and B - constants
 V - Speed of wind at building

Mechanical ventilation may be specified. Empirical factors are available to reduce freestream wind speed based on user's estimate of protection from wind.

5. Building Location and Structure

Latitude	Any latitude may be specified.
Height above sea level	Covered by weather data used.
Relation to surroundings	User directly specifies hourly shade provided by surrounding buildings, trees etc. allowing for change with time of year. User is also required to specify factors for diffuse radiation based on estimates of sky and ground "viewed" by facade.
Thermal storage	Through the values of transfer and internal admittances, lags and leads, it is accurately modelled.
Modular gains	Version 2.1 considers two habitable zones in addition to two attic spaces and sub-floor spaces being treated as additional separate zones. Output for each habitable zone.
Limits to size	Limited to ten each of vertical surfaces, horizontal surfaces and inclined surfaces. In use, different surfaces of the same orientations may be combined such that this is rarely limiting. (This restriction keeps the field length down, to make the package available to smaller computers). There is no problem in increasing the number of surfaces.
Facade orientation	Any number consistent with stated limit to size.

6. Radiation Transmission through Glass and Blinds

Glass thickness	Inbuilt data for two thicknesses and provision for factors to adopt to any thickness and type.
Double or triple glazing	Appropriate factors allow any combination of glazing to be used.
Special glass	Heat absorbing - for one type. Any others permissible by specification of factors related to the inbuilt data.
Ext. and int. blinds	Related to inbuilt glass data by appropriate factors.

Combination of special glass and blinds	As above
Shading devices	Considered in conjunction with shade by surrounding buildings. See paragraph 5.
Orientation	No limit.
Air to air glass gain	Input - design "U" value for glass or combination(s). Program varies transfer characteristics as affected by changing external air film resistance due to wind speed alterations.
Operation of blinds	Hours of operation specified and/or as determined by specified level of solar radiation through glass. This level to be specified by the user. (Data 44).

7. Gains through Opaque Walls and Roofs

Solar radiation	Solair temperatures. Increment due to solar radiation and long wave radiation calculated on the basis of hourly direct and diffuse solar radiation using absorptance coefficient, hourly variation in surface resistance (wind) and long wave radiation using empirical formulation based on cloud cover.
Thermal properties	U-value, modified 24 hour transfer and internal admittance, lags and leads.
Calculation of transfer	Method is based on modified response factor termed "advancing mean". Program tests hourly for direction of heat flow and if significant, uses factors appropriate to direction.
Casual gains	Hourly sensible gains only are input to version 2.0 program.

8. Load Profiles

Space loads	Heat added to or removed from space to maintain specified conditions is computed hourly.
Equipment loads	Not determined.

9. Simulation of Building Services Systems

Version 2.1 is used for buildings in general but it incorporates special features necessary for dwellings.

There is little point in simulating the building service system in most dwellings.

There is nothing in the nature of the algorithms used which precludes the inclusion of simulations of services other than that very real limitations would have to be imposed on the building performance section if the total package were to be held to reasonable length.

In the present program, as previously stated, days and time of operation of heating/cooling plant may be specified.

Air cooling/heating may be simulated; also radiant heating.

Mechanical ventilation can be specified. (Version 3.0 is more appropriate to commercial buildings)

10. Consumed Energy Profiles

Consumed energy added to or subtracted from space is presented in output on a daily, fortnightly and cumulative basis for each zone. Heating and cooling energy are simulated separately.

11. Output

Consumed energy	As above
Space loads	Frequency distribution within ten intervals (subdivision of maximum load) for each hour and totals.
Temperatures	Frequency distribution within ten intervals for each hour and totals. A summary of excessive and low temperatures in terms of number of days of each duration is also provided.

12. Specific Output

Daily	User may nominate a series of days for which complete information required. Output for each hour of each day is external air temperature, air change, internal temperature, loads.
Heat flow by paths	For a nominated day, heat flow via each path of building for each hour is provided.

Gains via Glass	For each fortnight output is provided of solar gains via glass, total and per square metre. The proportion of the gain that is actually used in each zone is also computed. In addition mean internal and external air temperatures for each period are provided.
Options	The package has been adapted to numerous special cases but these are not available in the standard package.

13. Significance of results

Matching of predictions with measured conditions for 14 houses has been consistently satisfactory.

14. Skills required for use

Data preparation	Within compass of architect or engineer. Some understanding and experience required to avoid errors. A training period is necessary.
Data input	Some computer programming ability is an advantage, and understanding of thermal performance is necessary so that data errors will be appreciated.
Output interpretation	Feedback indicates no great difficulty and format is greatly appreciated by users.
Time of user	Little greater than that required for comprehensive air conditioning calculations.

TDINPUT (TEMPAL Data Input File)

DATA 1:HEADING TO PRINTOUT

3-STOrey BUILDING (AIR-CONDITIONED)

NARROW FRONTAGE UNIT, N - S AXIS

ADELAIDE, H/W=0.5

WINTER, APL.-OCT.

DATA 2

DATA NO,NO.OF PERIODS,DAYS IN PERIOD,MIDDLE DAY OF 1ST.PERIOD

(MONTH AND DAY),SEASON CODE,PLOT ID.,DIAGNOSTICS(1,2,3,OR 4)

2,14,15,4,8,2,003,1

DATA 3:CLIMATIC DATA CONTROLS

DATA NO,ACCESS DAY,WIND FACTOR,LATITUDE

3,30,0.7,-35

DATA 4:GROUND TEMPERATURES

GROUND TEMPERATURES FOR EACH PERIOD IN RUN

4,20.7,20,7,18.0,18.0,14.4,14.4,12.6,12.6,11.4,11.4,12.0,12.0,13.8,13.8

DATA 5:ELEMENTS IN EACH OF SETS 1 TO 3

DATA NO,NO.OF ELEMENTS IN SET 1(HORIZONTAL),NO.IN SET 2

(VERTICAL-EXCEPT ATTIC),NO. IN SET 3(ATTIC-VERT.& HORIZ.) AND NON-ATTIC

INCLINED,NO.OF ELEMENTS IN EACH ZONE OF SET 1,SET 2,AND SET 3

5,0,4,2,0,0,2,2,0,0

DATA 6:SET 1 GLASS CODE AND ABSORPTANCES

DATA NO,GLASS CODE,ABSORPTANCES OF EACH SURFACE

DATA 7:SET 1 AREAS AND EXPOSURE TO DIFFUSE RADIATION

DATA NO,FOR EACH ELEMENT OF SET IN TURN:

OPAQUE AREA,SKY DIFFUSE FACTOR,REFLECTED DIFFUSE FACTOR,GLASS AREA,SKY

DIFFUSE FACTOR,REFLECTED DIFFUSE FACTOR

DATA 8:SET 2 GLASS CODE AND AZIMUTHS

DATA NO,GLASS CODE,NO.OF DIFFERENT AZIMUTHS

LIST OF DIFFERENT AZIMUTHS IN ANY ORDER

8,1,2,0,180

DATA 9:SET 2 AZIMUTH ORDER

DATA NO,THE LIST OF THE ORDER OF THE AZIMUTHS

9,1,2,1,2

DATA 10:SET 2 REFLECTANCES

DATA NO,MEAN REFLECTANCES OF SURROUNDING SURFACES

FOR EACH WALL IN TURN

10,0.3,0.2,0.3,0.2

DATA 11:SET 2 ABSORPTANCES

DATA NO,ABSORPTANCES FOR EACH EXTERNAL VERTICAL SURFACE

11,0.7,0.7,0.7,0.7

DATA 12:SET 2 AREAS AND EXPOSURE TO DIFFUSE RADIATION

DATA NO,FOR EACH ELEMENT OF SET IN TURN:

OPAQUE AREA,SKY DIFFUSE FACTOR,REFLECTED DIFFUSE FACTOR,GLASS AREA,

SKY DIFFUSE FACTOR,REFLECTED DIFFUSE FACTOR

12,
12,0.41,0.59,3,0.41,0.59
12,0.41,0.59,3,0.41,0.59
12,0.46,0.54,3,0.46,0.54
12,0.46,0.54,3,0.46,0.54
DATA 13:SET 3 GLASS CODE,AZIMUTH AND INCLINATION PAIRS

DATA NO,GLASS CODE,NO.OF DIFFERENT AZIMUTH/INCLINATION PAIRS
LIST OF PAIRS
13,9,2,0,73,180,73
DATA 14:SET 3 AZIMUTH INCLINATION ORDER,ABSORPTANCES

DATA NO,ORDER OF AZIMUTH/INCLINATION PAIRS,ABSORPTANCES
14,1,2,0,7,0.7
DATA 15:SET 3 AREAS AND EXPOSURE TO DIFFUSE RADIATION

DATA NO,FOR EACH ELEMENT OF SET IN TURN:
OPAQUE AREA,SKY DIFFUSE FACTOR,REFLECTED DIFFUSE FACTOR,GLASS AREA,SKY
DIFFUSE FACTOR,REFLECTED DIFFUSE FACTOR
15,27,0.95,0.8,0,0,0
27,0.95,0.8,0,0,0
DATA 16:RADIATION PLOT CONTROLS

DATA NO,PLOT CONTROL CODE,SELECTED SURFACE(DEFINED BY ORDER OF
AZIMUTH)
16,0,0
DATA 17:SHADING OF EXTERNAL ELEMENTS

DATA NO,THE FOLLOWING ENTRIES ARE REQUIRED
FOR EACH SURFACE IN TURN OF SETS 1,2,3(OMIT IF NO ELEMENTS IN SET)
AND REPEATED FOR EACH NEW MONTH OF SHADING SEASON
CODE X9(1 OR 0),NO. OF HOURS OF MIXED SUNLIGHT X8(IF 0 OMIT THE
FOLLOWING),HOUR WHEN MIX COMMENCES,HOUR ENDS,OPAQUE AREA IN SHADE
FOR
EACH HOUR,GLASS AREA IN SHADE FOR EACH HOUR(OMIT THE GLASS AREA IF
THERE
IS NO GLASS IN THE SURFACE)
17,1,1,
17,17,9,3,
1,0,
1,0,
1,0,
1,0,
1,0,
1,10,
7,16,12,0,0,0,0,0,0,0,0,5.4,3,0,0,0,0,0,0,0,0,6,
1,0,
1,0,
1,0,
1,0,
1,0,
1,10,
7,16,12,0,0,0,0,0,0,0,0,12,3,0,0,0,0,0,0,0,0,3,
1,0,
1,1,
7,7,9,3,
1,0,
1,0,

DATA NO, CODE, U, T, LAG, Y, LEAD

22,1

0.4, 0.26, 4.9, 0.82, 3.6

DATA 23: THERMAL PROPERTIES OF SET 3 (ALL EXTERNAL ELEMENTS ENCLOSING

ATTIC SPACES AND EXTERNAL INCLINED ELEMENTS ENCLOSING HABITABLE SPACES

DATA NO, CODE, U, T, LAG, Y, LEAD (FLOW IN), U, T, Y (FLOW OUT)

23,1

4.63, 3.71, 0.4, 4.65, 0.1, 5.66, 4.58, 5.68

DATA 24: THERMAL PROPERTIES OF SET 4

(PERIMETER SUBFLOOR WALLS)

DATA NO, CODE, U, T, LAG, Y, LEAD

24,1

3.34, 2.8, 3, 4.46, 1.3

DATA 25: THERMAL PROPERTIES OF SET 5

(CEILINGS BELOW THE ATTIC SPACES)

DATA NO, CODE, U, T, LAG, Y, LEAD (FLOW IN), U, T, Y (FLOW OUT)

25,1

0.42, 0.37, 1.0, 0.95, 3.7, 0.44, 0.39, 0.98

DATA 26: THERMAL PROPERTIES OF SET 6

(SUSPENDED FLOORS ABOVE GROUND)

DATA NO, CODE, U, T, LAG, Y, LEAD (FLOW IN), U, T, Y (FLOW OUT)

26,1,

2.07, 1.21, 4.3, 2.73, 2.4, 1.69, .79, 2.47

DATA 27: THERMAL PROPERTIES OF SET 7

(CONC. SLAB ON GROUND-PERIMETER STRIP)

DATA NO, CODE, U, T, LAG, Y, LEAD

DATA 28: THERMAL PROPERTIES OF SET 8

(CONC. SLAB ON GROUND-CORE OF SLAB)

DATA NO, CODE, U, T, LAG, Y, LEAD

DATA 29: THERMAL PROPERTIES OF SET 9

(FACES OF VERTICAL PARTITIONS BETWEEN ZONES)

DATA NO, CODE, U, T, LAG, Y, LEAD

DATA 30: THERMAL PROPERTIES OF SET 10

(FACES OF NON-VERTICAL PARTITIONS BETWEEN ZONES)

DATA NO, CODE, U, T, LAG, Y, LEAD (FLOW IN), U, T, Y (FLOW OUT)

30,2

2.07, 1.21, 4.3, 2.73, 2.4, 1.69, .79, 2.47,

1.69, 0.79, 4.3, 2.47, 2.4, 2.07, 1.21, 2.4

DATA 31: THERMAL PROPERTIES OF SET 11

(PARTITIONS INTERNAL TO A ZONE)

DATA NO, CODE, U, T, LAG, Y, LEAD (FLOW IN), U, T, Y (FLOW OUT)

31,1

1.94, 1.69, 0.5, 2.01, 0.8, 1.94, 1.69, 2.01

DATA 32: THERMAL PROPERTIES OF SET 12

(CONTENTS)

DATA NO, U, T, LAG, Y, LEAD

32,1

1.8,1.78,0.8,1.97,1.1

DATA 33:THERMAL PROPERTIES OF THE GROUND

DATA NO,U-VALUE OF GROUND,INTERNAL ADMITTANCE,LEAD

33,0.7,5.5,1

DATA 34:OPENINGS BETWEEN ZONES

DATA NO,TOTAL OPENING B/W ZONES,IF 2 STOREY-WHICH ZONE UPPERMOST
(OMIT IF SINGLE STOREY),MODE OF OPERATION, TYPE OF PLANT FOR EACH ZONE

34,4,2,2,20,20

DATA 35:ATTIC SPACES-RELATIONSHIP TO ZONES

DATA NO,NO.OF EXTERNAL SURFACES ENCLOSING ATTIC SPACES,FOR ZONE 1
AND 2:NO.OF EXTERNAL SURFACES FOR ANY ENCLOSED ATTIC SPACE WHICH
RELATES

TO THAT ZONE,NO.OF EXTERNAL SURFACES RELATING TO BOTH ZONES

35,2,0,2,0

DATA 36:ATTIC SPACES

DATA NO,FOR ATTIC SPACES RELATED TO ZONE 1(REPEAT FOR ZONE 2-OMIT
IF NONE):VOLUME,INITIAL TEMP.AT START OF RUN(2 ENTRIES IF MODE 3),
INFILTRATION FACTORS A & B,FOR ATTIC SPACES RELATED TO BOTH ZONES:
VOLUME,INITIAL TEMP.,FACTORS A & B

36,50,10,0,0

DATA 37:ZONE DATA

DATA NO,FOR EACH ZONE:VOLUME,FACTORS A & B FOR EACH OF THE FOLLOWING:
NATURAL INFILTRATION,NO COOLING PLANT-WINDOWS OPEN OR FAN,COOLING
PLANT

CV FACTORS FOR EACH TYPE OF VENTILATION

37,

132,0.3,0.1,3,15.5,0.3,0.1,

132,0.3,0.1,3,15.5,0.3,0.1,

1,1,3

DATA 38:ZONE DATA

DATA NO,FOR EACH ZONE:INITIAL DRY & WET BULB TEMPS.,2 PAIRS PER ZONE
MODE 3

UPPER COMFORT LIMIT,LOWER COMFORT LIMIT,START AND FINISH OF OCCUPANCY

38,15,10,27,18,7,22,

20,10,24,15,23,6

DATA 39:ZONE DATA

DATA NO,FOR EACH ZONE:DESIRED TEMP.IN ZONE,THERMOSTAT SWING(ABOVE &
BELOW), NUM. OPERATION PERIODS, FOR EACH TIME ON & OFF

39,21,1,2,2,7,9,17,22,

21,1,2,1,0,0

DATA 40:PLANT CHARACTERISTICS

DATA NO, FOR EACH ZONE, CONVECTIVE COOL OR HEAT: PLT. EFF, ACH,
THERM. LOC, TEMP.FLAG, PLANT CONFIG. FLAG.& CAP(KW)

40,100,5,0,1,1,4,

100,5,0,1,1,4

DATA 401:IF STORAGE HEATER - FOSH

DATA NO,CALC. TIME INCREMENT, NUM CHARGE PERIODS,FOR EACH TIME
ON & OFF, FOR EACH ZONE:MAX. HEATER POWER,INT. CORE TEMP,
SIM STAT (TEMP1,POW1),(TEMP2,POW2),ONSWING

DATA 402:IF STORAGE HEATER - COSH

DATA NO,CALC. TIME INCREMENT, NUM CHARGE PERIODS,FOR EACH TIME ON & OFF,
FOR EACH ZONE:MAX. HEATER POWER,INT. CORE TEMP, SIM STAT (TEMP1,POW1), (TEMP2,POW2),ONSWING, FAN PERIODS,FOR EACH TIME ON & OFF, THERMOSTAT SET.

DATA 41:ZONE DATA

DATA NO,FOR EACH ZONE:MEAN ABSORPTANCE OF FLOOR SURFACES,MEAN ABSORPTANCE OF OTHER SURFACES

41,0.4,0.3,0.4,0.3

DATA 42:ZONE DATA

DATA NO,FOR EACH ZONE,HOURLY SENSIBLE & LATENT HEAT LOADS (WATTS) LOAD PAIRS FOR HOURS 1 TO 24 INCL.

42,

0,0,0,0,0,0,0,0,0,0,0,0,0,700,400,700,400,150,100,150,100,150,100,500,250,

150,100,150,100,150,100,150,100,1000,500,700,400,700,400,700,400,700,

400,700,400,0,0,0,0,

300,200,300,200,300,200,300,200,300,200,300,200,300,200,0,0,0,0,0,0,0,0,

0,0,0,0,0,0,0,0,0,0,0,0,0,0,0,0,300,200,300,200

DATA 43:INTERNAL CONTROLS ON GLAZING

DATA NO,RADIATION CONTROLS(NO=1,YES=2:ZONE 1 THEN 2),BLINDS DRAWN AT NIGHT(NO=1,YES=2:ZONE 1 THEN 2),U-VALUE(BARE),U-VALUE(CURTAINS ETC.)

43,1,1,2,2,6,3.1

DATA 44:FACTORS FOR ACTUAL GLAZING USED

DATA NO,THREE ADJUSTMENT FACTORS TO CORRECT FOR DIFFERENCE IN GLASS TYPE AND TO ALLOW FOR ANY FIXED INTERNAL CONTROLS

44,0.97,0,1.6

DATA 45:INTERNAL RADIATION CONTROLS

DATA NO,FOR EACH ZONE(OMIT IF NONE IN ZONE):THREE FACTORS TO ALLOW FOR THE REDUCTION IN SOLAR RADIATION EFFECTS WHEN INTERNAL CONTROLS OPERATED

W/SQ.M ABOVE WHICH BLINDS DRAWN IN SUMMER OR BELOW WHICH DRAWN IN WINTER

DATA 46:OUTPUT CONTROLS

DATA NO,DAY OBNO.ON CLIMATIC DATA FOR BEGINNING OF 7 DAY DETAILED OUTPUT(COUNTED FROM ACCESS DAY),DAY NO.FOR HEAT FLOW BY PATHS(ONE OF 7 DAYS),PUT 0 IF EITHER NOT REQUIRED, PLOT OPTION 1=YES,2=NO

46,48,50,1